Vegetation and climate history of the southern Levant during the last 30,000 years based on palynological investigation

Dissertation

zur

Erlangung des Doktorgrades (Dr. rer. nat.)

der

Mathematisch-Naturwissenschaftlichen Fakultät

der

Rheinischen Friedrich-Wilhelms-Universität

zu Bonn

vorgelegt von

Vera Schiebel

aus

Troisdorf

Bonn, März 2013

Angefertigt mit Genehmigung der Mathematisch-Naturwissenschaftlichen Fakultät der Rheinischen Friedrich-Wilhelms-Universität Bonn

1. Gutachter: Prof. Dr. Thomas Litt

2. Gutachter: Prof. Dr. Dietmar Quandt

Tag des Promotionskolloquium: 06. Juni 2013

Erscheinungsjahr: 2013

Table of Contents

1 Introduction 4

2 Current state of research 6

2.1 Paleoclimate since the Last Glacial Maximum 6

2.2 Paleo-vegetation in the Levant 7

2.3 Settlement history in the Levant 8

3 Area of work 11

3.1 Topography 12

3.2 Geology 14

3.3 Modern climate conditions 15

3.4 Vegetation 18

3.5 Coring Sites 22

4 Material and methods 24

4.1 Coring campaign 24

4.2 Lake Kinneret 24

4.3 Birkat Ram 31

4.4 Reconstruction of vegetation based on pollen data 37

4.5 Dating of Late Pleistocene/Holocene lake sediments 38

5 Results 41

5.1 Lake Kinneret 41

5.2 Birkat Ram 47

6 Discussion 56

6.1 The Last Glacial Maximum (LGM) 56

6.2 The Late Glacial 58

6.3 The Younger Dryas (YD) 60

6.4 The Holocene 61

7 Summary 72

8 Zusammenfassung 74

9 Résumé 76

10 Appendix 78

11 Table of figures and charts 89

12 References 90

1 Introduction

Understanding the relations between variations of paleo-climate and its effects on the paleo-vegetation is of particular interest to a broad range of scientific disciplines. On the one hand, knowledge of past environmental scenarios may help to better understand modern processes, and to develop strategies to adapt plant growth and food production to the present and future climate variability (Pain, 2013). On the other hand, evaluation of human migration activities in the light of interactions between vegetation and past societies is of fundamental importance to explain the dynamics of human populations.

Being located in the transitional climate belt between North-Atlantic influenced climate systems at higher latitudes, and monsoonal influenced climate systems at lower latitudes (Ziv et al., 2006), the southern Levantine region comprises the arid-to-semi-arid climate boundary, and is thus highly sensitive to climate change (Robinson et al., 2006). Moreover, having a long history of human habitation, the Levant is discussed as migration corridor of humans to Europe (Issar and Zohar, 2004), and being part of the Fertile Crescent supposed to be the origin of crop cultivation and agriculture during the Neolithic (Belfer-Cohen and Goring-Morris, 2011; Kuijt and Goring-Morris, 2002). Effects of distinct rapid climate changes on environmental conditions in the Levant from Late Pleistocene until recent years might have caused or triggered changes in human behaviour including plant production, and migration activities of past societies (Robinson et al., 2006). Therefore, the Levantine region provides unprecedented opportunity to study relations of climatic and environmental change. Anthropogenic activities and development of human societies are interpreted in relation to climate and paleo-environmental change. Investigations on interference of humans with nature, as well as on possible responses to changes of climate and vegetation, namely adaptation or migration, have received considerable attention in geosciences for decades (e.g., Berglund et al., 1996; van Zeist and Bottema, 1991). Palynological investigations in the Levantine region have been performed since the 1950s at Lake Hula (Picard, 1952), since the 1970s at Lake Kinneret (Horowitz, 1971) and Birkat Ram (Weinstein, 1976a), and since the 1980s at the Dead Sea (Horowitz, 1984). Taking into consideration the uncertainties in dating of sediments, and in distinguishing between various pollen taxa especially in the earliest approaches (Meadows, 2005; Robinson et al., 2006; Rossignol-Strick, 1995), availability of consistent data is rather poor.

Baruch (1986) analysed a radiocarbon dated 5 m-core from Lake Kinneret at rather low sample resolution. From Birkat Ram, a high-resolution palynological analysis encompasses the last 6,500 years based on a consistent chronology (Neumann et al., 2007a; Schwab et al., 2004). Van Zeist et al. (2009) reviewed the chronology of a pollen record from Lake Hula, formerly published by Baruch and Bottema (1991; 1999), which provides palynological data since the early Holocene applying a revised age-to-depth model. Recently, a chronologically well constrained 10,000-year pollen record from the Dead Sea was published by Litt et al. (2012).

This study is a contribution to the Collaborative Research Centre 806 'Our Way To Europe', supported by the Deutsche Forschungsgemeinschaft (DFG), and dealing with culture-environment interaction and human mobility in the Late Quaternary. In particular, being part of sub-project B3 (main proponent Prof. T. Litt, University of Bonn), the presented investigations aim at highlighting the 'Environmental Response on Climate Impact in the Levant during the Last Glacial and Holocene and their Role in the Origin of Agriculture'. Lacustrine sedimentary archives of Lake Kinneret and Birkat Ram were cored to produce a new record at improved data availability, and most importantly to cover the climatically instable Pleistocene-to-Holocene transition, as well as the entire Holocene. Within this thesis, a time-model is presented, which is developed on the basis of radiocarbon dated debris. Variations of pollen compositions are used as paleo-environmental, as well as paleo-climatological proxy, and which are discussed as indications for human interference with natural vegetation. Possible evidence of rapid climate changes such as the '8.2 Climate Event' are evaluated. Those data are discussed within dating precision. By integrating pollen records from the Dead Sea (Litt et al., 2012) and Lake Hula (van Zeist et al., 2009), potential temporal offsets of vegetation changes along a north-to-south transect along the Dead Sea Rift are assessed in the following. Considering the limitations of the approach and potential implications of the presented data for reconstructing climate and settlement patterns, the present study concludes by distinguishing between climatically- and anthropogenically-induced variations of paleo-vegetation. Moreover, collected pollen data are being applied as proxy of quantitative paleo-climate reconstruction (Thoma, PhD thesis; in prep.).

2 Current state of research

2.1 Paleoclimate since the Last Glacial Maximum

The Last Glacial Maximum (LGM) chronozone is defined as the interval between 23,000 and 19,000 cal BP, centering on 21,000 cal BP by the EPILOG project (Mix et al., 2001). Since then, global climate went through considerable changes (Shakun and Carlson, 2010). In the Near East, very cold and dry conditions prevailed during the LGM (Gat and Magaritz, 1980; Robinson et al., 2006). However, reconstruction of the lake level of Lake Lisan, predecessor of the Dead Sea, and Lake Kinneret, reveals a highstand during the LGM. During the deglaciation after the LGM, mean global sea-level rose by 10-15 m due to the collapse of global ice-sheets and the subsequent meltwater pulses during the deglaciation period (MWP-1A and MWP-1B) (Bard et al., 2010; Deschamps et al., 2012).

Due to the subsequent disturbance of the thermohaline circulation of the North Atlantic, the global warming was interrupted by a fall-back into virtually glacial conditions during the Younger Dryas (YD). The YD is recorded between 12,900 and 11,700 cal BP with regional differences concerning intensity and timing (Broecker et al., 2010). Reconstructions of YD climate in the eastern Mediterranean diverge to some degree. Rossignol-Strick (1993; 1995) and Yechieli (1993) suggest an arid period with dry summers and cool winters whereas Stein et al. (2010) consider the YD as humid time interval. Some records do not reflect a distinct YD-event at all (Bottema, 1995). Reviewing multiple datasets on the Eastern Mediterranean region, Robinson et al. (2006) conclude that the YD was extremely arid and cold compared to the Late Glacial and Holocene.

Although interrupted by several abrupt climate variations, Holocene climate has been rather warm and humid in comparison to the YD (Kotthoff et al., 2008; Mayewski et al., 2004). Even if not reflected in each paleo-environmental record, these rapid climate changes (RCCs) are possibly of global significance (Mayewski et al., 2004). Numerous records prove RCCs from 9,000-8,000 BP ("8.2-event"), 6,000-5,000 BP, 4,200-3,800 BP, 3,500-2,500 BP, 1,200-1,000 BP and since 600 BP (Alley et al., 1997; Bar-Matthews et al., 1999; Bond et al., 1997; Rohling et al., 2009; Rohling and Pälike, 2005), which are marked by intensified Eurasian winter conditions and enhanced Siberian High intensity in the eastern Mediterranean (Rohling et al., 2009). Disturbances of the global oceanic

circulation, and local climatic regimes, induced by rapid input of cold freshwater into the North Atlantic may also have been linked to the development of RCCs (Robinson et al., 2006).

2.2 Paleo-vegetation in the Levant

Temporal variations of the composition of Levantine vegetation during Late Pleistocene- to Holocene times are being investigated since the 1970s, and controversially discussed also for the spatial scale and evolution particularly during climatically crucial periods, e.g. the Younger Dryas (Rossignol-Strick, 1995). The reliability of the applied age-to-depth models of the studied sediment records, as well as possible differences in climate and vegetation on regional or local scale are discussed by Rossignol-Strick (1995), Meadows et al. (2005), and Robinson et al. (2006). Most of the records show evidence for anthropogenic pressure on the vegetation, for example, forest clearance, cultivation of crops, and livestock husbandry or grazing during periods of settlement (e.g., Litt et al., 2012; Neumann et al., 2007a; van Zeist et al., 2009; Yasuda et al., 2000). Significance and interpretation of these indications is also controversially discussed (e.g., Litt et al., 2012; Yasuda et al., 2000).

Southern Levantine lacustrine palynological records are available from the Bekaa Valley in Lebanon (encompassing ~14,500 years; Hajar et al., 2010; Hajar et al., 2008), and the Ghab Valley in Syria (Niklewski and Van Zeist, 1970; Van Zeist and Bottema, 1982; Van Zeist and Woldering, 1980; Yasuda et al., 2000) setting in at the onset of the Late-Glacial Interstadial after the chronology proposed by (Rossignol-Strick, 1995). On Israeli territory, sediment cores and outcrops were analysed from the Hula Basin (estimated chronology encompassing ~11,500 years; Baruch and Bottema, 1991; Baruch and Bottema, 1999; van Zeist et al., 2009), Birkat Ram (encompassing ~6,500 years; Neumann et al., 2007a; Schwab et al., 2004; Weinstein, 1976b), and Lake Kinneret (encompassing max. 5,300 years; Baruch, 1986) in the north, as well as from the Dead Sea (encompassing ~2,500 years Leroy, 2010; ~10,000 years, Litt et al., 2012; ~3,500 Years, Neumann et al., 2010; ~6,800 years, Neumann et al., 2007b) in the south. In addition, pollen records from the marine sediment core 9509 near the southern Israeli coast (encompassing ~86,000 years; Langgut et al., 2011), and a record from a Holocene fluvial marsh site in Jordan (Tzedakis et al., 2006) add information on the Quaternary vegetation of the Levantine region.

2.3 Settlement history in the Levant

Israel is part of the "Fertile Crescent", which is said to be the origin of agriculture (Belfer-Cohen and Goring-Morris, 2011; Goring-Morris and Belfer-Cohen, 2011). Therefore, the evolution of the vegetation in Israel is affected by past societies and vice versa since the transition from Pleistocene to Holocene. Table 2.1 summarises archaeological periods in the Near East assigned to the corresponding time periods. Early- and Middle-Epipaleolithic people (24,000-14,900 cal BP / 22,050 BCE-12,950 BCE) led a nomadic hunter-gatherer lifestyle (Goring-Morris and Belfer-Cohen, 2011), whereas the Natufian people, who inhabited the southern Levant from about 14,900 to 11,700 cal BP (12,950 BCE-9750 BCE) (Goring-Morris and Belfer-Cohen, 2011), are said to have been the first community, living on systematically collected wild cereals (Bar-Yosef, 2000; Grosman, 2003; Valla, 1995).

During Pre-Pottery and Pottery Neolithic times (11,700-8,400 cal BP / 9,750 BCE-6,450 BCE and 8,400-6,500 cal BP / 9,759 BCE-4,550 BCE, respectively; Kuijt and Goring-Morris, 2002), hunter-gatherer societies began to develop a sedentary lifestyle, and agricultural techniques arose and spread throughout the Levant (Goring-Morris and Belfer-Cohen, 2011; Kuijt and Goring-Morris, 2002). Describing these socio-economic changes, Childe (1936) established the term "Neolithic Revolution". In the vicinity of Lake Kinneret, archaeological findings show evidence of settlement activity (Bar-Yosef, 1995) whereas the Golan Heights seem to have been sparsely populated until the Chalcolithic period (Gopher, 1995; Mazar, 1992).

Throughout the southern Levant, the Chalcolithic period (approx. 6,500-5,500 cal BP / 4,550 BCE-3,550 BCE; after Burton and Levy, 2001) was characterised by the marked growth of population, combined with the development of more complex, inter-regional connected societies (Epstein, 1998; Gibson and Rowan, 2006; Rowan and Golden, 2009). The Lake Kinneret area, as well as the Golan Heights and the Mt. Hermon region, were affected by small rural communities, whose inhabitants lived on olive and fruit cultivation, livestock husbandry, and farming (Epstein, 1977; Epstein, 1998). Evidence for settlement activity decreased towards the end of the Chalcolithic period (Mazar, 1992; Rowan and Golden, 2009).

Table 2.1: Chronology of archaeological and historical periods in the Near East after Bar-Yosef (1995), Kuijt and Goring-Morris (2002), and Finkelstein et al. (2004)

Age [BCE / CE]	Age [cal BP]	Archaeological Periods
Recent - 1917	Recent - 33	Modern times
1917 - 1516	33 - 434	Ottoman period
1516 - 1291	434 - 659	Mamelukes
1291 - 1099	659 - 851	Crusaders
1099 - 638	851 - 1312	Early Islamic period
638 - 324	1312 - 1626	Byzantine period
324 CE - 63	1626 - 2013	Roman period
63 - 332	2013 - 2282	Hellenistic period
332 - 586	2282 - 2536	Babylonian-Persian period
586 - 1200	2536 - 3150	Iron Age
1200 - 1550	3150 - 3500	Late Bronze Age
1550 - 2200	3500 - 4150	Middle Bronze Age
2200 - 3550	4150 - 5500	Early Bronze Age
3550 - 4550	5500 - 6500	Chalcolithic period
4550 - 6450	6500 - ~8400	Pottery Neolithic
6450 - 9750	~8400 - ~11700	Pre-Pottery Neolithic
~9750 - ~13000 BCE	~11700 - ~14900	Natufian period

The Early Bronze Age (EBA) in the Levant (5,500-4,150 cal BP / 3,550 BCE-2,200 BCE; after Levy, 1995) was characterised by the "Urban Revolution" (Childe, 1936; Gophna, 1995). Population density rose and urban societies developed. Surrounding Lake Kinneret, several EBA settlements are recorded. Bet Yerah, near the exit of the Jordan River, is assumed to have had 4,000-5,000 inhabitants during the EBA (Greenberg, 2011). Besides, there is archaeological data documenting further EBA communities in the vicinity of the lake (Dever, 1995). Also on the Golan Heights, enhanced settlement activity during the EBA can be shown, but is said to have decreased again towards the end of this period (Paz, 2011).

In general, the Middle Bronze Age (MBA, 4,150-3,500 cal BP / 2,200 BCE-1,550 BCE; after Levy, 1995), too, is characterized by continuous agricultural activities in the southern Levant (Berelov, 2006; Fall et al., 2004). In contrast, in the Lake Kinneret region as well as

on the Golan Heights, settlements have been abandoned, agricultural yields have declined (Greenberg and Paz, 2005), and population was less dense compared to the EBA (Ilan, 1995; Thompson, 1979). Although detailed chronology is a controversially discussed issue (Fantalkin et al., 2011; Finkelstein and Piasetzky, 2009; Plicht et al., 2009), settlement history during the Late Bronze Age (LBA, 3,500-3,150 cal BP / 1,550 BCE-1,200 BCE; Levy, 1995) as well as the Iron Age (IA, 3,150-2,536 cal BP / 1,200 BCE-586 BCE; after Levy, 1995) in the Levant is generally known as unsteady, and characterized by conflicts and short intervals of rise and decline of cultures. Finkelstein and Piasetzky (2009) describe at least ten destruction horizons within 400 years in LBA to IA settlements. In general, archaeological investigations show little evidence for settlement activity in northern Israel during the LBA and the IA (Bunimowitz, 1995; Holladay Jr, 1995). A distinct, relatively denser populated period is stated by Finkelstein and Piasetzky (2009) during Middle to Late IA I (approx. 3,000 cal BP / 1,050 BCE), when an expansion of highland Israelits to the northern valleys can be documented.

Not until the Hellenistic period (2,282-2,013 cal BP / 332 BCE-63 BCE), quantity and size of settlements increased again (Berlin, 1997; Dar, 1993; Urman, 1985). Roman (2,013-1,626 cal BP / 63 BCE-324 CE) and Byzantine (1,626-1,312 cal BP / 324 CE-638 CE) periods were densely populated and economically flourishing, too (Anderson, 1995; Chancey and Porter, 2001; Dar, 1993; Sayej, 2010; Urman, 1985). However, some temporally and spatially limited setbacks are recorded in northern Israel (Aviam, 2011; Pastor, 1997). The transition to the Early Islamic period (1,312-851 cal BP / 638 CE-1,099 CE; after Levy, 1995) was marked by an economic regression and a decline of agriculture as well as population density in the southern Levant (Safrai, 1994). This setback does not terminate until the end of the 19th century, when resumption of agriculture and livestock husbandry as well as development of industry and tourism effected an economic revival.

3 Area of work

This study investigates evolution of vegetation and environment in the southern Levant, which encompasses Israel, Palestine, Syria, Lebanon, Cyprus, western parts of Jordan, and southern parts of Turkey. The analysed sediment material originates from the Birkat Ram and the Lake Kinneret, both located in the southern Levant on Israeli territory (Fig. 3.1).

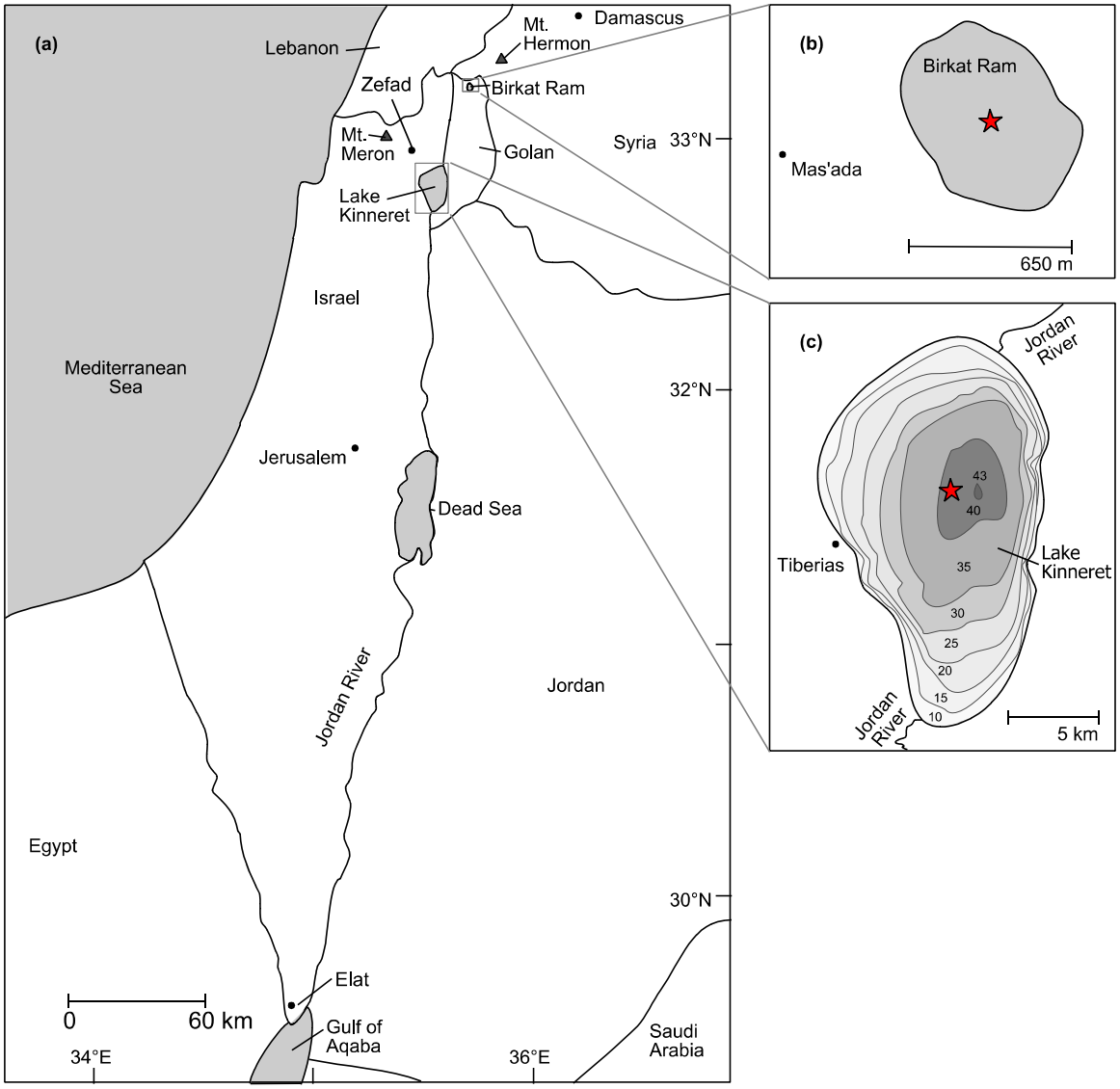

Fig. 3.1: (a) Map of Israel and adjacent areas showing relevant cities (•), rivers, and mountains (▲); (b) Birkat Ram, red star indicates coriing site; (c) Lake Kinneret including bathymetric data after Sade et al. (2008), red star indicates coring site

3.1 Topography

The topography of the eastern Mediterranean (Fig. 3.2) is rather diversified, and strongly influences regional climate (van Zeist and Bottema, 1991). Tectonic events since the early Tertiary led to predominantly north-to-south directed topographic patterns. The region is subdivided into four longitudinal belts (Zohary, 1982). Adjacent to the Mediterranean Sea, the coastal plains span from the Lebanese mountain ranges in the north to the Sinai coastal belt in the south. The coastal plains broaden southward up to a maximum width of ~60km. Bordering the coastal plain, the western mountain ranges with their gently rising western slopes extend from the foot of Mount Lebanon in the north to the Sinai Desert in the south. Being composed of the Upper and Lower Galilee as well as the Central Mountains, they form a barrier for moisture-bearing western winds (van Zeist and Bottema, 1991). The average height of the mountain ranges is ~600 m, comprising the highest summit Mount Meron (1208 m, Upper Galilee). Several west-to-east running valleys incise the mountain ranges. The steep eastern slopes descend abruptly to the Jordan Valley. The Jordan Valley is the lowest depression of the Earth's continental surface (424 m below mean sea level; Israel-Oceanographic&Limnological-Research, 2010), extending from Syria to the Red Sea, and connected to the south with the East African Rift Valley. The Jordan River drains the valley, passing Lake Hula, Lake Kinneret, and into the Dead Sea. North of Lake Kinneret, the Jordan River flows on Israeli territory along the western edge of the Golan Heights, a mountain range extending to the south-western part of Syria. Highest summit of the study area is Mount Hermon (2814 m above mean sea level (amsl)). The Golan Heights average at 1200 m amsl in the northern part, and at about 300 m amsl in the southern part. The southern section of the Jordan River forms the border between Israel and Jordan. On the Jordanian eastern shore, the steep escarpments of the Transjordan Plateau elevate up to 1200 m, and the highest summit Jabal Ram (1754 m), located at the southern part of the plateau. Several east-to-west running rivers cross the Transjordan Plateau, and drain into the Jordan River as well as the Dead Sea. To the east, the Transjordan Plateau gently down-slopes, and merges with the Syrian Desert.

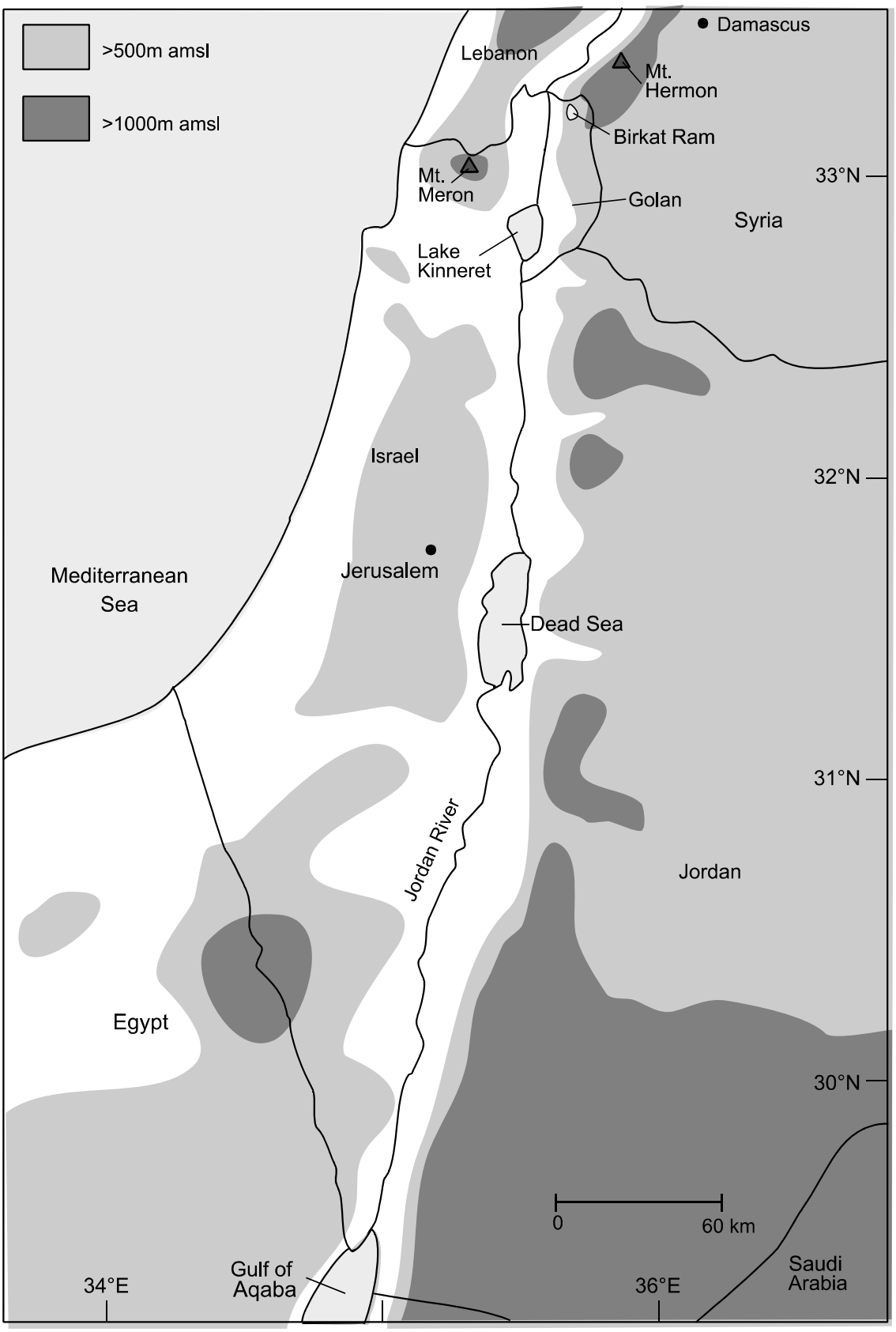

Fig. 3.2: Topographical map of Israel and adjacent areas distinguishing contour lines of 500 m above mean sea level (amsl), and 1000 m amsl (after Geological-Survey-of-Israel, 2012)

3.2 Geology

The study area is composed of various geological formations (Fig. 3.3) (Segev and Rybakov, 2011). In the northern part of the Golan Heights, the Hermon Formation is exposed. It is composed of Mid Jurassic limestones and dolomites and borders southward on Upper Jurassic and Lower Cretaceous as well as Upper Cretaceous limestones, sandstones, and dolomites. Quaternary deposits are formed of gravels, sands and clays, and overlie the older formations in some areas. Large parts of the Golan Heights consist of Late Pliocene to Late Pleistocene basalts, enclosing numerous volcanic cones. Extending southward, those basalt plateaus adjoin Tertiary lime-, sand-, and mudstones, as well as Quaternary alluvial deposits. Those alluvial deposits fill the Jordan Rift Valley, and occur scattered between older structures. West of the Dead Sea Transform Fault, Cretaceous formations, consisting of limestones, and marls alternate with Tertiary sand- and limestones, Pliocene basalts, and Quaternary gravels, sands, and clays. The Birkat Ram crater rim is formed by Late Pleistocene Golan basalt sequences. Within the northern part of the Birkat Ram drainage area, Lower and Upper Cretaceous lime- and sandstones are exposed. Furthermore, Jurassic formations and Quaternary alluvial deposits affect the lake system. The Lake Kinneret watershed is composed of Pliocene basalts, Cretaceous limestones, sandstones, dolomites, marls, as well as Tertiary formations, and Quaternary sequences (Horowitz, 1979).

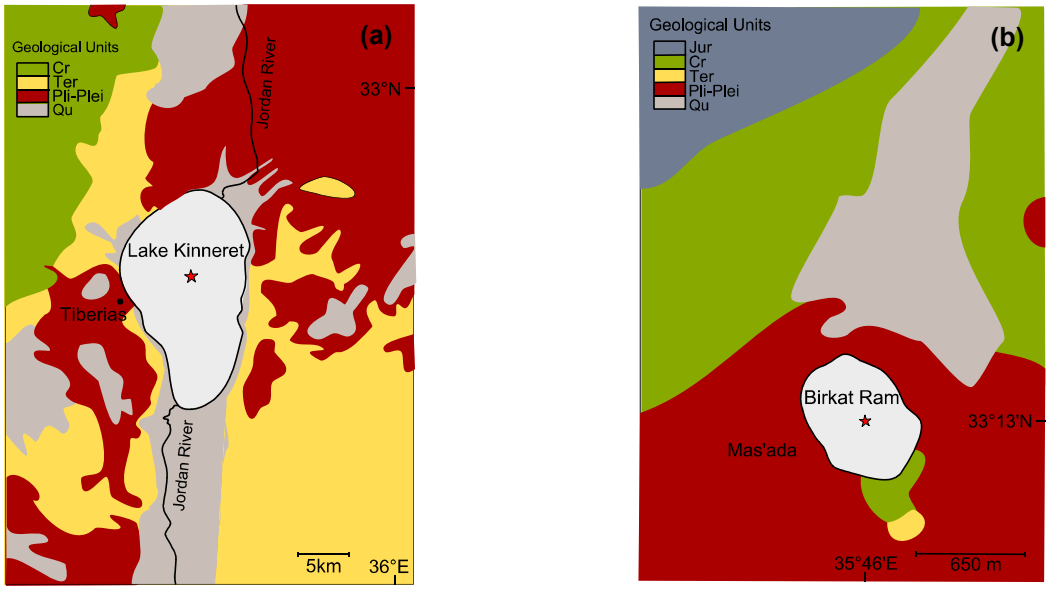

Fig. 3.3: Geological map of the (a) Lake Kinneret area, and (b) Birkat Ram area; Jur=Jurassic formations, Cr=Cretaceous formations, Ter=Tertiary formations, Pli-Plei=Pliocene / Pleistocene formations; Qu=Quaternary deposits (after Geological-Survey-of-Israel, 2012); red stars indicate coring sites

3.3 Modern climate conditions

The eastern Mediterranean region encompasses the transitional climate zone between the North African deserts and the Central European West Wind Drift (Boucher, 1975). Due to seasonal changes of the predominant North African anticyclone, two different regimes affect the eastern Mediterranean climate. During boreal summer, the northern position of the North African subtropical high-pressure system covers the eastern Mediterranean, characterised by high temperatures, and widespread droughts (Rohling et al., 2009). Developing over the Persian Gulf, Red Sea, and Cyprus, steady low-pressure systems stabilise the climate. The wind system affecting Israel is part of the general westerly flow, typical of the eastern Mediterranean basin (Levantine Basin) during summer. It is dominated by the Mediterranean breeze, which develops in spring and declines in autumn. Due to large differences in altitude, these westerly to north-westerly winds accelerate and strengthen, while air masses heat up adiabatically. They reach the Jordan Rift Valley as hot winds with high wind speeds (50km/h in average), and superimpose diurnal elements on the local wind systems. At night, local conditions in the vicinity of the lakes are affected by katabatic winds and land breezes caused by land-to-water temperature gradients (Bitan, 1974; Bitan, 1981).

During boreal winter, climatic conditions in the Eastern Mediterranean are less stable. The air pressure trough over the Persian Gulf collapses, and the northern edge of the subtropical high-pressure system is displaced southward to North Africa. The Mediterranean Sea is exposed to intensive cyclonic activity (Bitan, 1981). Most of the west-to-east passing extratropical cyclones, i.e. “Cyprus Lows”, originate in the western Mediterranean while some develop near Cyprus (Alpert et al., 1990; Dayan et al., 2008). While moving over the warm Mediterranean waters, air-masses gain moisture, and facing the north-to-south directed mountain ridges cause intensive rainfall over the Levant (Sharon and Kutiel, 1986). The rainy season lasts from the end of October to early May, and 70% of the annual precipitation occurs between December and February (Karmon, 1994). The eastern Mediterranean trough is associated with a high pressure ridge expanding over Western Europe. Therefore, cold and wet winters in the Levant coincide with warm and dry winters over Western Europe and vice versa (Ziv et al., 2006). The wind system is less steady during winter than summer, too. Frequency and force of Mediterranean breezes are weaker in winter than summer due to the lower land-to-sea

temperature gradient. Westerlies do not reach the Jordan Rift Valley in winter. In contrary to summer, the study area is affected by southerly, south-westerly, and easterly winds (Bitan, 1974).

In Israel, latitude, altitude, and topographic conditions cause steep gradients in temperature and precipitation. The average annual temperature increases from less than 16°C in the north to approximately 23°C in the south (Fig. 3.4) (Zohary, 1962). Within a range of four degrees of latitude, average annual precipitation decreases from more than 1000 mm in the northern mountainous regions to approximately 25 mm in the southernmost part of Israel, the Negev desert (Fig. 3.5). Snowfall is unique to the northernmost part of the Golan Heigths. The summit of Mt. Hermon is snow-capped for about six month per year. The zonal distribution of precipitation is less regular than the meridional changes, caused by the topography (Zohary, 1982).

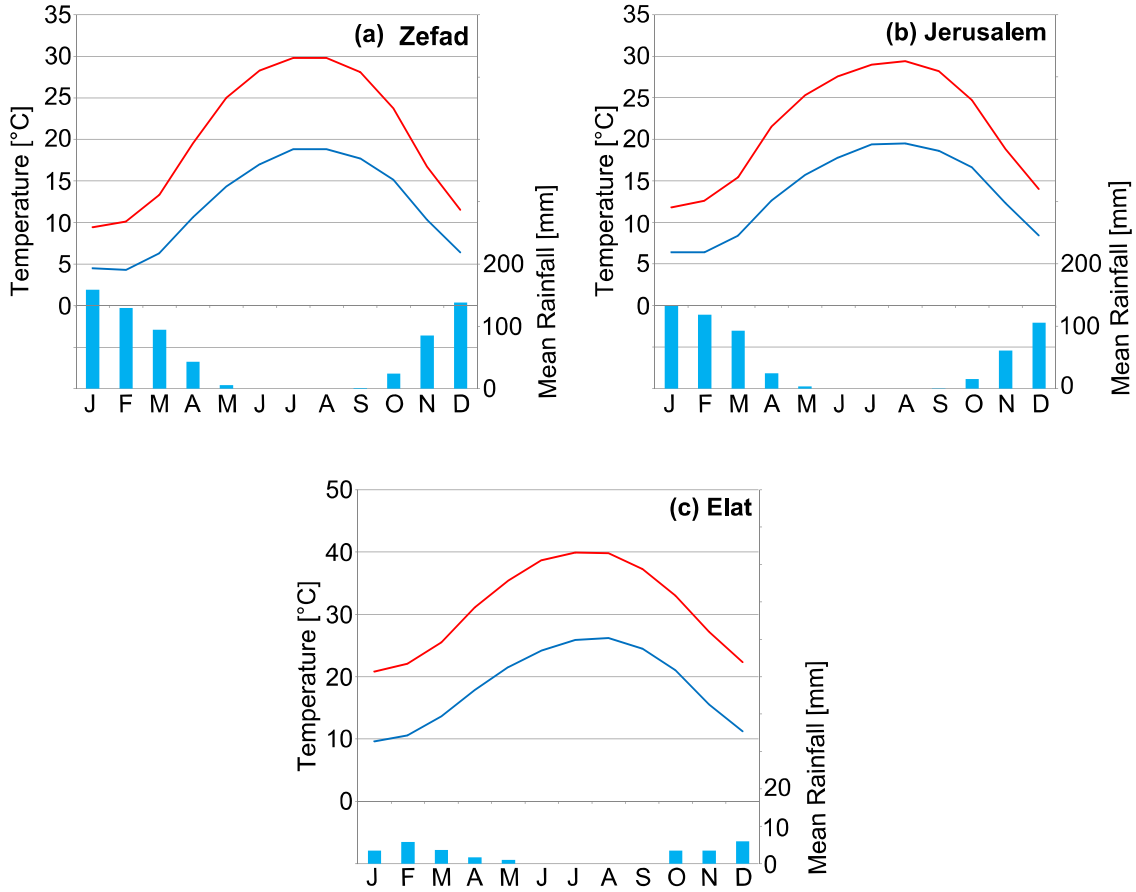

Fig. 3.4: Israeli climate diagrams based on data from Appendix 1; x-axis shows months from January to December; red line: mean maximum air temperature, blue line: mean minimum air temperature, blue bars: mean rainfall

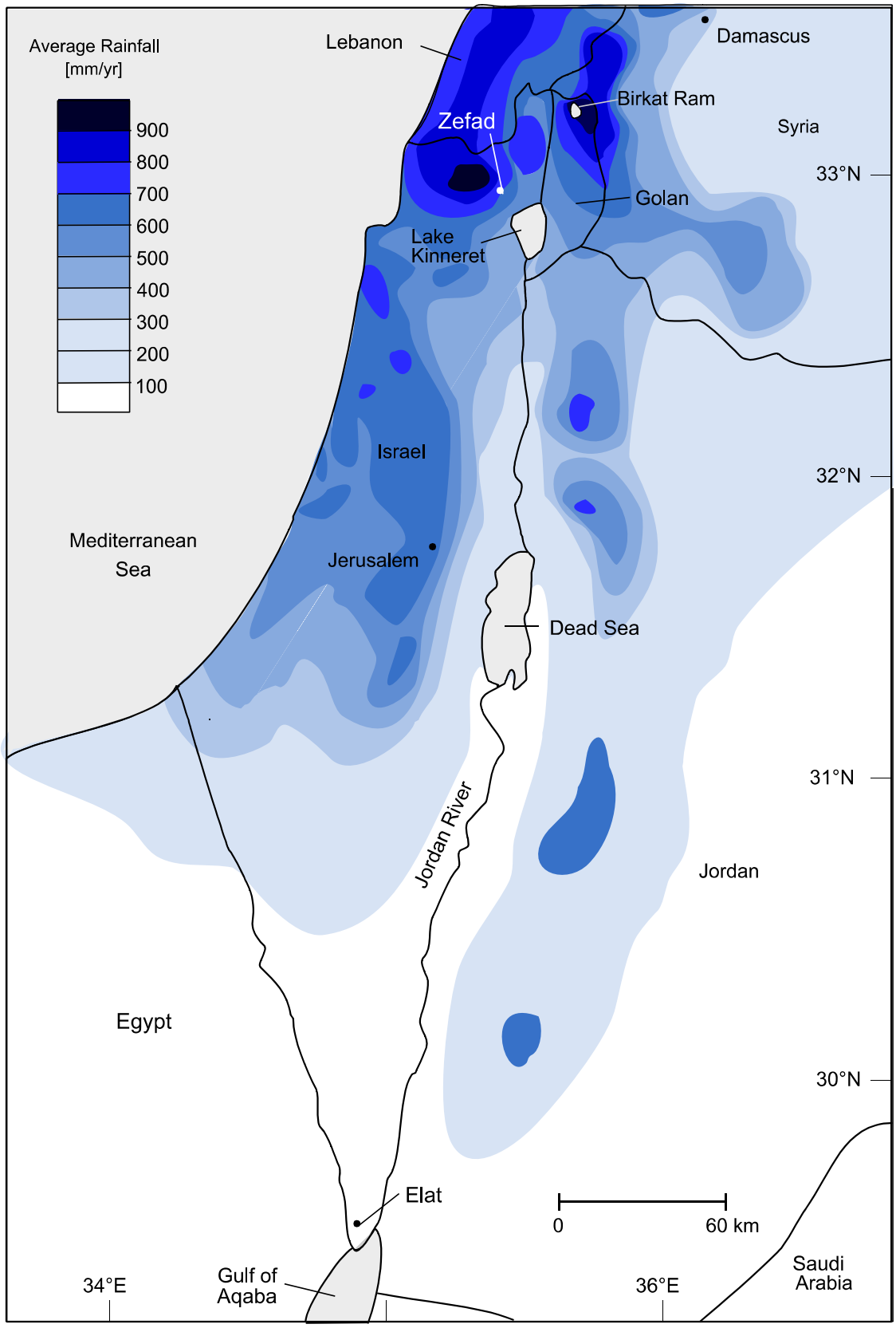

Fig. 3.5: Map of Israel and adjacent areas indicating mean annual precipitation in mm (after Jaffe, 1988)

3.4 Vegetation

3.4.1 Vegetation zones in Israel

Vegetation in Israel is exceptionally diverse due to its location in a climatic transition zone and its diversified orography. Danin and Plittman (1987) and Danin (1988) revised previous classifications of phyto-geographical regions (Eig et al., 1931; Zohary, 1962; Zohary, 1966) and subdivided the flora of Israel into seven vegetation zones, and assemblages of species with particular distributional areas:

1. Mediterranean (M) species, which are distributed around the Mediterranean Sea
2. Irano-Turanian (IT) species, which also inhabit Asian steppes of the Syrian Desert, Iran, Anatolia in Turkey, and the Gobi desert
3. Saharo-Arabian (SA) species, which also grow in the Sahara, Sinai, and the Arabian deserts
4. Sudano-Zambesian (S) species, typical of the subtropical savannahs of Africa.
5. Euro-Siberian species, also known in countries with a wetter and cooler climate than that of Israel; growing mainly in wet habitats, and along the Mediterranean coasts, and on the high-altitude slopes of Mount Hermon
6. Bi-regional, tri-regional, and multi-regional species that grow in more than one of the regions mentioned above
7. Alien species from remote countries. These plants propagate without human assistance. The principal countries of origin are the Americas, Australia, and South Africa. The percentage of aliens in the Flora Palaestina area is 5.7% of the entire flora (Danin, 2001)

The Mediterranean (M) territory (Danin, 1999; Eig et al., 1931) is dominated by macchia and batha vegetation. Predominant taxa are the summer-green oaks *Quercus ithaburensis* and *Quercus boisseri*, the evergreen oak *Quercus calliprinos*, as well as olive (*Olea europaea*). The distribution area of *Olea europaea* largely matches the Mediterranean territory (Walter and Straka, 1970). Further characteristic taxa are *Pistacia lentiscus*, *Arbutus andrachne*, *Ceratonia siliqua*, *Pinus halepensis* and *Sarcopoterium spinosum* (Danin, 1988; Zohary, 1982). Average precipitation exceeds 300mm per year. Characteristic taxa of the Irano-Turanian (IT) territory are *Artemisia herba-alba*, *Thymelea hirsute*, *Achillea santolina*, and some Poaceae and Chenopodiaceae (Danin, 1988; Zohary, 1982). Average annual precipitation ranges between 300 and 150mm. Characteristic taxa

of the Sudano-Arabian (SA) territory are Chenopodiaceae and Tamarisks (Zohary, 1982). The average precipitation is below 150mm/year. Sudano-Zambesian (S) taxa, which grow in oases along the Jordan Valley, are for example *Acacia*, *Balanites aegyptica*, and *Phoenix dactylifera* (Zohary, 1982). Danin (1988) further subdivides the vegetation zones by adding composite zones in the transitional areas. Composite zones are named after the most frequent zone in combination with the second most frequent in parentheses: M(M-IT), SA(M), SA(IT), SA(S), IT(S), IT(SA), S(SA). Regarding the studied area, the Mediterranean and the Irano-Turanian as well as composite zones are the relevant vegetation zones (Danin, 1988).

3.4.2 Regional distribution of vegetation zones

In general, the composition of the potential natural vegetation depends on climatic factors (e.g., temperature and precipitation), lithology, and soil. In the southern Levant, precipitation is the predominant limiting factor for the presence and growth of plant taxa. Human impact has affected vegetation since the Neolithic (Bar-Yosef, 1995; Rollefson and Köhler-Rollefson, 1992). Therefore, reconstructing the potential natural plant cover is rather complicated (Zohary, 1962). FigureFig. 3.6 outlines the distribution of the vegetation zones. The palynological archives located in the study area are affected by components of the Mediterranean and the Irano-Turanian vegetation zone.

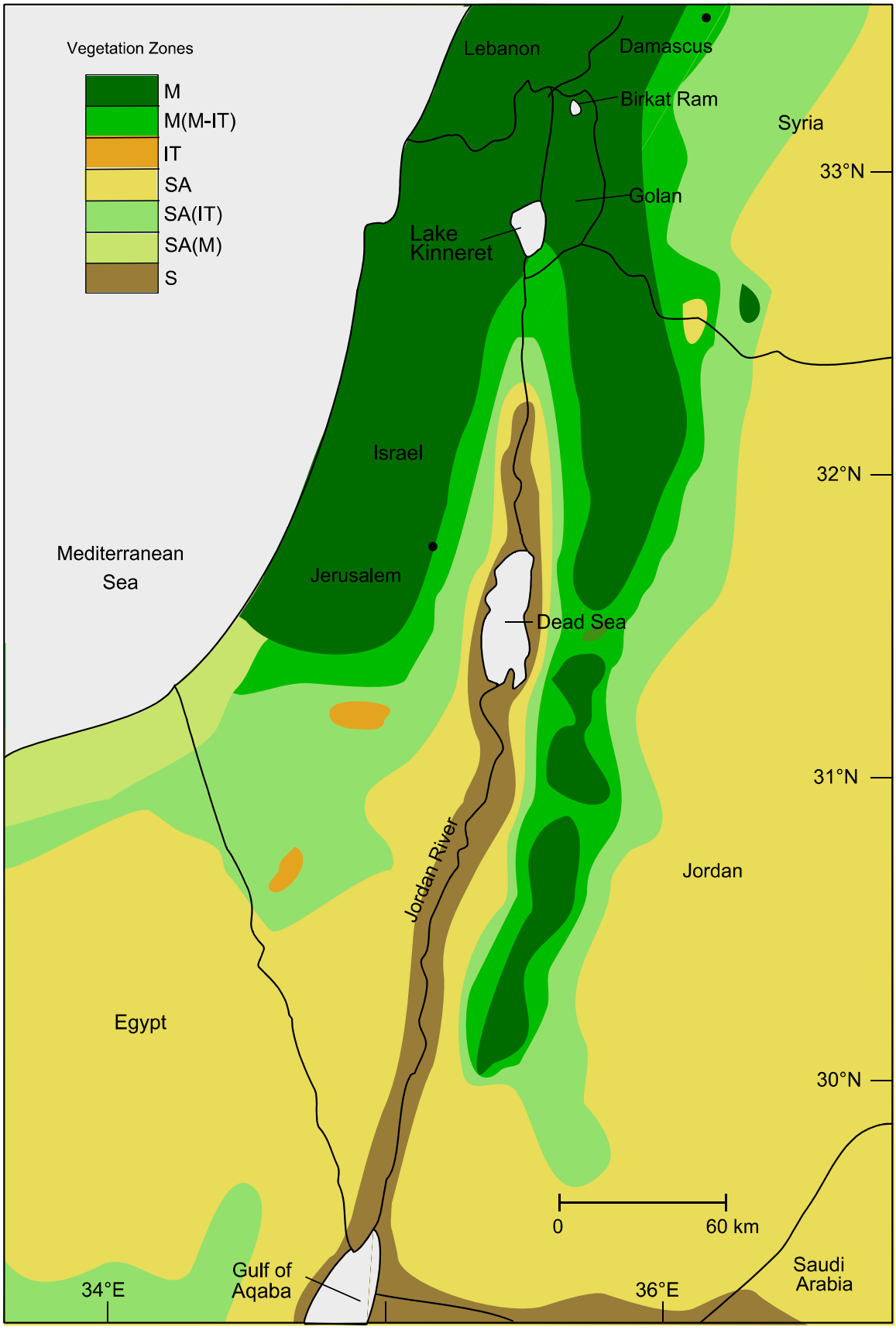

Fig. 3.6: Distribution of vegetation zones in Israel and adjacent areas; M = Mediterranean veg. zone; IT = Irano-Turanian veg. zone; SA = Saharo-Arabian veg. zone; S = Sudano-Zambesian veg. zone (after Danin, 1988)

3.4.2.1 The Mediterranean zone (M)

The Mediterranean woodland, macchia, and batha vegetation zone comprises areas that are characterised by an average precipitation >300mm/year, i.e. the coastal plains, the northern and the western Golan Heights, as well as the mountains of Judea, Carmel and Galilee (Danin, 1988; Zohary, 1982). The composition of taxa varies depending on elevation, topography and edaphic conditions. At elevations between 0 and 500 m amsl, deciduous oaks are the main element of the potential natural tree cover on sandy loam soil, Terra Rossa, Dark Rendzina, and basalt. Sparsely scattered patches of *Quercus ithaburensis* are modern remnants of formerly more widespread open-forest dispersal, diminished by deforestation (Shmida, 1980). Arboreal companions are for example *Pistacia palaestina*, different Rhamnaceae, and *Ziziphus spina-christi*. The Aleppo pine (*Pinus halepensis*) populates the lower elevations of the Upper Galilee mountain range on marly, chalky bedrock covered with Light Rendzina soil (Danin and Plitmann, 1987; Weinstein, 1989). Areas between tree and shrub patches are covered by grasses, for example wild wheat (*Triticum dicoccoides*), wild barley (*Hordeum spontaneum*), and wild oat (*Avena sterilis*), as well as some herbaceous taxa and semi-shrubs, as various Cistaceae species, and *Sarcopoterium spinosum* (Danin, 1988).

Lower elevations from 0 to 300 m amsl in combination with limestones, as the coastal plains and the western foot of Upper Galilee, are dominated by evergreen olive (*Olea europaeae*), pistachio (*Pistacia lentiscus*), and carob tree (*Ceratonia siliqua*). Habits are primarily shrub-like, and well-developed trees are rare. These taxa are well adapted to heat but sensitive to cold temperatures (van Zeist and Bottema, 1991). *Olea europaea* requires a mean minimum temperature of the coldest month of more than 6°C (Rubio de Casas, 2002) and constitutes an important part of the natural Mediterranean vegetation (Baruch and Bottema, 1999). Evidence for olive cultivation is found since the beginning of the Chalcolithic period 6,500 cal BP (Neef, 1990; Zohary and Hopf, 1988). The shrub associations are accompanied by Mediterranean semi-shrubs and herbaceous vegetation, as for example *Sarcopoterium spinosum*, and different rockroses (*Cistus salvifolius*, *Cistius creticus*).

Mountainous territories between 500 m and 1200 m amsl are dominated by evergreen oaks (*Quercus calliprinos*). In the Upper Galilee, the most humid area of Israel, evergreen oaks grow on Terra Rossa soils and are accompanied by different buckthorns (*Rhamnus lycioides*, *R. alaternus*, *R. punctata*), whitethorns (*Crataegus azarolus*, *C. monogyna*),

Styrax officinalis, *Phyllirea media*, as well as many semi-shrubs, as for example *Sarcopoterium spinosum*, and herbaceous species, (e.g., *Fumana arabica*) and different Cistaceae (Danin, 1988; van Zeist and Bottema, 1991). On the volcanic substrates on the Golan Heights, a dense macchia of *Quercus calliprinos* is accompanied by *Pistacia palaestina*, *Quercus boisseri*, *Crataegus monogyna*, *C. aronia*, and *Prunus ursine* (Danin, 1988; Zohary, 1972). The interspaces between patches of trees and shrubs are covered by vast assemblages of ephemeral herbaceous vegetation. The composition of the vegetation at the highest elevations at the Mount Hermon (1300-1800 m amsl) is named "Oro-Mediterranean" by Danin and Plitmann (1987). Characteristic arboreal taxa are for example *Quercus boisseri*, *Q. libani*, and *Juniperus drupacea*, accompanied by perennial and annual grasses, and semi-shrubs. The montane forest vegetation tolerates low temperatures and strong winds.

3.4.2.2 The Irano-Turanian zone (IT)

Characteristic taxa of the Irano-Turanian zone require an average precipitation of 150-300 mm/year (Zohary, 1982). Within the IT assemblage, plant habits are largely dwarf-shrubby (van Zeist and Bottema, 1991). Predominant taxa are several species of the aster family (Asteraceae), for example *Artemisia herba-alba*, accompanied by different Ephedraceae, and *Achillea santolina* (Danin, 1988; Zohary, 1962; Zohary, 1982). After Zohary (1962), the IT assemblage occupies a rather narrow strip east and south of the Mediterranean vegetation zone on Israel territory, and on Jordanian territory it encircles the Mediterranean vegetation from south, east, and west. Danin and Plitmanns (1987) plant geographical map distinguishes a distinct IT area in the Judean Mountains and describes a transitional zone, i.e. M(M-IT), along the boundary of the Mediterranean territory. Neither the Saharo-Arabian (SA) nor the Sudano-Zambesian (S) vegetation zones affect the composition of pollen assemblages deposited in the sediments of Lake Kinneret and Birkat Ram.

3.5 Coring Sites

3.5.1 Lake Kinneret

Lake Kinneret (Fig. 3.1) also known as the Sea of Galilee or Lake Tiberias is a hard-water lake located in the northeast of Israel. It is a relic of different-sized water bodies, which filled the tectonic depressions along the Dead Sea Transform Fault (DST) since the Neogene (Hazan et al., 2005). The modern Lake Kinneret occupies one of a series of pull-

apart basins along the DST. At a lake level of 211 m below mean sea level (bmsl), the central basin is 43 m deep. The maximum length of the lake is 21 km (N-S), its maximum width is 12 km (W-E). Lake Kinneret's surface spans 166 m^2, containing a water body of $4.1x10^6$ m^3. The lake is monomictic, and stratification lasts from mid-March to late December (Nishri et al., 1999). The catchment area encompasses 2760 m^2. Approximately two-thirds of the inflow, i.e. $477x10^6$ m^3/year derive from the Jordan River, and one-third originates from minor sources, i.e. other streams and seasonal floods (16%), direct rainfall (9%), and subaqueous springs (8%). Average precipitation over the Lake Kinneret area is 400 mm per year, and evaporation amounts to $250x10^6$ m^3/year (±10%) (Stiller, 2001; Stiller et al., 1988). Between 1970 and 1995, the residence time of water was 5.5 years on average (Nishri et al., 1999). Adjacent to the shoreline, steep slopes elevate up to a difference in altitude of about 450 m west of the lake, and almost 600 m eastward. Limited sections of the north-western and north-eastern shorelines, as well as the Jordan River mouth in the south form broad plains (Bitan, 1981).

3.5.2 Birkat Ram

The maar lake Birkat Ram (Fig. 3.1) is located in the northern Golan Heights at 940 m amsl about 80 km north-east of Haifa. It developed as a result of Pleistocene volcanic and tectonic activities (Ehrlich and Singer, 1976). Birkat Ram's origin is dated at 129,000 years BP by Shaanan (2011). The lake's characteristics are an average surface of 0.45 km^2 , a maximum length of 900 m, and a maximum width of 650 m. Water depth seasonally ranges between 6 m and 12 m, and includes fluctuations of water volume between $1.41x10^6$ m^3 and $5.1x10^6$ m^3 (Singer and Ehrlich, 1978). Precipitation over Birkat Ram is 1042 mm/year on average, and is the main water-source of the lake together with local run-off. The drainage area spans 1.5 km^2. Minor inflow is contributed by some subaquatic springs. Total annual input of 2.1 $x10^6$ m^3 is largely balanced by evaporation and seepage (Ehrlich and Singer, 1976). The modern lake is eutrophic and anoxic (Singer and Ehrlich, 1978).

4 Material and methods

4.1 Coring campaign

Sediment cores were obtained during a drilling campaign in March 2010, as part of SFB 806 “Our Way To Europe”, funded by the Deutsche Forschungsgemeinschaft (DFG). A UWITEC Universal Sampling Platform (http://www.uwitec.at) was employed, and drilling was carried out using a gravity corer to recover short cores, and a piston corer to obtain long cores. Either of the tools were produced by UWITEC. Plastic liners with a length of 2m, and diameters of 90 mm or 60 mm were used. Sediment cores were opened at the Steinmann Institute in Bonn. One half of each core-segment was used for non-destructive analyses, and archived subsequently, and the other half was sampled for palynological analyses.

4.2 Lake Kinneret

The Lake Kinneret coring site at 32°49’13.8”N, 35°35’19.7”E, is located in the very central lake basin at a water depth of 38.8 m (Fig. 3.1). Two parallel cores Ki I (13.3 m recovery), and Ki II (17.8 m recovery) were taken at a distance of 2 m. A 17.8m-composite profile was developed (Appendix 2 and Fig. 4.2). The upper 25 cm of the sediment core are varved (Fig. 4.1). The varves are assumed to have formed after damming of the natural outflow by the National Water Carrier in 1964 (Nishri, Ami, personal communication). Below, sediment cores consist of homogenous greyish to brown silts to clays. No major changes in appearance, colour, and texture were found (Appendix. 3). For detailed description of the core segments see Appendix 5 after Rüßmann (2010).

Fig. 4.1: Lake Kinneret; core segment Ki10_V1_top, uppermost 25 cm laminated sediments; scale unit [cm]

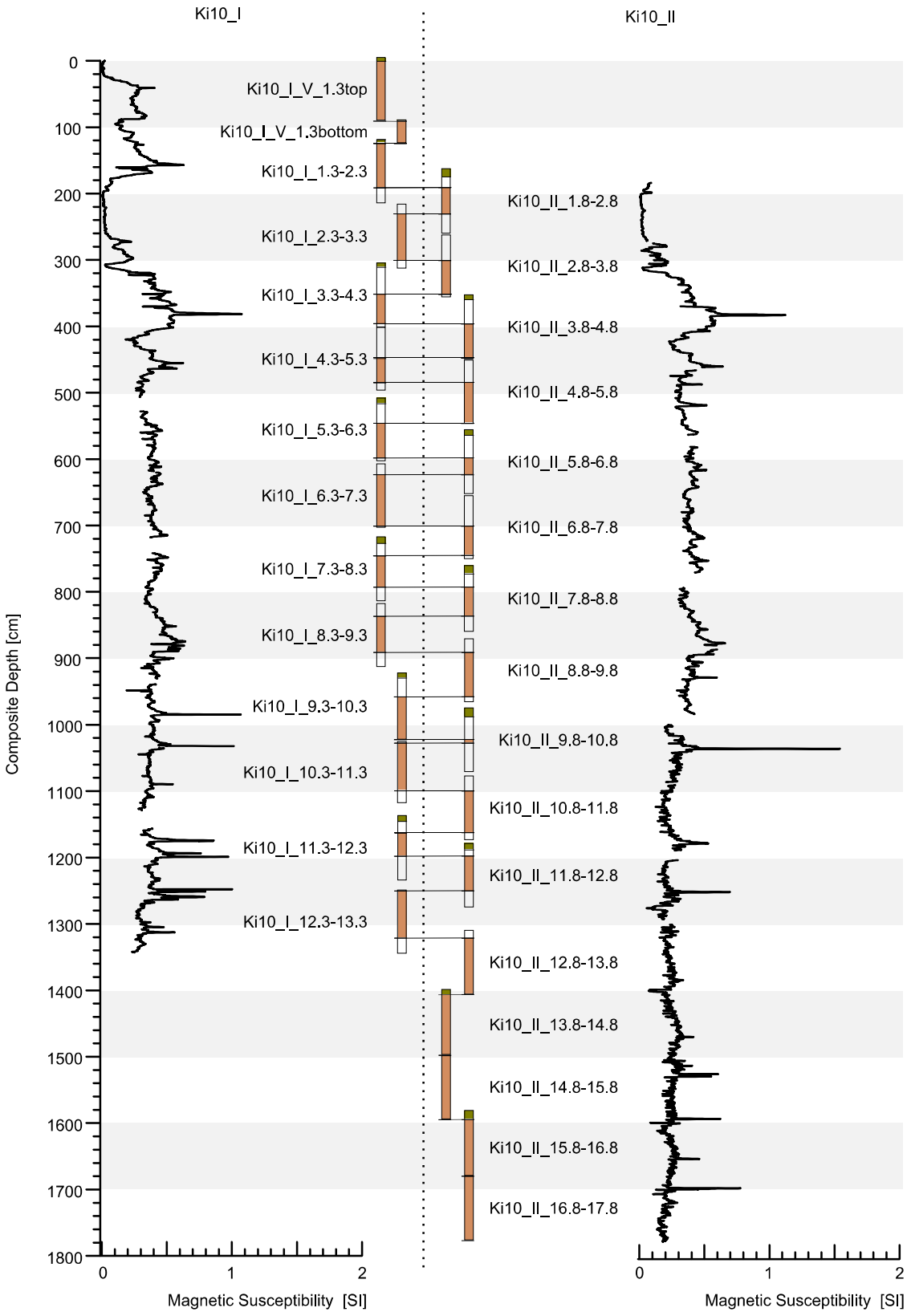

Fig. 4.2: Lake Kinneret; composite profile of parallel cores based on correlation of magnetic susceptibility; in beige sections constituting master section of composite profile, in green core filling compound

4.2.1 Methods applied

4.2.1.1 Magnetic susceptibility

High resolution magnetic susceptibility data were produced at the Institute of Geology and Mineralogy at the University of Cologne, and were used to correlate the parallel cores, and to define the composite profile (Fig. 4.2). Measurement on longitudinally split core surface was carried out using a spot-reading Bartington MS2E sensor. Response area of the sensor is 3.8 mm x 10.5 mm, and the operating frequency was 2 kHz. At a vertical depth of 1 mm, response is reduced by approximately 50%, and reduction at a depth of 3.5 mm is approximately 90% (Bartington-Instruments-Limited, 1995). Data were measured at 1mm intervals, and measurement period was 15 seconds.

4.2.1.2 Palynological analysis

Sediment cores were sampled for palynological analyses at 25 cm intervals (Appendix 6). Average sample volume was approximately 5 cm^3. One *Lycopodium* tablet (Batch 483216, Department of Quaternary Geology, University of Lund) containing a defined number of spores was added to each sample to calculate absolute pollen concentration (Stockmar, 1971). Subsequently, chemical treatment followed the standard procedure according to Faegri and Iversen (1989), including application of [HCl] (10%), [KOH] (10%), [HF] (40%), and acetolysis ([$C_4H_6O_{3(conc.)}$], and [$H_2SO_{4(conc.)}$], ratio 9:1). Sieving was carried out two times during the procedure (mesh widths: 200 µm and 10 µm, ultrasonic sieving). Samples were stained with safranine and stored on glycerol. At least 500 pollen grains per sample were counted using transmitted-light microscopy (Leica DME, ZEISS Lab.A1 AX10, 400 x magnification). Pollen grains were identified to the highest possible systematic level. The extensive comparative collection of palynomorphs available at the Department of Paleobotany at the Steinmann-Institute (University of Bonn) was utilised as reference for identification. In addition, different textbooks of circum-Mediterranean pollen grains (Beug, 2004; Moore et al., 1991; Reille, 1990-1999) were used. Pollen diagrams (Fig. 5.1 and Appendix 10) were plotted with Tilia software (version 1.7.14 by Eric Grimm, (2011) Illinois State Museum, Springfield). Borders between local pollen assemblage zones (LPAZ) were defined visually. Data were approved by applying a constrained cluster analysis (CONISS) (Grimm, 1987) (see Appendix 10).

4.2.1.3 AMS radiocarbon dating

Six macrofossil remains of terrestrial plants and 16 samples of bulk organic material were radiocarbon dated utilising Accelerator Mass Spectrometry (AMS) (Table 4.1). The

measurements were operated at the "Leibniz-Laboratory for Radiometric Dating and Isotope Research" in Kiel (5 macrofossils, 14 bulk samples), and at "Beta Analytic Radiocarbon Dating" in London (1 macrofossil, 2 bulk samples). Pre-treatment of macrofossils included dispersion of samples in deionised water, and elimination of mechanical contaminants such as associated sediments. Subsequently, hot HCl-washes were applied to eliminate carbonates, and alkali-washes (NaOH) were applied to remove secondary organic acids. Each solution was neutralised prior to the subsequent procedure. Bulk sample sediments were dispersed in deionised water, and repeatedly treated with HCl at 60° C to remove carbonates. Remaining carbon from each sample was burned at 900° C in a quartz ampoule filled with copper oxide (CuO) and silver wool. Obtained CO_2 was reduced to graphite ($C_{(conc.)}$) at 600° C, and subsequently detected in an accelerator mass spectrometer. ^{14}C concentrations are results of comparisons of the measured ^{14}C, ^{13}C, and ^{12}C contents with the concentrrations of the CO_2-references (oxalic acid II). Data were corrected for isotopic fractionation using the simultaneously measured $^{13}C/^{12}C$-ratio which includes effects occurring during graphitisation and within AMS-processes. ^{14}C-ages were calculated after Stuiver and Polach (1977) (Table 4.1). Age-to-depth models (Fig. 4.3 and Fig. 4.4) were developed using "clam"-software (Blaauw, 2010), which is a component of the open-source statistical environment "R" (Development-Core-Team, 2011). ^{14}C ages were calibrated in clam, basing on the IntCal09 calibration curve (Reimer, 2009). Data were operated on a 95% confidence interval (2σ), and intermediate values were established by linear interpolation between dated levels.

Table 4.1: Lake Kinneret; AMS ^{14}C data, computed reservoir corrections printed in bold type

Lab ID	Composite Depth [cm]	Age [14C years BP]	cal BP	Processed in	Material	Applied Reservoir correction [yrs] / Age-to-Depth Model I	Applied Reservoir correction [yrs]/ Age-to-Depth Model II
KIA48028	97.0	1470 +/- 35	1356 +/- 53	Kiel	bulk sediment	469	469
KIA48029	199.0	2175 +/- 30	2264 +/- 48	Kiel	bulk sediment	582	582
KIA48030	304.0	2670 +/- 25	2773 +/- 26	Kiel	bulk sediment	701	701
Beta-327805	358.0	2990 +/- 30	3171 +/- 95	London	bulk sediment	**835**	**835**
KIA44213	359.5	2155 +/- 25	2120 +/- 62	Kiel	plant remains	0	0
KIA48031	394.0	3275 +/- 30	3508 +/- 66	Kiel	bulk sediment	802	802
KIA48032	495.0	3545 +/- 30	3858 +/- 52	Kiel	bulk sediment	915	915
KIA48033	605.0	4515 +/- 35	5124 +/- 77	Kiel	bulk sediment	1040	1040
KIA48035macro	794.0	3800 +/- 45	4190 +/- 109	Kiel	plant remains	0	0
KIA48035	794.0	4765 +/- 30	5527 +/- 62	Kiel	bulk sediment	**965**	**965**
Beta-336208	921.0	4230 +/- 30	4831 +/- 24	London	plant remains	0	0
Beta-327806	943.5	5800 +/- 40	6585 +/- 92	London	bulk sediment	**1635**	**1635**
KIA44214	945.0	4165 +/- 40	4674 +/- 99	Kiel	plant remains	0	0
KIA44215	946.5	4100 +/- 25	4587 +/- 64	Kiel	plant remains	0	0
KIA48037	992.0	5900 +/- 40	6719 +/- 80	Kiel	bulk sediment	1635	1475
KIA44216	993.0	5870 +/- 60	6665 +/- 134	Kiel	plant remains	0	0
KIA48038	1093.0	6655 +/- 45	7525 +/- 67	Kiel	bulk sediment	1635	1589
KIA48039	1181.0	7145 +/- 50	7982 +/- 67	Kiel	bulk sediment	1635	1688
KIA48041	1378.0	7700 +/- 40	8483 +/- 73	Kiel	bulk sediment	1635	1910
KIA48042	1472.0	8480 +/- 45	9489 +/- 48	Kiel	bulk sediment	1635	2016
KIA48043	1572.0	8860 +/- 45	9970 +/- 202	Kiel	bulk sediment	1635	2128
KIA48045	1778.0	9805 +/- 45	11223 +/- 55	Kiel	bulk sediment	1635	2359

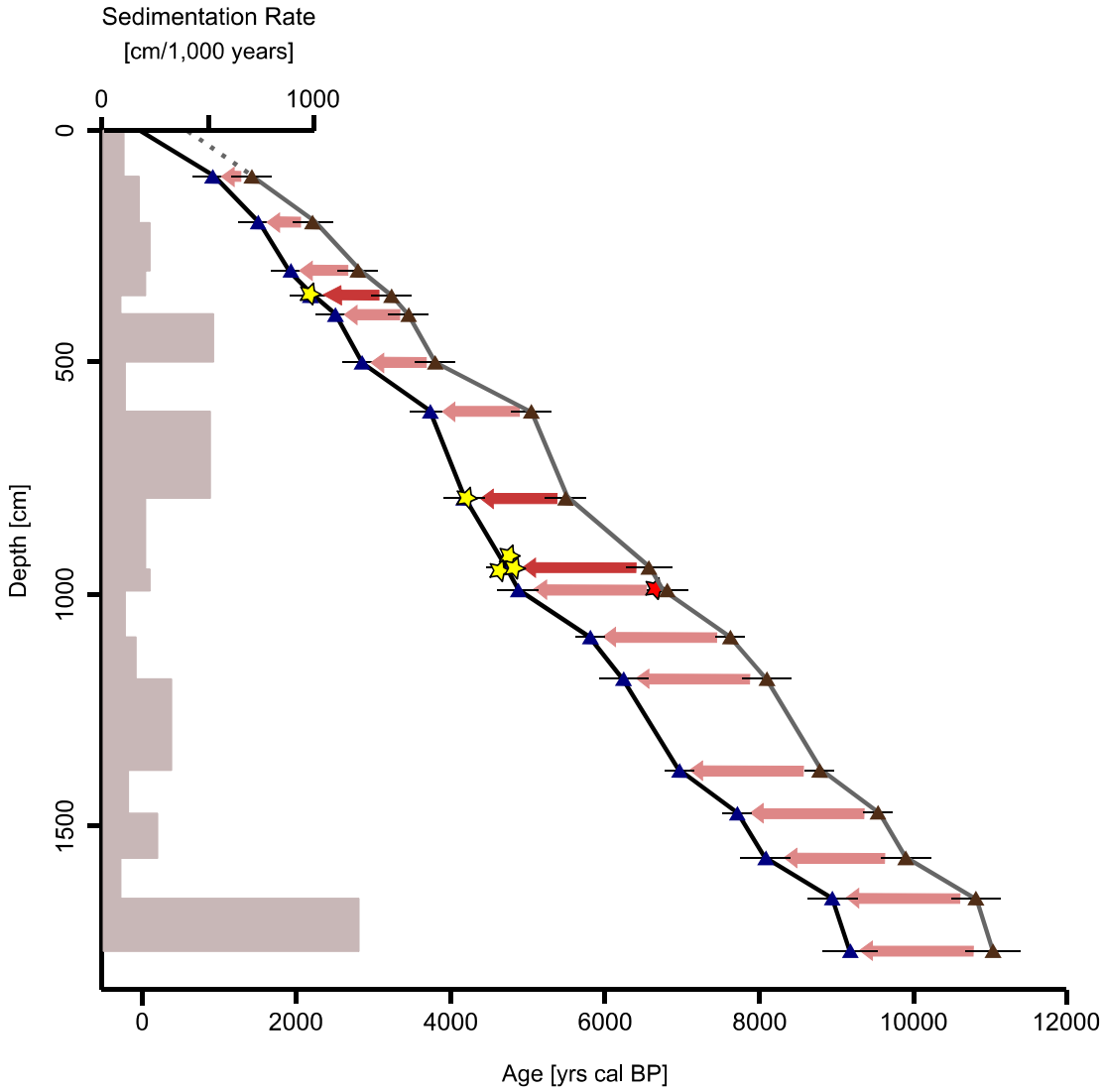

Fig. 4.3: Lake Kinneret; age-to-depth model I of composite profile based on calibrated radiocarbon data (Table 4.1); yellow stars indicate data from terrestrial plant remains, red star indicates data of probably reworked terrestrial plant remain, brown triangles indicate data from bulk organic material, blue triangles indicate data from bulk organic material corrected for reservoir effects, error bars indicate 2 σ-range, dark red arrows indicate computed reservoir correction at depth horizons with available macro and bulk organic sample, light red arrows indicate interpolated reservoir correction at depth horizons with only bulk organic samples available, below lowermost dark red arrow constant correction is applied, for detailed discussion of reservoir effects see chapter 5.1.2; grey bars show sedimentation rates in cm per 1000 years

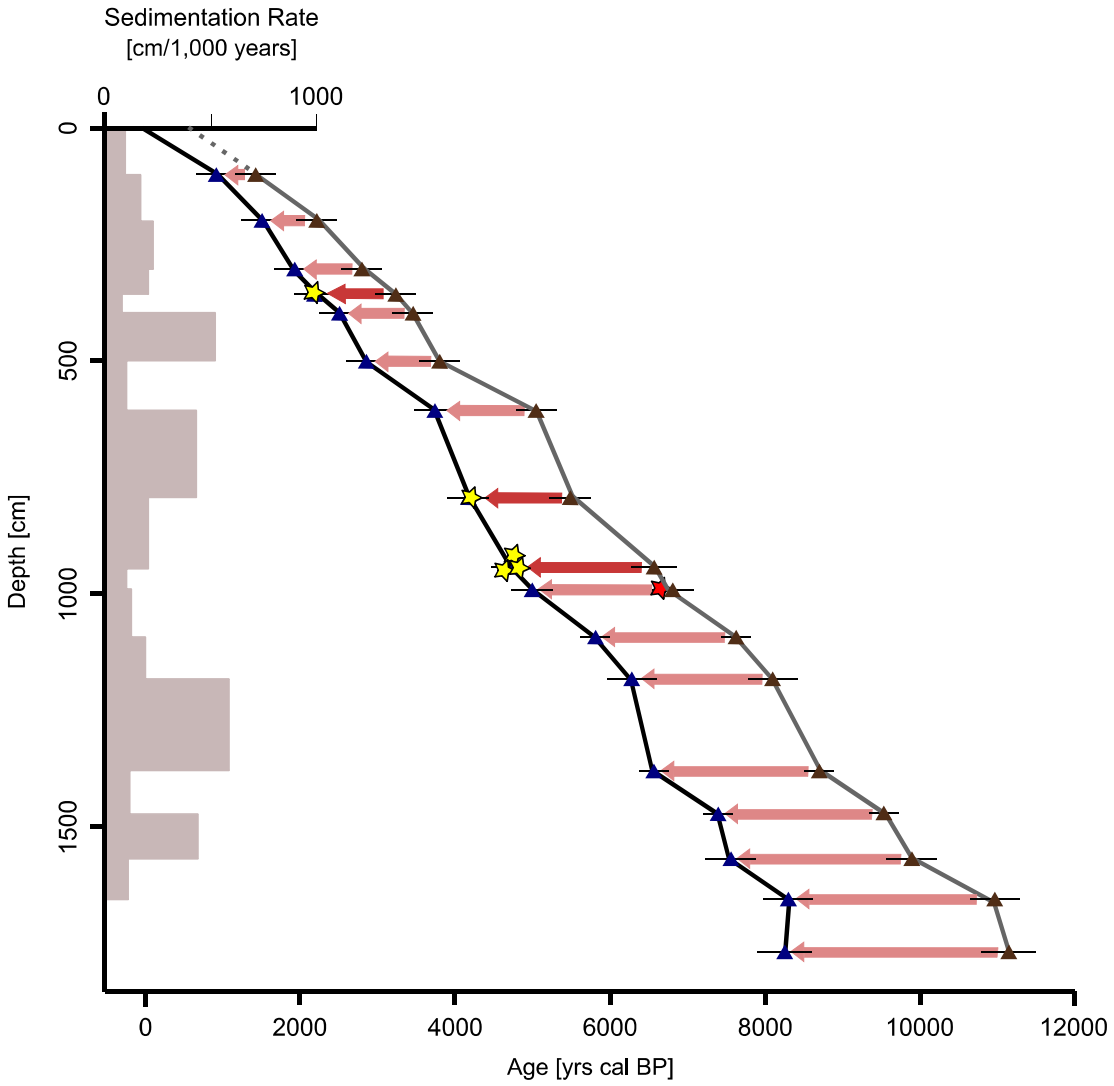

Fig. 4.4: Lake Kinneret; age-to-depth model II of composite profile based on calibrated radiocarbon data (Table 4.1); yellow stars indicate data from terrestrial plant remains, red star indicates data of probably reworked terrestrial plant remain, brown triangles indicate data from bulk organic material, blue triangles indicate data from bulk organic material corrected for reservoir effects, error bars indicate 2 σ-range , dark red arrows indicate computed reservoir correction at depth horizons with available macro and bulk organic sample, light red arrows indicate increasing interpolated reservoir correction at depth horizons with only bulk organic samples available, approximated by the linear equation y = 1.1259x + 358.39, for detailed discussion of reservoir effects see chapter 5.1.2; grey bars show sedimentation rates in cm per 1000 years

4.3 Birkat Ram

The Birkat Ram sampling site is located at 33°13’54.3”N, 35°46’1.4”E (Fig. 3.1). Water depth was 14.5 m. Core recovery at location BR I was 10 m, and at location BR II, recovery was 11.5 m. Distance between the sites was 2 m. A 10.96 m-composite profile was produced (Appendix 7 and Fig. 4.6). Sediments consist of silty fine sand and clay. Sporadically, fine gravel layers are interspersed. Between 4 m and 6 m core depth, sediments are dark brown. Above and below, colour is greyish to brown (Appendix 4). For detailed description of the core segments see Appendix 8 after Rüßmann (2012) and Geiger (2011). Between 732 cm and 756 cm composite core depth, several oxidised root cast fragments occurred (Fig. 4.5).

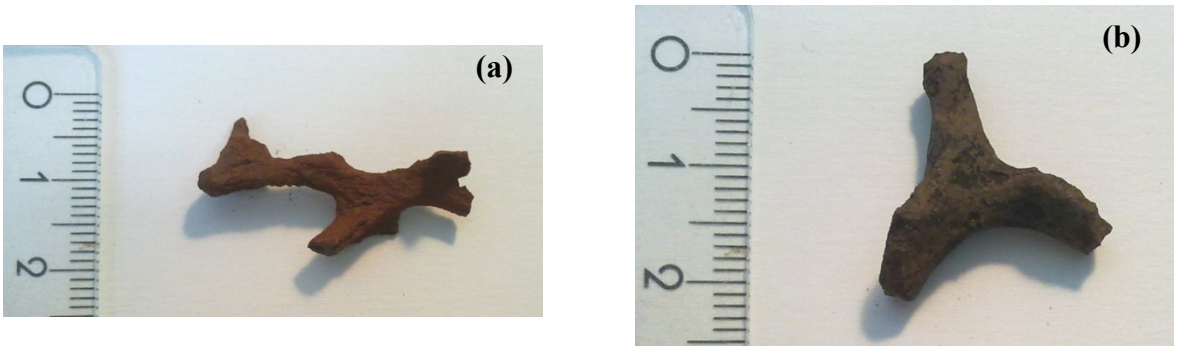

Fig. 4.5: Birkat Ram; oxidised root cast fragments; extracted from BR10_I_7-8 at (a) 733 cm, and (b) 745 cm composite core depth; scale unit [cm]

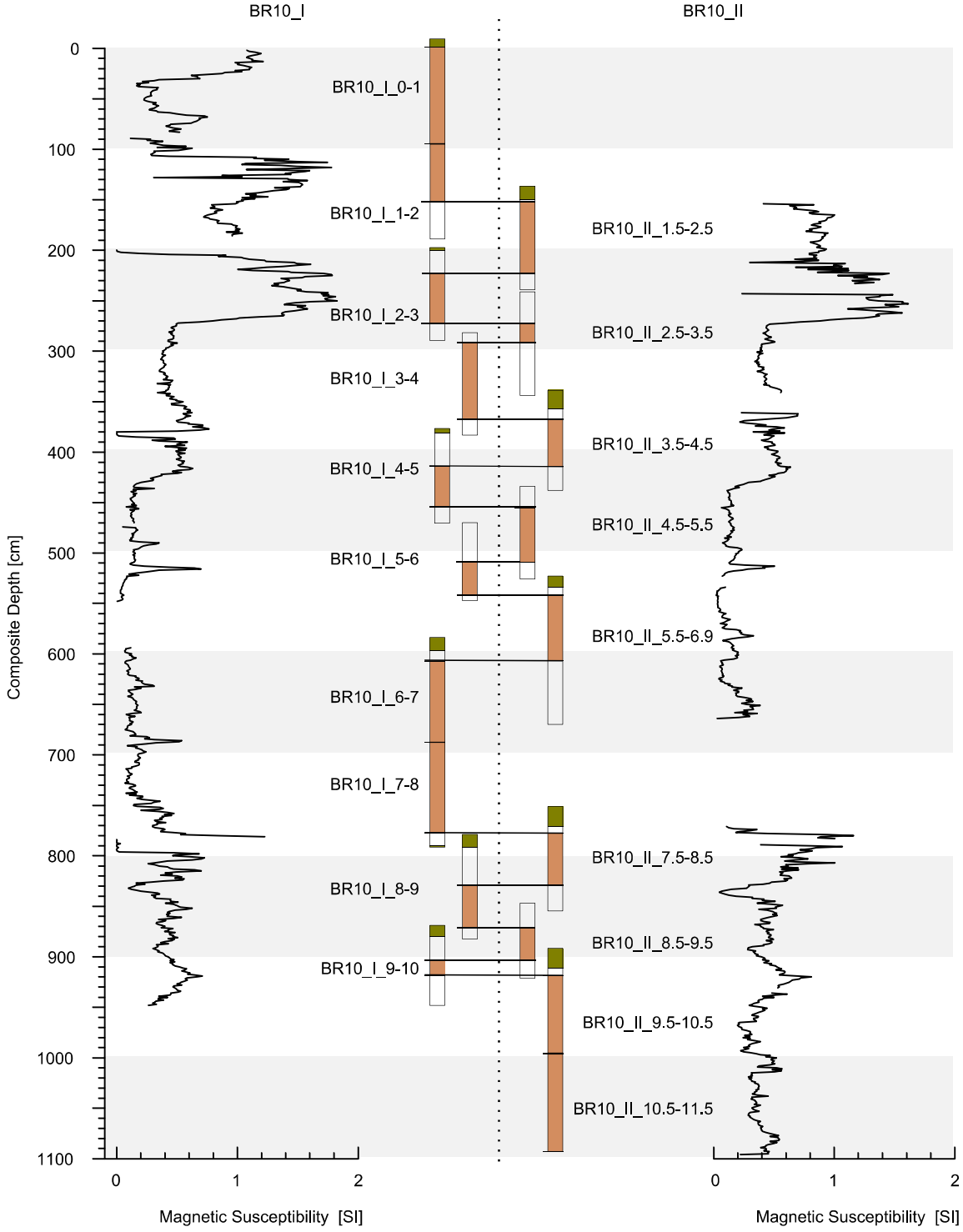

Fig. 4.6: Birkat Ram; composite profile of parallel cores based on correlation of magnetic susceptibility; in beige sections constituting master section of composite profile, in green: core filling compound

4.3.1 Methods applied

4.3.1.1 Magnetic susceptibility

From Birkat Ram sediment cores, high resolution magnetic susceptibility data were produced at the Institute of Geology and Mineralogy at the University of Cologne. Cores were scanned utilising a Bartington MS2E sensor, implemented in a GEOTEK (UK) Multi-Sensor Core Logger. Data were measured at 1 cm intervals. For details about Bartington MS2E see chapter 4.2.1.1. Magnetic susceptibility data of the parallel cores were correlated to identify reference layers, and a composite profile was defined (Fig. 4.6).

4.3.1.2 Palynological analysis

Sampling of Birkat Ram sediment cores for palynological analysis was carried out at 25cm intervals. In the segment between 6.25 m and 7.75 m, samples were taken each 5 cm to get more detailed information on the interval, which is assumed to include the Pleistocene-to-Holocene transition (Appendix 9). Average sample volume was $5cm^3$. The samples were treated in exactly the same way as the Lake Kinneret samples (chapter 4.3.1.2). Pollen diagrams are shown in Fig. 5.3 and in Appendix 11. Manually established borders of local pollen assemblage zones (LPAZ) were verified by a constrained cluster analysis (CONISS) (Grimm, 1987) (see Appendix 11).

4.3.1.3 AMS radiocarbon-dating

Four terrestrial plant macrofossils, two samples containing macro remains from water plants (*Potamogeton*, *Ranunculus aquatilis*, *Zanichellia palustris*), and six samples containing bulk organic material were extracted from the Birkat Ram sediment cores, and were radiocarbon dated (AMS) (Table 4.2). All measurements were executed at "Beta Analytic Radiocarbon Dating", London. In addition, two radiocarbon dates from terrestrial macrofossils, twelve radiocarbon dates from water plant macrofossils, and four radiocarbon dates from bulk organic material were adopted from another sediment core recovered in 1999 at Birkat Ram (Neumann et al., 2007a; Schwab et al., 2004) (Table 4.3). For details concerning sample treatment, measurement procedures, and tools used for the development of the age-to-depth model see chapter 4.2.1.3. The age-to-depth model is shown in figure Fig. 4.7.

Table 4.2: Birkat Ram; AMS ^{14}C data

Lab ID	Composite Depth [cm]	Age [14C years BP]			cal BP			Processed in	Material	Applied Reservoir Correction [yrs]
Beta-327807	537	7260	+/-	40	8086	+/-	85	London	bulk sediment	no corr. applied
Beta-327808	635	11600	+/-	60	13462	+/-	167	London	bulk sediment	no corr. applied
Beta-337247	703	9110	+/-	40	10251	+/-	50	London	water plant remains	600
Beta-327809	736	13480	+/-	50	16629	+/-	251	London	bulk sediment	no corr. applied
Beta-331274	746	14140	+/-	50	17225	+/-	295	London	plant remains	0
Beta-327810	836	19720	+/-	80	23580	+/-	313	London	bulk sediment	no corr. applied
Beta-327811	936	21330	+/-	80	25478	+/-	393	London	bulk sediment	no corr. applied
Beta-327900	938	21130	+/-	90	25262	+/-	339	London	plant remains	0
Beta-337249	1009	24250	+/-	100	29016	+/-	426	London	water plant remains	600
Beta-337250	1046	25080	+/-	100	29906	+/-	351	London	plant remains	0
Beta-337251	1061	21980	+/-	90	26422	+/-	394	London	plant remains	0
Beta-327812	1089	24860	+/-	140	29812	+/-	387	London	bulk sediment	no corr. applied

Table 4.3: Birkat Ram; AMS ^{14}C data from Birkat Ram profile, cored in 1999 (after Neumann et al., 2007a; Schwab et al., 2004)

Lab ID	Composite Depth [cm]	Age [14C years BP]	cal BP	Processed in	Material	Applied Reservoir Correction [yrs]
Poz-639	49.5	800 +/- 30	710 +/- 35	Poznan	water plant remains	600
Poz-637	99.5	1260 +/- 30	1229 +/- 62	Poznan	water plant remains	600
Poz-634	99.5	1141 +/- 30	1030 +/- 60	Poznan	water plant remains	600
Poz-633	100.5	1210 +/- 30	1122 +/- 63	Poznan	water plant remains	600
KIA-11666	105.5	980 +/- 45	877 +/- 88	Kiel	water plant remains	600
Poz-3293	144.5	1755 +/- 30	1651 +/- 86	Poznan	water plant remains	600
Poz-3261	144.5	1780 +/- 30	1750 +/- 65	Poznan	water plant remains	600
Poz-3292	144.5	2435 +/- 30	2448 +/- 94	Poznan	bulk sediment	no corr. applied
Poz-3294	198.5	3555 +/- 30	3872 +/- 55	Poznan	bulk sediment	no corr. applied
Poz-3401	247.5	3580 +/- 30	3902 +/- 74	Poznan	bulk sediment	no corr. applied
KIA-11667	317.0	2685 +/- 30	2799 +/- 47	Kiel	plant remains	0
Poz-638	321.5	2600 +/- 30	2741 +/- 30	Poznan	plant remains	0
Poz-3295	323.5	3700 +/- 30	4034 +/- 66	Poznan	bulk sediment	no corr. applied
Poz-636	355.0	3180 +/- 35	3410 +/- 57	Poznan	water plant remains	600
Poz-641	400.5	4140 +/- 35	4697 +/- 128	Poznan	water plant remains	600
Poz-640	456.0	5440 +/- 35	6243 +/- 53	Poznan	water plant remains	600
Poz-3296	505.0	5980 +/- 40	6832 +/- 106	Poznan	water plant remains	600
Poz-642	533.0	6070 +/- 35	6927 +/- 85	Poznan	water plant remains	600

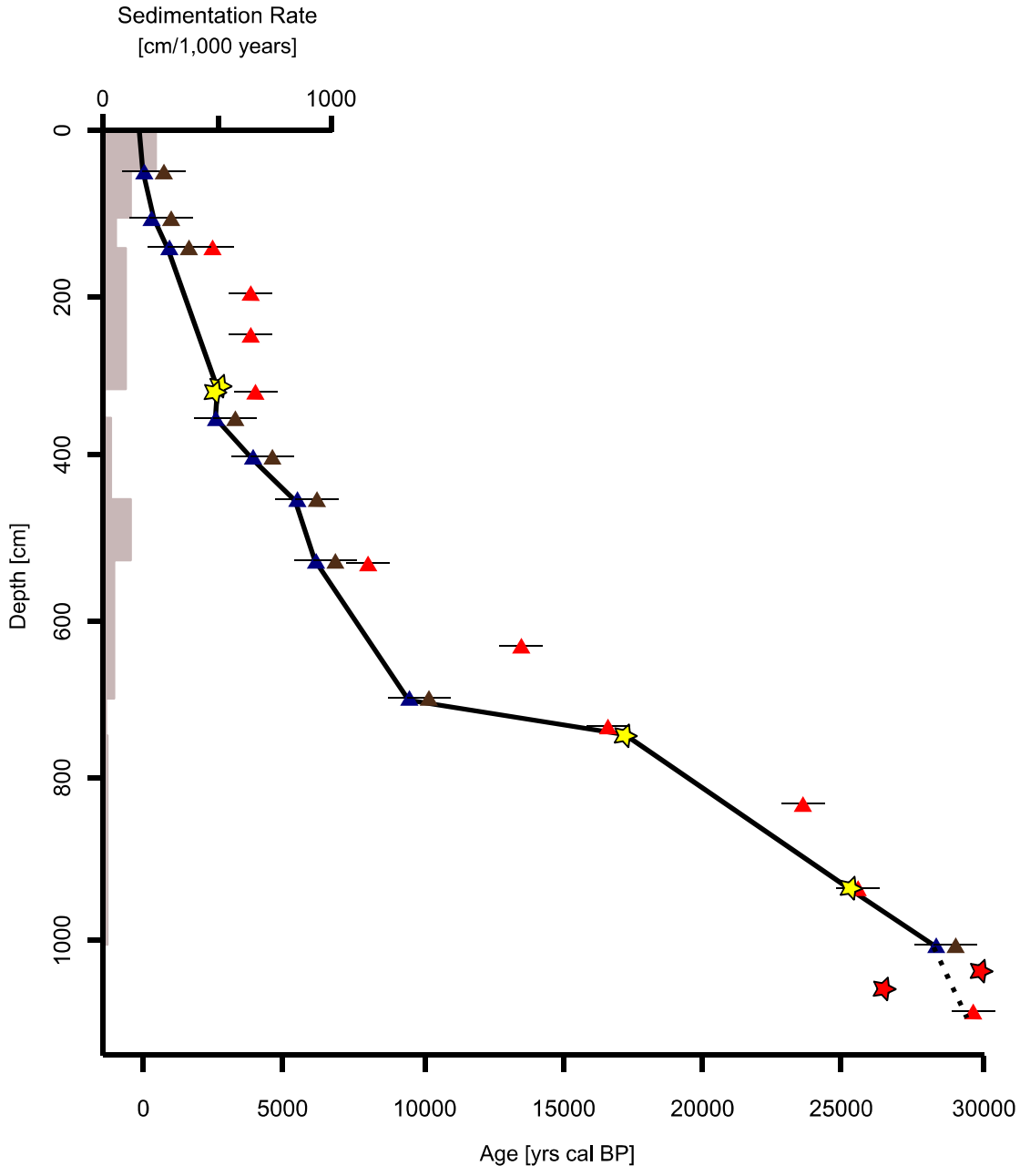

Fig. 4.7: Birkat Ram; age-to-depth model of composite profile based on calibrated radiocarbon data (Table 4.2 and Table 4.3); yellow stars indicate data from terrestrial plant remains, red stars indicates data of probably reworked terrestrial plant remains, brown triangles indicate data from water plant remains, blue triangles indicate data from water plant remains corrected for reservoir effects (600 years), for detailed discussion of reservoir effects see chapter 5.2.2; red triangles indicate data from bulk organic material, error bars indicate 2 σ-range, grey bars show sedimentation rates in cm per 1000 years

4.4 Reconstruction of vegetation based on pollen data

Pollen grains are common proxy to reconstruct paleo-vegetation, -environment, and -climate (Berglund and Ralska-Jasiewiczowa, 1986). Being dispersed by plants for reproduction, pollen grains are deposited in the vicinity of vegetation patches. Pollen grains can be identified and attributed to the source plant taxa. Therefore, knowledge about ecological requirements of the taxa, for example temperature, amount of precipitation, and composition of soils enables identification of relations between the pollen grains and the environment. Changing ratios of characteristic pollen taxa and pollen assemblages in a geological archive, for example lake sediments, reflect changing compositions of the vegetation. Thus, varying conditions of environmental parameters in the pollen source area can be reconstructed. However, several characteristics have to be considered: Size of the pollen source area positively correlates with the size of the lake surface (Janssen, 1973). Increasing distance of vegetation to the investigated archive implies decreasing relevance in the pollen record (Sugita, 1994). Therefore, the occurrence of vegetation changes in the pollen signal is affected by extent, distance, and position of the vegetation changes in relation to the archive, and by the size of the archive (Sugita, 1997).

Besides the advantages and analytical potential, the method possesses certain limits, which have to be considered: Most of the pollen grains can only be identified at a genus- or family-level. Within the eastern Mediterranean flora, some of those (e.g. *Quercus* and Poaceae) nevertheless reflect specific climatic conditions, because the whole genus or family, respectively, shares equal requirements. Other taxa, for example Brassicaceae, have to be interpreted with caution because different species of the family grow in different environments. Another aspect is the possible discrepancy between the proportion of taxa in the pollen rain, and its proportion in the vegetation (Davis, 2000). In general, wind pollinated taxa produce far more pollen grains than insect pollinated taxa. Depending on their shape and structure, the distances of pollen grain transport vary up to ranges of several hundred kilometres (Birks and Birks, 1980; Davies and Fall, 2001). Pollen grains of oak, olive, and pine, for example, belong to the most widely dispersed taxa. Therefore, the source region has to be reconstructed carefully, considering direction and strength of wind systems (van Zeist and Bottema, 1991). In terms of preservation, the risk of over- and under-representation of certain taxa in the pollen record has to be considered. Fragile Cupressaceae pollen grains, for example, are far more severely affected by corrosion than,

for example, Asteraceae pollen grains (van Zeist and Bottema, 1991). Besides these aspects, the dependency of taxa ratios among themselves, if presented as percentage diagrams, cause non-linearity between the pollen ratio, and the share in vegetation of particular taxa. This phenomenon is named Fagerlind-effect (Prentice and Webb, 1986). To estimate those discrepancies, investigations of the correlation of modern vegetation, and modern pollen rain are required (Fall, 2012; Horowitz, 1979). Being affected by humans for thousands of years, natural vegetation in the eastern Mediterranean is nearly non-existent in modern times (Zohary, 1982). Beyond that, pollen traps rarely simulate authentic depositional conditions in lakes (Giesecke et al., 2010). To reliably reconstruct paleoenvironment, -vegetation, and -climate based on ratios of pollen assemblages, it is inevitable to consider the effects of those parameters (e.g., Theuerkauf et al., 2012).

Drawing conclusions on paleo-pollen composition implies considering possible indications for anthropogenic impact. Primary and secondary anthropgenic indicators can be distinguished (Behre, 1990). Pollen from primary anthropogenic indicators directly reflect human interference with the natural vegetation, for example crop cultivation. In general, cereals are one of the most important evidences for agricultural activities, but which cannot be used in the Levant, since being element of the natural vegetation assemblage. In the Levant, olives (*Olea europaea*), walnut (*Juglans regia*), and grapewine (*Vitis vinifera*), for example, are crops, which can be traced in the pollen record. Secondary anthropogenic indicators indirectly point to human pressure on the natural vegetation. Behre (1990) defines secondary anthropogenic indicators asspecies which are not intentionally grown by man but are favoured in various ways or unintentiaonally introduced by man and his economy. *Sarcopoterium spinosum*, for example, is considered to reflect overgrazing, and to invade abandoned, formerly cultivated areas (Baruch, 1986). Numreous particular Poaceae and Brassicaceae positively correlate with human activity, too, but which cannot be determined to species level, and thus are inappropriate in terms of interpreting pollen records (Behre, 1990).

4.5 Dating of Late Pleistocene/Holocene lake sediments

Multiple absolute and relative dating methods can be applied to Late Pleistocene and Holocene lake sediments. Relative methods include the correlation of characteristic changes of particular proxies, such as pollen assemblages (palynostratigraphy, e.g., Litt et al., 2001; van Zeist et al., 2009), and the correlation of lithological events, such as tephra

layers (tephrochronology, e.g., Lowe, 2011; Zanchetta et al., 2011) or magnetic anomalies (magnetostratigraphy, e.g., Bonhommet and Zähringer, 1969; Plenier et al., 2007), with the adjacent records and global standard records (e.g., Dansgaard et al., 1993; Grootes et al., 1993; Petit et al., 1999). Varves can be counted if sediments are annually laminated and undisturbed (e.g., Litt et al., 2001; Litt and Stebich, 1999; Wick et al., 2003).

Radiocarbon (^{14}C) dating of deposited terrigenous plant macrofossils provides accurate reference points for the absolute chronology unless samples are reworked (e.g., Neumann et al., 2007a; Schwab et al., 2004). Since terrestrial plant material is often scarce in sediment cores, macrofossils from submerged plants, as well as bulk organic material are optionally for radiocarbon dating (e.g., Neumann et al., 2007a; Schwab et al., 2004). The organic fraction of bulk samples can be composed of fragments of terrestrial and / or water plants, phytoplankton, as well as plant- and animal detritus. Therefore, possible age discrepancies due to the hard-water effect, and the reservoir effect have to be considered (e.g., Grimm et al., 2009; Stein et al., 2004). The hard-water effect describes the dilution of the ^{14}C concentration of lake waters caused by ^{14}C-depleted “dead carbon”, washed in from carbonate-containing bedrock (e.g., limestone). Therefore, submerged plants that photosynthesise sub-aquatically and thus assemble the ^{14}C-diluted lake water, and animals that feed on these plants might produce exaggerated radiocarbon ages (Deevey et al., 1954). The ‘reservoir effect’ refers to the exchange between water and air is relatively slow, and thus the CO_2 of the lake water might not be in isotopic equilibrium with atmospheric CO_2, i.e. the ^{14}C activity of the water is lower than in air. The reservoir effect is increased if the residence time of the water in the lake is short (Stiller, 2001). The initial specific radiocarbon activity of dated samples might hence be considerably lower than that of the contemporaneous atmosphere, which leads to erroneously high ^{14}C ages (Deevey et al., 1954; Geyh et al., 1998). Furthermore, varying lake levels, and other changes in volume of the water body, as well as seepage of older ^{14}C-depleted groundwater into the lake affect the magnitude of the reservoir effect (Olsson, 1991; Stein et al., 2004). Since the influencing parameters are not necessarily stable, the hard-water-effect, as well as the reservoir effect is temporally variable (Zhou et al., 2011).

Depending on the particular hydrological and environmental conditions, varying magnitudes of these effects between 0 and 8,000 years are possible. Commonly, discrepancies between 500 and 2,000 years are determined (Geyh et al., 1998; Grimm et al., 2009). Specifically required reservoir corrections can be evaluated by dating bulk

organic material, and terrestrial macrofossils within one horizontal level. Subsequently, radiocarbon ages of bulk samples can be corrected for reservoir errors. An age-to-depth-model based on ^{14}C dates that can be confirmed through correlation with other well-dated records utilising proxy- and event-stratigraphy is possibly the most reliable base for further analyses (e.g., Rossignol-Strick, 1995).

5 Results

5.1 Lake Kinneret

5.1.1 Composite profile

A continuous 17.80 m-composite profile was constructed for the two sediment cores Ki10_I and Ki10_II to fill sampling gaps resulting from the applied coring technique. Magnetic susceptibility data were utilised for stratigraphic correlation (Fig. 4.2). Horizons of sufficient and reliably consistent magnetic susceptibility signals were defined as reference layers (Appendix 2).

5.1.2 Chronology

The occurrence of *Eucalyptus* pollen grains in the uppermost sample prove Recent age of the sediment-to-water interface of the Lake Kinneret sediment core. The neophyte is native to Australia, and was introduced to the area not before the end of the 19th century. They are component of the modern pollen rain (Horowitz, 1979). Besides the upper 25 cm, any visible lamination of sediments is absent and organic material of terrestrial origin is rarely deposited in datable amounts. Consequently, bulk organic material was used for AMS radiocarbon dating (Table 4.1). In addition, six macro remains of plants of terrestrial origin were dated (Table 4.1). In total, three depth horizons were dated for their ^{14}C ages from plant macro remains as well as from bulk sediments, and are available to calculate the magnitudes of the reservoir effect. Age discrepancies increase with increasing depth, since the reservoir effect is highly variable through time (Geyh et al., 1998).

At a depth of 358 cm, the age difference between the plant sample and the bulk sample is 835 years (Table 4.1). At a depth of 794 cm, an age discrepancy of 965 years was measured, and the lowermost horizon at 944 cm features a difference of 1,635 years (Table 4.1). Assumptions concerning the magnitude of the reservoir effects of the Lake Kinneret water and deposited sediments diverge to some degree (Lev et al., 2007; Stiller, 2001). However, neither the evolution of lake level nor carbonate source system is entirely understood so far (Hazan, 2004; Hazan et al., 2005).

Therefore, two approaches to create an age-to-depth model of the sediment cores are proposed. (1) Figure Fig. 4.3 presents an approach, in which the reservoir effect correction of 1,635 years at 944 cm core depth is applied to all bulk sample data points below (age-to-depth model I). (2) In age-to-depth model II an increase of age discrepancies was approximated by the linear equation y = 1.1259x + 358.39 (Fig. 4.4). Reservoir corrections at the bottom part of the sediment core are extrapolated. Table 4.1 shows the applied reservoir corrections for each age-to-depth model approach. Regarding both approaches, all data points are in stratigraphic order and no inversion occurs. Two dated macro remains (KIA44214 and KIA44215) were recovered from adjacent depth horizons at 945 cm and 946.5 cm, respectively. One ^{14}C date (KIA44216, 993 cm) appears to be significantly too old, i.e. the dated material was possibly reworked.

The presented Lake Kinneret record spans approximately 8,300 years (age-to-depth model II, Fig. 4.4) to 9,200 years (age-to-depth model I, Fig. 4.3). Changing sedimentation rates are displayed in figuresFig. 4.4 and Fig. 4.3. Average sedimentation rates amount to 194 cm per 1,000 years in age-to-depth model I, and 213 cm per 1,000 years in age-to-depth model II. Evidence for any hiatus in the sediment records was not found. Thus, sediment deposition can be reliably considered continuous, whereas age-to-depth correlations are rather regarded approximate.

5.1.3 Pollen analysis

Percentages of pollen types are calculated on the basis of total pollen sums, which include arboreal and non-arboreal pollen taxa, and exclude aquatic taxa as well as indeterminable pollen grains. The pollen record can be subdivided into seven palynostratigraphic units, titled Local Pollen Assemblage Zones (LPAZ) (Fig 5.1 and Table 5.1). LPAZ are distinguished by either specific composition of taxa (“Assemblage Zone”) or significant changes of frequency of particular taxa (“Abundance Zone”) (Murphy, 1999; Steininger, 1999). Zonation of the Lake Kinneret pollen record is based on pollen ratios of *Olea europaea*, *Quercus ithaburensis*-type, and *Quercus calliprinos*-type.

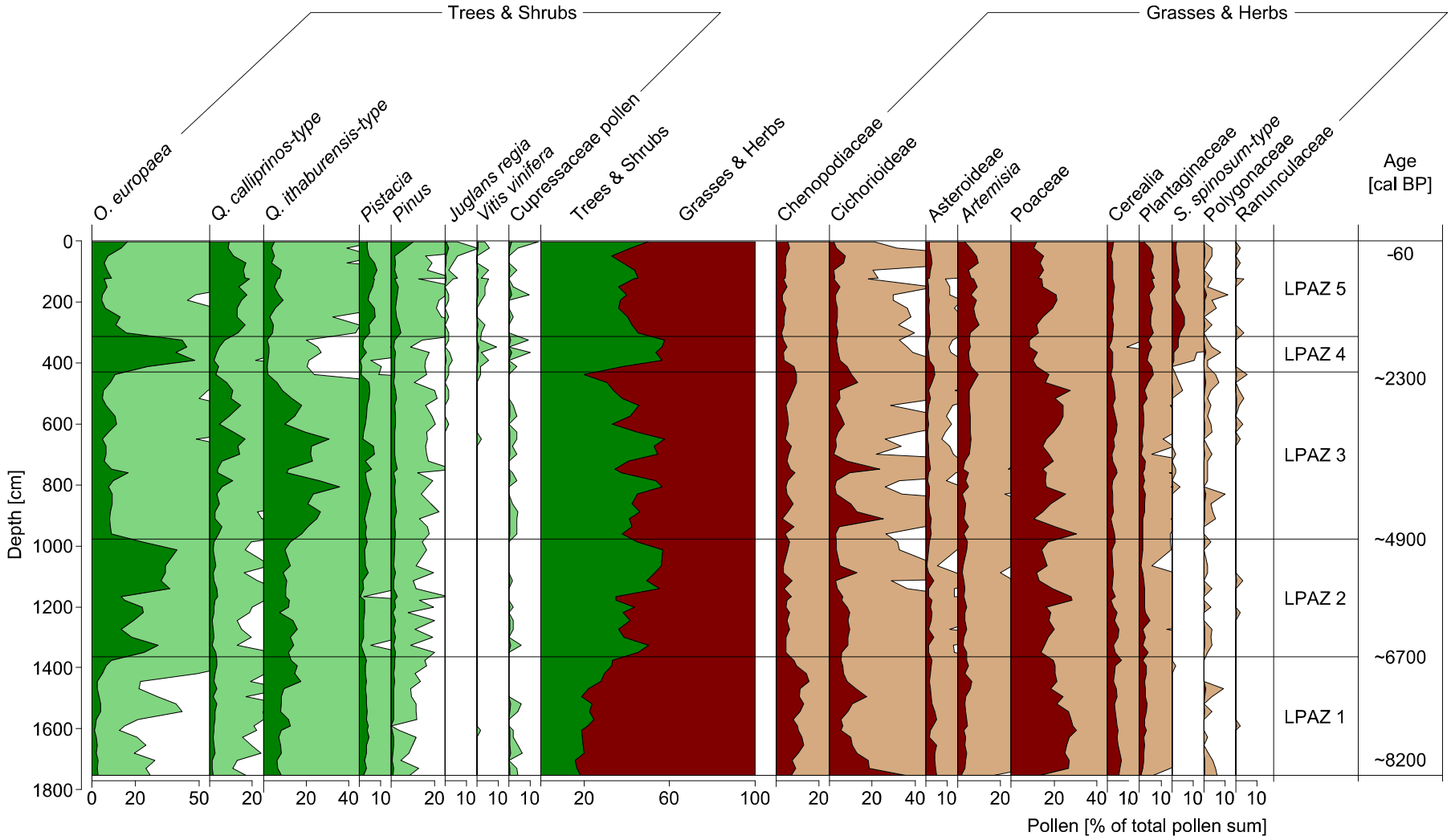

Fig. 5.1: Lake Kinneret; pollen diagram showing most relevant taxa; LPAZ indicate local pollen assemblage zones; ages are given within dating precision, for detailed information see chapter 5.1.2

Table 5.1: Lake Kinneret; pollen zonation of composite pollen profile (see Fig 5.1 and Appendix 10)

Local Pollen Assemblage Zone (LPAZ)		Composite Depth [cm]			Criterion for Lower Boundary	Features AP	Features NAP
Quercus calliprinos-type - *Pistacia* LPAZ	5	0	-	311.5	*Quercus calliprinos*-type >10%	predominance of *Quercus calliprinos*-type, remarkable values of *Pinus*, occurance of *Eucalyptus* as neophyte in uppermost part	remarkable amounts of *Sarcopoterium spinosum*
Olea europaea - *Sarcopoterium spinosum* LPAZ	4	311.5	-	428	*Olea europaea* >20%	highst values of *Olea europaea*, onset of continuous occurance of *Vitis vinifera* and *Juglans regia*	low values of Poaceae, onset of continuous occurance of *Sarcopoterium spinosum*
Quercus ithaburensis-type LPAZ	3	428	-	976.5	*Quercus ithaburensis*-type >15%	highest values of *Quercus ithaburensis*-type, *Quercus calliprinos*-type increasing, two distinct peaks of *Olea europaea*	Poaceae fluctuating on high level, three distinct peaks of Cichorioideae
Olea europaea LPAZ	2	976.5	-	1365	*Olea europaea* >15%	predominance of *Olea europaea*, fluctuations in lower half	low values, Poaceae fairly fluctuating
Poaceae - Cerealia LPAZ	1	1,365	-	1780	not defined	moderate Quercus ithaburensis-type values, increasing towards top	remarkable amounts of Chenopodiaceae and Poaceae pollen, remarkable peak of Cichorioideae in upper half

LPAZ 1 (1,780 cm - 1365 cm) is characterised by high values of non-arboreal pollen (NAP), fluctuating above 80% in the lower part of the zone, and slightly decreasing towards its top. Main constituent of NAP are Poaceae pollen, peaking at a depth of 1,604cm at about 30%, and declining towards the top of LPAZ 1. The Chenopodiaceae ratio is below 10% at the bottom of the zone, increases towards the middle part reaching its global maximum value of 15%, and decreases again towards the top. The very bottom of the record is marked by a major peak of Cichorioideae pollen ratio of above 30%, succeeded by a decline and a second minor peak (~17%) in the upper part of LPAZ 1. Low arboreal pollen (AP) ratio primarily consists of the following taxa. *Quercus calliprinos*-type pollen range at 2% throughout LPAZ 1, whereas *Quercus ithaburensis*-type pollen increase from below 10% at the bottom to nearly 20% at the top of LPAZ 1, showing two distinct peaks at a depth of 1,589 cm and 1,444 cm. Pollen values of *Olea europaea* range at 2%, and increase not before the very top of LPAZ 1.

Transition to LPAZ 2 at a depth of 1,365 cm is marked by *Olea* pollen ratio exceeding 15% of the total pollen sum. AP values are significantly higher in LPAZ 2 (1365 cm - 976.5 cm), fluctuating between 35% and 57%. Dominating taxon is *Olea europaea*, showing two peaks of 31% at a depth of 1,325 cm, and 24% at a depth of 1,219 cm in the lowermost half of the zone, each followed by a sharp decline to 14% and 13%, respectively. *Olea* pollen ratios increase steeply in the upper half of the zone, reaching 36% at a depth of 1,140 cm, and remaining high up to a sharp drop at the very top of LPAZ 2. Oak pollen values remain fairly constant. *Quercus calliprinos*-type ratio ranges at 2%, *Quercus ithaburensis*-type at 12%. Again, Poaceae pollen constitute the major share of NAP, fluctuating between 12% and 20% with one distinct peak of 29% at a depth of 1177 cm. None of the other NAP taxa exceeds 10% of the total pollen sum in LPAZ 2. *Quercus ithaburensis*-type pollen ratio rises towards the very top of LPAZ 2, and exceeds 15% of the total pollen sum at a depth of 976.5 cm, defining the onset of LPAZ 3 (976.5 cm - 428 cm).

LPAZ 3 is marked by considerable fluctuations of the AP/NAP-proportion. The AP ratio, dominated by *Quercus ithaburensis*-type (2%-36%), and *Quercus callprinos*-type (2%-17%) pollen, varies between 20% and 58% of the total pollen sum. *Olea* pollen values range between 5% and 9%, featuring two distinct peaks (17% at 761 cm, and 12% at 599 cm), and a slight increase towards the very top of the zone. *Pistacia* pollen, averaging about 3% in general, and peak at 7% at a depth of 699 cm, and 674 cm. The NAP ratio (42

- 80%) is dominated by Poaceae pollen (11 - 31%). The Cichorioideae pollen ratio ranges at 5%, and peaks at 25% (911 cm), 23% (747 cm), and 13% (464 cm) in LPAZ 3. Towards the top of the zone, *Plantago* pollen values rise from an average of about 2% up to 7%. In the middle of LPAZ 3, the *Artemisia* pollen ratio doubles from about 3% to about 6%. *Olea europaea* pollen dominate the overlying pollen zone, and an increase of *Olea europaea* above 20% at a depth of 428 cm is defined as the onset of LPAZ 4 (428 cm - 311.5 cm).

The strong increase of *Olea* pollen values is marked by a double-peak (global maximum of 48% at a depth of 390 cm, and 44% at a depth of 348 cm), followed by a conspicuous decrease towards the uppermost part of LPAZ 4. AP trace the course of the *Olea* pollen graph, showing somewhat higher quantities (56% at a depth of 390 cm, and 58% at a depth of 323 cm). Oak pollen values range about 2% in *Quercus ithaburensis*-type, and 5% in *Quercus calliprinos*-type pollen. Albeit playing a minor role with respect to the relative abundance, it should be emphasised that *Quercus calliprinos*-type pollen outnumber *Quercus ithaburensis*-type pollen for the first time in the record. Within NAP taxa, highest values are reached by Poaceae pollen, ranging steadily at 10%. Being discontinuous in the lowermost part of the record, *Vitis vinifera*, *Juglans regia*, and *Sarcopoterium spinosum* pollen ratios continuously occur since the onset of LPAZ 4.

The increasing *Quercus calliprinos* ratio is criterion for the transition to LPAZ 5, exceeding 10% at a depth of 311.5cm, levelling off at about 15% at around 300 cm core depth, and falling below 10% at the very top of the record. *Quercus ithaburensis*-type pollen as well as *Pistacia* pollen ranges consistently around 7% in LPAZ 5. *Olea* pollen values decrease at the bottom of the zone, level off at 6% in the middle part of LPAZ 5, and recover up to 17% at the very top. Increasing Poaceae pollen ratios peak at 21% (195 cm, and 175 cm) and decrease again towards the top of LPAZ 5. AP/NAP-proportions fluctuate between 40/60 and 50/50.

5.2 Birkat Ram

5.2.1 Composite profile

At Birkat, two parallel sediment cores BR10 I and BR 10 II were obtained. Based on the stratigraphic correlation of reliably consistent peaks of the magnetic susceptibility data of both cores, a 10.96 m-composite profile was produced (Fig. 4.6 and Appendix 7).

5.2.2 Chronology

Birkat Ram is a small lake, and remarkable differences of sedimentation rates are not considered to be likely. Therefore, the chronology of a 543 cm-profile cored at Birkat Ram in 1999, and established by Schwab et al. (2004) and Neumann et al. (2007a) was adopted for the upper part of this profile (0-534 cm composite core depth). Consistent correlation of pollen ratios as well as magnetic susceptibility signals of both Birkat Ram composite profiles support the adoption of the age-to-depth model of Neumann et al. (2007a) and Schwab et al. (2004) (Fig. 5.2).

Correction for hard-water and reservoir effect for water plant macrofossils is assumed 500-700 years, resulting from the correlation of a water plant macrofossil with the established date of the first occurrence of neophytes in the pollen record of the composite profile from 1999. For bulk organic material, a reservoir effect of approximately 1,000 years is supposed (Neumann et al., 2007a; Schwab et al., 2004), but which appears to differ to some degree in the bottom part of the composite profile from 2010. Low lake levels might have improved the isotopic exchange between the CO_2 of the lake water with the atmospheric CO_2, and hence caused lower reservoir effects. However, available data are insufficient to draw more precise conclusions.

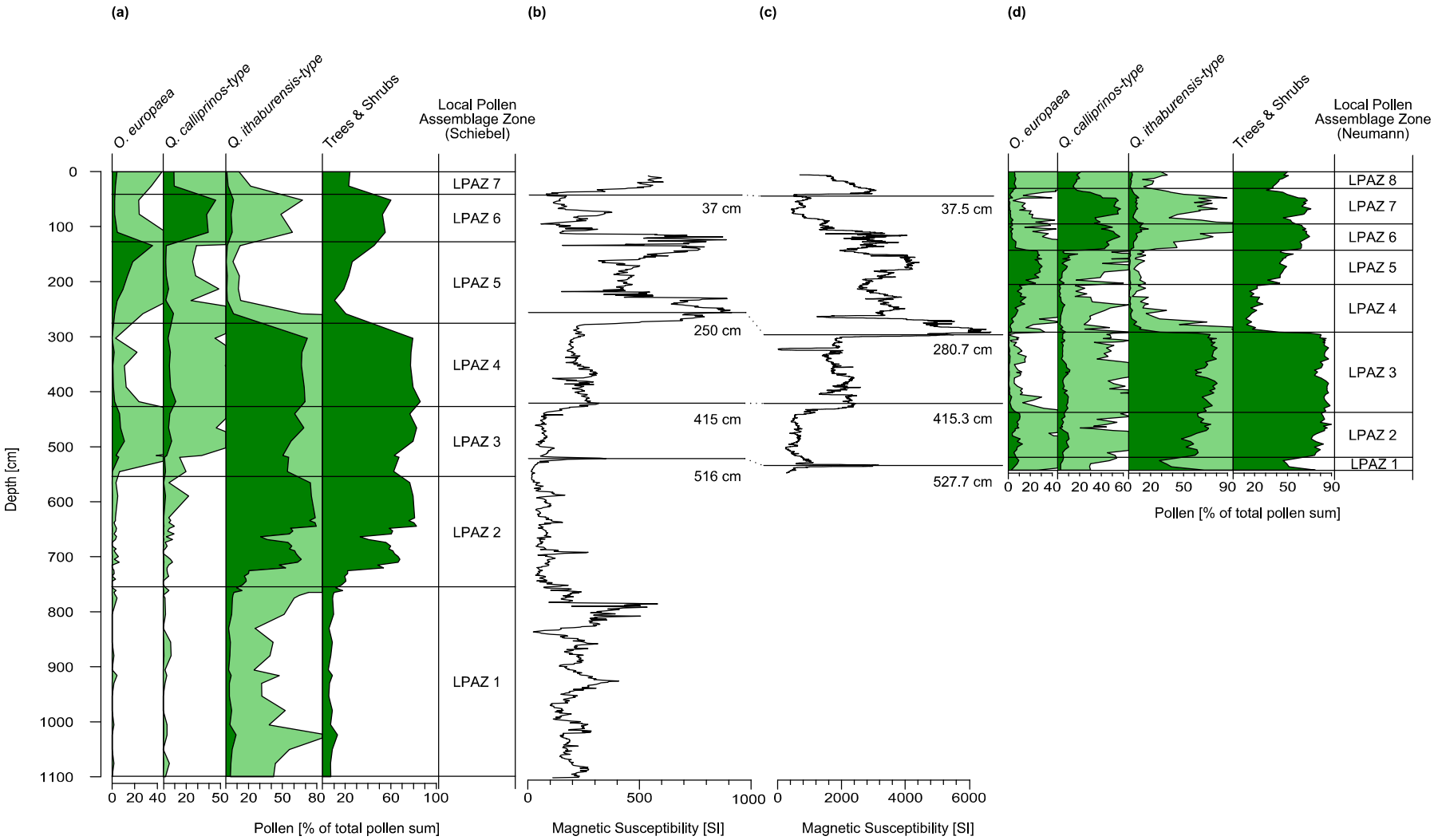

Fig. 5.2: Birkat Ram; correlation of the presented profile with a profile from cores recovered at Birkat Ram in 1999 based on (a)(d) palynostratigraphical, and (b)(c) magnetostratigraphical reference horizons; (c) and (d) after Schwab et al. (2004), and Neumann et al. (2007a)

The age-to-depth model shown in figure Fig. 4.7 includes all available data points (Table 4.2 and Table 4.3), assuming the sediment-to-water interface being Recent because of the occurrence of the neophytes *Eucalyptus* and *Casuarina* in the uppermost sample. Introduction of these plants from Australia dates to the end of the 19th century (Horowitz, 1979). Radiocarbon ages from water plant macrofossils were reduced by 600 years to correct for hard-water and reservoir effect (Table 4.2 and Table 4.3). Data points obtained from bulk organic material were plotted without precise correction due to above-mentioned uncertainties. No evidence for any disturbance of the deposition of sediments is obvious in the upper part of the profile (Fig. 4.7).

Average sedimentation rate between sediment-to-water interface and the data point at a composite depth of 703 cm (Beta-337247) is ~73 cm per 1,000 years. Below, a conspicuous drop of the average sedimentation rate to ~6 cm per 1,000 years in the segment between 703 cm and 746 cm (Beta-331274) clearly indicates a period of very low and partly discontinuous sedimentation of about 7,000 years around between ~10,000 and ~17,000 cal BP (746 cm core depth, Table 4.2). The deduced root cast horizon between around 732 cm and 756 cm composite core depth (see chapter 4.3) supports the assumption of a sedimentation gap. In the bottom part of the record, sediments seem to have been deposited without considerable gaps. Average sedimentation rate between 746 cm and 1,009 cm core depth (Beta-337249) is ~24 cm per 1,000 years (Fig. 4.7).

In the very bottom part, three data points are available (Table 4.2). The deviation of Beta-337251 (1,061 cm core depth) from the assumed age-to-depth model might be explainable by a dating error due to the rather low amount of organic material. Since the lowermost bulk organic sample (Beta-327812) dates younger than the terrestrial plant sample above (Beta-337250), the latter appears to be reworked. Although the consistency of available data points in the bottom part of the record is rather low, and therefore, minor disturbances of the deposition of sediments cannot be ruled out, the record is assumed to span approximately 30,000 years.

5.2.3 Pollen analysis

Arboreal and non-arboreal pollen taxa constitute total pollen sum of the Birkat Ram record. Indeterminable pollen grains are excluded from further assemblage analyses. Aquatics are likewise excluded from the total pollen sum, but yet evaluated for their relative abundance of total pollen sum. Classification into LPAZs is predicated on *Olea europaea*, *Quercus*

ithaburensis-type, and *Quercus calliprinos*-type pollen ratios (Table 5.2). Figure Fig. 5.3 shows pollen curves of important taxa, as well as the AP/NAP-ratios.

LPAZ 1 (1,096 cm - 756 cm) is entirely dominated by NAP, which reach a maximum value of 95% at 896 cm core depth. Main constituents are Polygonaceae and Poaceae, which fluctuate at about 20% of the total pollen sum. Chenopodiaceae ratios decrease from 23% at the bottom of the record to about 10% at 1,015 cm core depth, levels-off and recovers not before the upper part of LPAZ 1 to 23% at a depth of 768 cm core depth, where Poaceae pollen ratio drops to 10% contemporaneously. *Artemisia* pollen values reach high values in LPAZ 1, too. In the uppermost part of LPAZ 1, a distinct peak of 15% at a core depth of 758 cm is discernible. AP values are low throughout LPAZ 1. The only continuously occurring taxa are *Quercus ithaburensis*-type pollen (accounting for approx. 5%) and *Pinus* pollen (varying at 2%). *Olea europaea* pollen only occur sporadically. Virtually no pollen of aquatics occur in LPAZ 1.

The transition from LPAZ 1 to LPAZ 2 (756 cm - 555 cm) is determined at a depth of 756 cm, where *Quercus ithaburensis*-type ratios exceed 10% of the total pollen sum. Between 756 cm and 718 cm, *Quercus ithaburensis*-type pollen increase slightly to 21%, and then steeply to 66% to 698 cm core depth. After an abrupt decrease to 31% at a depth of 657 cm, *Quercus ithaburensis*-type ratios recover rapidly, peaking at a global maximum of 79% at core depths of 638 cm and 622 cm. As no other arboreal taxon reaches remarkable pollen ratios, AP ratios largely trace the trend of *Quercus ithaburensis*-type ratios. A global maximum of 82% of *Quercus ithaburensis*-type pollen appears at a depth of 638 cm. In the lowermost part of LPAZ 2, Chenopodiaceae and Polygonaceae are the most contributing NAP taxa. After varying about 20% up to a depth of 728 cm, the former decreases and levels-off at values between 1% and 7%, except for a single distinct peak of 14% at a depth of 657 cm. Polygonaceae vary between 14% and 26% up to a depth of 718 cm, and then decreases to values of approximately 5% in the upper part of LPAZ 2. One distinct peak of Polygonaceae pollen of 13% is visible at a depth of 662 cm. *Artemisia* pollen ratios peak at 9-10% between 737 cm and 728 cm, but show negligible amounts in large parts of the zone. Poaceae pollen values fluctuate with a slight downward tendency. Describing LPAZ 2, it is worth mentioning that two sharply separated peaks of aquatic *Myriophyllum* appear at core depths of 708 cm (103% of the total pollen sum) and 662 cm (67%).

The lower boundary of LPAZ 3 (555cm-426cm) is defined by a decrease of *Quercus ithaburensis*-type pollen below 70%. After further decrease to 50% at a core depth of 510 cm, *Quercus ithaburensis*-type pollen ratios recover up to 68% (460 cm). *Olea europaea* pollen quantities not only occur continuously in LPAZ 3 for the first time in the record, but even peak at 11% at a core depth of 485 cm. Furthermore, *Quercus calliprinos*-type pollen vary between 1% and 7%, and *Pistacia* pollen reach values of 1-2%, and are continuously present from LPAZ 3 on. The first appearance of *Vitis vinifera* is observed at a core depth of 460 cm. After peaking at 9% in the lowermost section of LPAZ 3, *Artemisia* pollen ratios decrease to 1-2% again. Poaceae pollen decrease to 6% at 435 cm core depth. Plantaginaceae as well as Ranunculaceae show distinctively higher values throughout LPAZ 3 than in LPAZ 2. As a result, AP/NAP proportions vary between 62/38 (539 cm) and 83/17 (460 cm). *Myriophyllum* percentages decline from 89% down to 12% during LPAZ 3.

Although LPAZ 4 is dominated by AP taxa, *Olea europaea* ratios drop to 1-2%. The lower boundary of LPAZ 4 is defined at a depth of 426 cm, where the *Oleae europaea* pollen ratio falls below 5%. *Quercus calliprinos*-type pollen values range between 5% and 11%, whereas *Quercus ithaburensis*-type pollen ratios range at high levels, peaking at 72% at a depth of 299 cm, and decreasing steeply afterwards. *Vitis vinifera* pollen grains occur frequently in LPAZ 4. The lowermost appearance of *Juglans regia* occurs at the bottom of LPAZ 4. In total, AP range between 77% (349 cm) and 86% (413 cm). Regarding NAP ratios, Poaceae show highest values, amounting to 5% at the bottom of the zone, and to 10% at depths of 349 cm and 299 cm with an increasing trend towards the top of LPAZ 4. Further NAP taxa ratios are rare throughout the zone, with Cichorioideae as well as Asteroideae increasing towards the very top. No major peaks of aquatics are discernible in LPAZ 4.

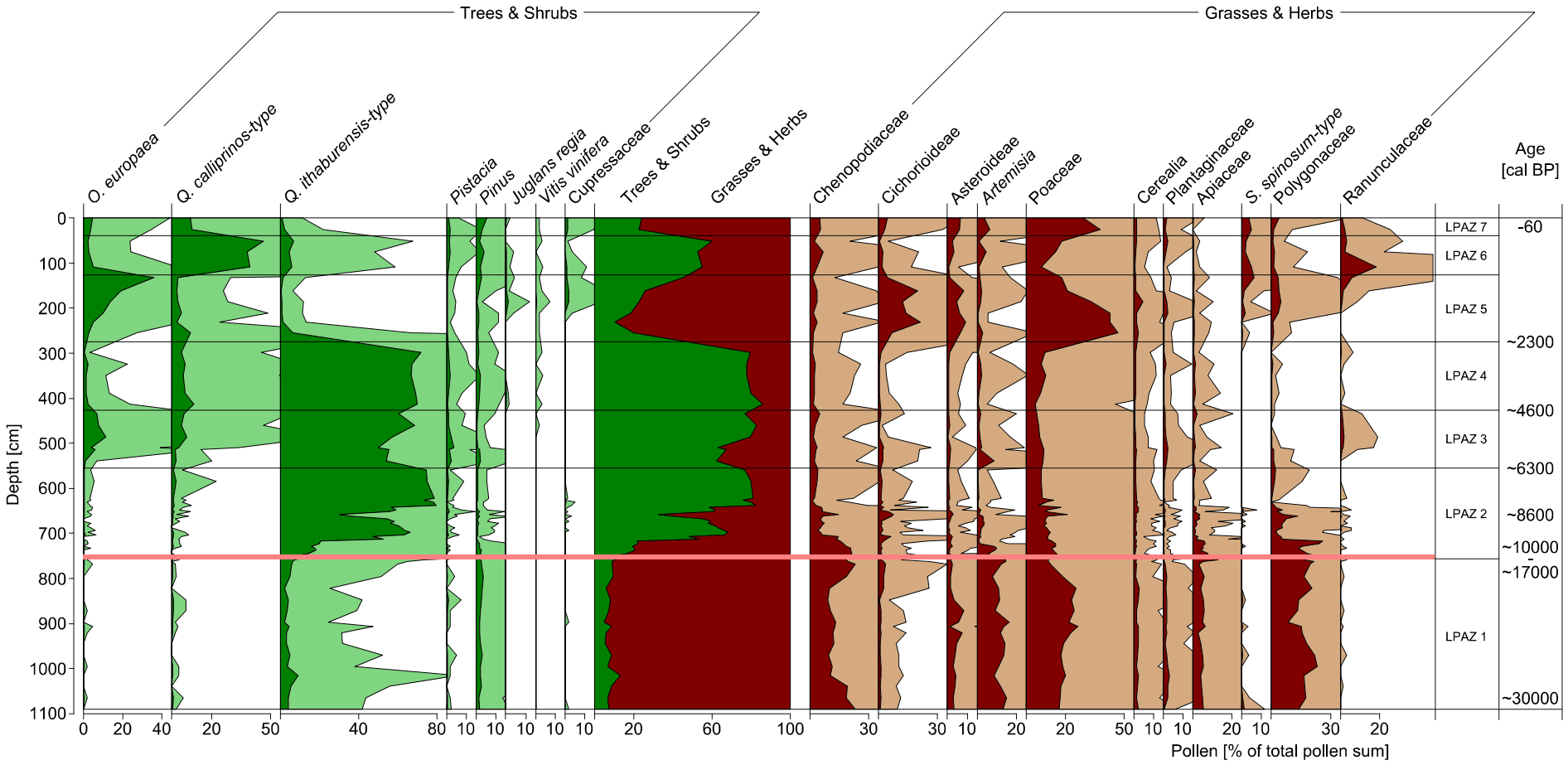

Fig. 5.3: Birkat Ram; pollen diagram showing most relevant taxa; LPAZ indicate local pollen assemblage zones; red horizon indicates assumed hiatus in the pollen record due to discontinuous sedimentation; ages are given within dating prcision, for detailed information see chapter 5.2.2

Table 5.2: Birkat Ram; pollen zonation of composite pollen profile (see Fig. 5.3 and Appendix 11)

Local Pollen Assemblage Zone (LPAZ)		Composite Depth [cm]			Criterion for Lower Boundary	Features AP	Features NAP
Poaceae - *Pinus* LPAZ	7	0	-	40	*Quercus calliprinos*-type <30%	low values, *Quercus ithaburensis*-type and *Quercus calliprinos*-type decrease, *Pinus* comparatively high, occurance of *Eucalyptus* and *Casuarina* pollen in uppermost part	high valus of Poaceae, distinct peaks of Cichorioidae, Asteroidae and *Artemisia*
Quercus calliprinos-type - *Pistacia* LPAZ	6	40	-	127	*Quercus calliprinos*-type >10%	steep decline of *Olea europaea*, *Quercus calliprinos*-type rises sharply, slightly increased values of *Quercus ithaburensis*-type, remarkable higher values of *Pinus*	low values, local minimum of Poaceae, remarkable values of Ranunculaceae
Olea europaea - Poaceae LPAZ	5	127	-	275	*Quercus ithaburensis*-type <50%	sharp drop of Quercus ithaburensis-type, Olea europaea increases steadily up to global maximum, onset of continuous occurance of *Juglans regia*	predominance of Poaceae, high values of Cichorioidae and Asteroidae, onset of continuous occurance of *Sarcopoterium spinosum*
Quercus ithaburensis-type - *Quercus calliprinos*-type LPAZ	4	275	-	426	*Olea europoaea* <5%	*Quercus ithaburensis*-type recovers to highest values, sharp decline in uppermost part, *Quercus calliprinos*-type moderate, *Olea europaea* values low, onset of continuous occurance of *Vitis vinifera*	quite low values, Poaceae, Cichorioidae and Asteroidae start increasing towards top
Olea europaea - *Quercus ithaburensis*-type LPAZ	3	426	-	555	*Quercus ithaburensis*-type <70%	Quercus ithaburensis-type values lower but still predominant, *Olea europaea* peaks, onset of higher values of *Quercus calliprinos*-type, first occurance of *Vitis vinifera*	quite low values, peak of *Artemisia* at bottom, remarkable values of Ranunculaceae
Quercus ithaburensis-type LPAZ	2	555	-	756	*Quercus ithaburensis*-type >10%	*Quercus ithaburensis*-type increases slightly at bottom, then sharply, distinct cutback in central part	Chenopodiaceae and Polygonaceae drop in lower part, then peak in central part, double-peak of *Artemisia*, Poaceae values rather low, fluctuating in central part
Polygonaceae - Poaceae LPAZ	1	756	-	1096	not defined	quite low values, *Quercus ithaburensis*-type and *Pinus* continuous	predominance of Polygonaceae and Poaceae, *Artemisia* and Chenopodiaceae show high values and peak in uppermost part

The transition to LPAZ 5 (275 cm - 127 cm) is characterised by the *Quercus ithaburensis*-type pollen ratio falling below 50%. After the rapid decrease, *Quercus ithaburensis*-type pollen values level-off at about 1% of the total pollen sum, whereas *Quercus calliprinos*-type pollen fluctuate at 5%. The dominant AP taxon in LPAZ 5 is *Olea europaea*. Its quantities grow steadily throughout the zone, reaching a global maximum of 36% at a depth of 132 cm. *Vitis vinifera* pollen are continuously present. Incessant appearance of *Juglans regia* as well as Cupressaceae pollen set in at a depth of 186 cm. In total, AP pollen percentages drop in the lower part of LPAZ 5, reach a minimum value of 11% at a depth of 230 cm, and then increase up to 45% (132 cm). Therefore, besides *Olea europaea*, NAP taxa dominate this part of the pollen record. Poaceae pollen ratios increase sharply at the LPAZ4/5 transition, reaching a global maximum of 47% at a depth of 255 cm, and then decreases steadily down to 18% at 132 cm. Cichorioideae as well as Asteroideae pollen increase in abundance, followed by a double peak, and then a decrease in the uppermost part of the zone. Cichorioideae peak at 21% (230 cm) and 20% (161 cm), and Asteroideae at 9% (230 cm) and 8% (161 cm). The onset of continuous presence of *Sarcopoterium spinosum* is located at the LPAZ 4/5 transitional zone. Ranunculaceae pollen values are rather low in the lower part of LPAZ 5, and increase towards its top.

The onset of LPAZ 6 (127cm-40cm) is defined where *Quercus calliprinos*-type pollen exceed 10% of the assemblage. The taxon dominates the entire zone, with a maximum of 46% at a depth of 50 cm. Above the peak, an abrupt decline of *Quercus calliprinos*-type pollen sets in. *Quercus ithaburensis*-type pollen range between 5% and 7% in LPAZ 6, whereas *Olea europaea* decrease to 2%. *Pinus* pollen show slightly higher values than in the subjacent zones. Regarding NAP taxa, which range about 45% in total in LPAZ 6, Poaceae pollen ratios predominate. After falling to 8% at a depth of 108 cm, a steady increase to 18% (50 cm) is noticed. A distinct peak of Ranunculacea appears in the lower half of the zone (18% at 108 cm). Values of other NAP taxa are rather low, and display only slight fluctuations with low amplitudes. Ratios of aquatics increase steadily up to 63% (50 cm).

The onset of the most recent LPAZ 7 (40 cm - 0 cm) is characterised by a decrease of *Quercus calliprinos*-type pollen ratios under the 30% threshold. *Quercus calliprinos*-type pollen range at 10% throughout the zone whereas *Olea europaea*, as well as *Quercus ithaburensis*-type pollen ratios do not exceed 5% of the total pollen sum. *Pinus* reaches 5% in the uppermost sample, which is also characterised by the occurrance of *Eucalyptus*, as

well as *Casuarina* pollen. However, NAP ratio predominates LPAZ 7. Poaceae pollen value reaches a local maximum of 38% (25 cm), and adds up with any other NAP taxa to total ratios of about 77% in this zone.

6 Discussion

Reconstructing vegetation changes from the palynological assemblage composition over the Late Pleistocene and Holocene in the Levant implies considering varying impacts of anthropogenic pressure, and climatic change as predominant causes. Furthermore, spatial extents and particular limits of recorded vegetation patterns are to be figured out. Therefore, the interpretation of the results of the presented pollen analyses is approached in an interdisciplinary way, considering pollen records from adjacent lakes, climate reconstructions being based on other proxies as well as archaeological findings.

6.1 The Last Glacial Maximum (LGM)

Applying the proposed chronology on the Birkat Ram pollen record, LPAZ 1 sediments appear to have been deposited during the Pleniglacial from 30,000 cal BP (28,050 BCE) including the Last Glacial Maximum (23,000-19,000 cal BP / 21,050 BCE-17,050 BCE; Mix et al., 2001; and discussion in Tzedakis, 2007). The pollen record points to a steppe-like character of the vegetation in the vicinity of Birkat Ram. Chenopodiaceae-, *Artemisia*-, and Polygonaceae-ratios reach their maximum values in LPAZ 1, i.e. the LGM (Fig. 5.3).

The LGM can be assumed to reflect the natural vegetation of the area under cold and dry environmental conditions before human activities affected the vegetation. Goosefoots (Chenopodiaceae) and wormwoods (*Artemisia*) are components of a dwarf-shrub steppe vegetation type, which is also part of the modern vegetation of north-western Jordan (van Zeist et al., 2009). During the LGM, this plant assemblage possibly predominated in northern Israel.

The rather low values of the most frequent AP-taxon, *Quercus ithaburensis*-type, indicate patches of open woodland of deciduous oaks, most likely growing on the mesoclimatically favourable western slopes (Karmon, 1994). Constantly high Poaceae pollen-ratios point to grasses in the open woodland understorey, and to grasslands in higher elevated areas, as well as in the vicinity of the lake.

Patches of *Pinus halepensis*, growing on the Mount Meron in the Upper Galilee is assumed to constitute the origin of the pines and their pollen in the Birkat Ram record (van Zeist et

al., 2009). Pine pollen continuously reach values of about 2% in the LGM, and are the second most important tree pollen taxon. The Aleppo pine (*Pinus halepensis*) is the only pine species occurring in the modern vegetation of the southern Levant, and which can be assumed also for the past (van Zeist et al., 2009; Zohary, 1973). Very good pollen production and pollen dispersal of *Pinus halepensis* generally leads to an over-representation in pollen records especially in open-landscape environments (van Zeist et al., 2009).

The overall composition of the pollen taxa of LPAZ 1 points to relatively arid climatic conditions, and low amounts of precipitation and low temperatures can be deduced from the pollen assemblage (Fig. 5.3). A resulting low evaporation rate would provide an explanation for a relatively high lake level, and a continuous existence of the Birkat Ram lake despite little precipitation, which, at first glance, might not appear obvious. Similar patterns are documented from the Lake Lisan, precursor of the modern Dead Sea (Kushnir and Stein, 2010; Stein et al., 2010). Reconstructions from Lake Lisan suggest high lake levels, though with decreasing tendency, during the LGM (Kushnir and Stein, 2010; Stein et al., 2010). Correspondingly, dry and cold conditions during the LGM are recorded from the eastern Mediterranean by Tzedakis (2007), and which are supported by the results of climate models ran by Robinson et al. (2006).

Dry and cold climatic conditions over the LGM reconstructed from the pollen record are in good agreement with the findings from speleothem analyses from different caves in Israel (Ayalon et al., 2013; Vaks et al., 2003). The growth rate of speleothems can be applied as proxy to reconstruct paleo-precipitation (Vaks et al., 2003). In the Ma'ale Efrayim Cave, located in the rain shadow on the eastern side of the central ridge of Israel, growth of speleothems was interrupted from about 25,000 to 19,000 yrs BP, owing to a lack of precipitation (Vaks et al., 2003). In the Mizpe Shelagim Cave, located within the Alpine karst region of Mount Hermon, temperature is the limiting factor of speleothem growth (Ayalon et al., 2013). No growth of speleothems is recorded between about 36 and 15,500-14,500 yrs BP indicating average annual temperature <3° C (Ayalon et al., 2013). However, in the Soreq Cave, located on the western side of the central ridge, speleothems grew continuously during the last Glacial-Interglacial cycle, which points to a sufficient temperatures and water availability (Bar-Matthews and Ayalon, 2005). Correlation of pollen data and the isotopic composition of speleothems appears not to be reasonable in this context, since the signal is discussed to reflect the source-water composition of

Mediterranean Sea, rather than being as proxy of paleo-rainfall in the eastern Mediterranean (Frumkin et al., 1999; Kolodny et al., 2005; Litt et al., 2012).

Regarding other pollen records in the area, AP values in the pollen assemblage in the marine Core 9509 drilled off the southern Israeli coast, are the lowest of the entire record between 27,100 and 16,200 years BP, centring at about 19,000 years BP, indicating very dry and cold conditions (Langgut et al., 2011). Reconstructions based on the pollen record of the Yammoûneh basin (Lebanon) also indicate very arid conditions during the LGM (Develle et al., 2011). However, according to Niklewski and van Zeist (1970), climatic conditions in north-western Syria were more humid according to on the interpretation of a pollen record from Ghab Valley. Since no reservoir correction was applied to any radiocarbon age, Rossignol-Strick (1995) and Meadows (2005) argue for a revision of the chronology utilising biostratigraphic correlation, though.

During the LGM, Early- and Middle-Epipaleolithic people inhabited the southern Levant, leading a hunter-gatherer lifestyle without any impact on the vegetation (Goring-Morris and Belfer-Cohen, 2011).

6.2 The Late Glacial

Apparently, the deposition of sediments at Birkat Ram was discontinuous during the period of Late Glacial climate amelioration between the Last Glacial Maximum and the Younger Dryas (12,900-11,700 cal BP / 10,950 BCE-9,750 BCE; Broecker et al., 2010). Oxidised root cast fragments were found in the composite profile at 732 cm to 756 cm core depth, which necessarily have been exposed to atmospheric oxygen, and which thus indicate low lake levels or even desiccation of Birkat Ram. One of the samples was radiocarbon dated at 17,225+/-295 cal BP (Beta-331274, 746 cm composite core depth). Besides those findings, oospores from stonewort, which grows submerged in the photic zone, and fruit from Polygonaceae, which belong to the bankside vegetation, were recorded in the sediment above (at 703 cm core depth) and below (at 776 cm core depth) the root cast horizon (Fig. 6.1). Based on the radiocarbon ages of these samples (Fig. 4.7), the period low lake levels or even complete desiccation of Birkat Ram is chronologically attributed to the Deglaciation period.

Fig. 6.1: Birkat Ram; fruit of *Polygonum sp*., extracted from BR10_I_7-8 at a composite core depth of 776 cm; picture by G. Oleschinski

Consequently, the pollen record would be discontinuous at the bottom part of LPAZ 2, and no conclusion concerning a possible dispersion of Mediterranean vegetation during the Late Glacial climatic amelioration can be drawn. Although the lake levels of Birkat Ram as well as the Dead Sea appear to have dropped significantly (Kushnir and Stein, 2010; Stein et al., 2010), a tendency towards an increased precipitation can be seen in several paleoclimate reconstructions throughout the eastern Mediterranean during the Last-Glacial Interstadial (~15,000-13,000 cal BP / 13,050 BCE-11,050 BCE; Robinson et al., 2006).

In their marine record, which reflects a large source area, Langgut et al. (2011) describe a conspicuous increase of Mediterranean taxa initiating at 16,200 years BP. Pollen records from archives with a smaller scaled catchment area show a slighter increase of Mediterranean vegetation, but nevertheless assume an increase in precipitation (Hajar et al., 2010; Hajar et al., 2008). Niklewski and van Zeist (1970) assume decreasing (pollen assemblage zone Y4) and low (pollen assemblage zone Y5) AP-values during the Late-Glacial Interstadial period in the Ghab Valley (Syria). In contrast, Rossignol-Strick (1995)

and Meadows (2005) identify pollen assemblage zones Y1 to Y4 as the Last-Glacial Interstadial period. Adopting that approach, the high AP-values in the Ghab Valley pollen record indicate the development of Mediterranean macchia vegetation in Syria during the Deglaciation period. The concluded increase of available precipitation, which is essential for the expansion of Mediterranean plant taxa, could have been superimposed by an enhanced evaporation resulting from a pronounced increase of temperature (Tzedakis, 2007). The development and expansion of Mediterranean vegetation contemporaneous with falls and low stands of lake levels, which seems to be contradictory at first sight, could be explained by this hypothesis.

Regarding the interaction between vegetation and humans, an effect of vegetation on the development of human lifestyle is more possible than anthropogenic influence on the vegetation. Although the triggers for the development and degree of sedentism of the Natufian people in the Levant are subject of discussion (Bar-Yosef, 1998; Boyd, 2006; Grosman, 2003), the climatic conditions appear to have been favourable in terms of food availability to humans during this final period of the Last Glacial.

6.3 The Younger Dryas (YD)

The distinct peak of *Artemisia* at a composite core depth of 733 cm (Fig. 5.3), which occurs synchronous with high ratios of Chenopodiaceae, is assumed to reflect the characteristic YD (12,900-11,700 cal BP / 10,950 BCE-9,750 BCE; Broecker et al., 2010) pattern in eastern Mediterranean pollen records (Rossignol-Strick, 1995). Following this assumption, decreasing temperatures during the YD (Robinson et al., 2006), and the resulting reduced evaporation could have led to a regeneration of the Birkat Ram lake and a re-initiation of the deposition of sediments during the YD. AP-values are again dominated by *Quercus ithaburensis*-type, and, ranging about 15%, approximately double their share in the total pollen sum compared to the LGM period. Nevertheless, steppe taxa like Polygonaceae, Poaceae, Chenopodiaceae, and *Artemisia* dominate the pollen composition, indicating an arid climate.

Indicating dry and cold conditions during the YD, the results of this study correspond to findings reviewed by Tzedakis (2007). However, Rossignol-Strick's (1995) classification of the YD being the most arid period of the Late Pleistocene in the Near East cannot be confirmed by the Birkat Ram data. The magnitude of the impact of the YD climatic fall-

back on the vegetation cannot be determined quantitatively due to the gap in the pollen record during the Late Glacial (Fig. 5.3). Langgut et al. (2011) describe a moderate decrease of AP-taxa, and conclude a less intense severity of the YD event in comparison to the LGM. On the contrary, the revised pollen diagram from the Ghab Valley shows a sharp decline of the Mediterranean macchia vegetation to LGM values.

Reconstructions of the Dead Sea lake level assume a highstand during the YD, which might either reflect more humid conditions as a result of possible regional differences of the magnitude of this climatic event, or caused by a pronounced reduction of evaporation due to decreased temperatures (Kushnir and Stein, 2010; Stein et al., 2010).

Gvirtzman and Wieder (2001) identified a 0.7 m thick layer of loess between 12,500 and 11,500 yrs BP, which points towards low temperatures and increased wind stress during the YD. An extremely arid period is assumed for the YD, and considered the most significant event during the last 53,000 years by Gvirtzman and Wieder (2001).

Interpretations of the role of the YD in the context of the origin of agriculture diverge to some degree. Among others, Bar-Yosef (2011) and Belfer-Cohen and Bar-Yosef (2002) conclude that people initiated the cultivation of crops because the availability of wild edible plants was insufficient during the YD climatic deterioration. In contrast, e.g. Rosen and Rivera-Collazo (2012) and Zeder (2011) argue that no causal connection is evident. According to Rosen and Rivera-Collazo (2012) and Zeder (2011), it is possible that the development of agricultural techniques was a result of the evolution of human cultures, regardless of climatic forcing. In the pollen record of Birkat Ram, no evidence for agricultural activities can be observed during the transition from the Pleistocene to the Holocene (Fig. 5.3). Since cereals are part of the natural vegetation in Israel (Bottema, 1992), the occurrence of Cerealia pollen cannot be considered as indicator for the onset of agriculture as is the case in Central Europe (Behre, 1990). A distinction between wild and domesticated Cerealia pollen is impossible (Behre, 1990; van Zeist et al., 2009).

6.4 The Holocene

6.4.1 11,700-6,500 cal BP (The Neolithic period)

After the climatic deterioration during the YD, the most pronounced change of the pollen composition reflects the onset of the present interglacial, the Holocene, in the Birkat Ram

pollen record. The AP-ratio, namely its main component *Quercus ithaburensis*-type pollen, slightly increases by about 5% between 733 cm and 718 cm composite core depth, and subsequently increases over only 3 cm very steeply by about 30% at 715 cm composite core depth (Fig. 5.3). A similar pattern of an early Holocene change in plant assemblages characterises the record from Lake Van in eastern Anatolia (Litt et al., 2009). Apparently, the precipitation in northern Israel continuously exceeded 300 mm per year since the beginning of the Holocene, but which might well have been considerably higher. Beyond a precipitation threshold of 300 mm yr^{-1}, growth and expansion of Mediterranean plants can be expected (Danin, 1988). The low altitude slopes of the Golan Heights were obviously characterised by widespread open woodland, dominated by the deciduous Tabor oaks (*Quercus ithaburensis*), growing between 0 m and 500 m amsl. Although pollen grains of Tabor oaks and another deciduous oak, *Quercus boisserii*, cannot be distinguished, the latter has been limited to the uppermost mountain zones of the Golan Heights, and unlikely to be abundant at the lower slopes of the Golan Heights (van Zeist et al., 2009). The slightly increasing the *Quercus calliprinos*-type pollen in the Neolithic period (LPAZ 2) might reflect the occurrence of patches of Kermes oak on the higher elevated slopes of the Golan Heights (500 m – 1200 m amsl; Danin, 1988). Obviously, Mediterranean taxa expanded into higher altitudes, indicating not only an increase in precipitation, but additionally a temperature rise.

Synchronously with the increase of oak pollen values, the ratio of pine pollen declined, and only sporadically exceeded one per cent of the total pollen sum in the Neolithic period. This tendency is most probably a consequence of the change in the pollen composition rather than an indication of a reduction of pine populations. The high pollen productivity of *Quercus ithaburensis* can be assumed to have reduced the degree of over-representation of *Pinus halepensis* (Rossignol-Strick, 1995). The continuous occurrence of pollen grains of *Olea europaea*, originating from wild olives, in the Neolithic period provides further support for the assumed climate amelioration. Regarding the steppe taxa in the Birakt Ram pollen record, the considerable decline of Chenopodiaceae, Polygonaceae, Apiaceae and *Artemisia* clearly reflect a reduction of the influence of the Irano-Turanian plant assemblage on the vegetation in northern Israel. Compared to the above-mentioned taxa, the magnitude of decrease of the Poaceae pollen values was rather small. A variety of grasses appears to have constituted the understorey of the oak woodland.

The retraction of the Mediterranean vegetation belt, indicated by a distinct, conspicuous decrease of the pollen ratios of Mediterranean taxa at a composite core depth of ~660 cm (Fig. 6.32) might have been caused by rapid climate change around 8,200 cal BP (6,250 BCE) (Alley and Ágústsdóttir, 2005) or rather the underlying climate deterioration between 8,500 and 8,000 cal BP (6,550 and 6,050 BCE) (Rohling and Pälike, 2005). According to the proposed chronology, the decrease in AP-values occurred as early as 8,600 cal BP (6,650 BCE), and considering the uncertainties of the age-to-depth model does not necessarily present a caveat in the argumentation (see also chapter 5.2.2). The decrease of the Mediterranean vegetation zone can be considered as response to a return to colder and dryer conditions in the Northern Hemisphere. Oak woodland appears to have been replaced by Irano-Turanian steppe vegetation, largely composed of goosefoots, wormwoods, knotweeds (Polygonaceae), and grasses. The fast recovery of the arboreal pollen ratio up to a maximum value of ~80% in the late Neolithic period (upper part of LPAZ 2) points to a rapid amelioration of the climatic conditions. A similar pattern can be seen in the pollen record of Tenaghi Philippon (Pross et al., 2009), but which is indiscernible in Dead Sea record (Litt et al., 2012).

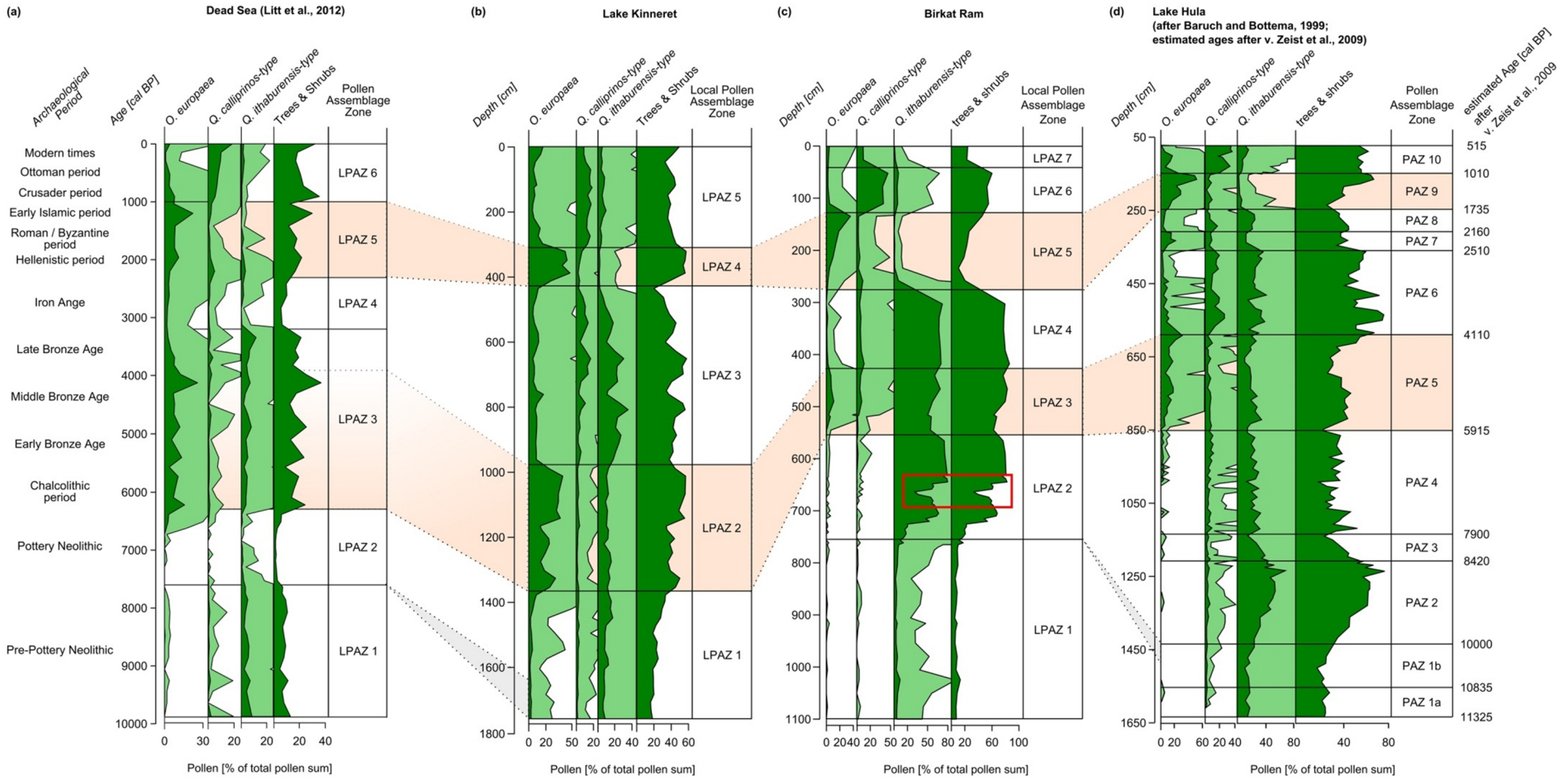

Fig. 6.2: Correlation of pollen records along a north-to-south-transect along the Dead Sea Rift; (a) record from the Dead Sea after Litt et al. (2012) plotted against reliable chronology and correlated to archaeological periods; (b) presented record from Lake Kinneret plotted against depth; (c) presented record from Birkat Ram plotted against depth; (d) record from Lake Hula after Baruch and Bottema (1999) plotted against depth, and supplemented by an estimated chronology after van Zeist et al. (2009); upper coloured horizon indicates olive cultivation during Hellenistic and Roman / Byzantine periods, lower coloured horizon indicates olive cultivation during the Chalcolithic period, Early Bronze Age (EBA), and Middle Bronze Age in the Dead Sea record, and during the Chalcolithic period and EBA in the other records, respectively; red box indicates decrease of AP, assumed to reflect the 8.2-event, faded grey conjunctions indicate tentative correlation of patterns

The Birkat Ram pollen record supports the supposed early Holocene climate optimum between 9,000 and 6,000 cal BP (Roberts et al., 2011; Rossignol-Strick, 1995). The composition of the pollen assemblage in the early Holocene counterpart of the Lake Kinneret record (LPAZ 1) differs to some degree from the Birkat Ram, though (Fig. 6.32). In contrast to the Birkat Ram record, NAP-taxa at Lake Kinneret reach values up to about 80% in the bottom part, and decrease towards the Chalcolithic period (LPAZ 2). The domination of Poaceae, Chenopodiaceae, and Cichorioideae indicates a strong influence of steppe vegetation in the catchment area. This vegetation zone can be assumed to have stretched along the shorelines of Lake Kinneret, and to have been part of the understorey of the open woodlands on the slopes of the mountain ranges. Beneath being part of the local vegetation, pollen grains of steppe taxa could well have been brought in via long-distance transport from Syrian steppe regions (Baruch, 1986). Prevailing taxon within the Mediterranean trees and shrubs is the Tabor oak varying around 15% of the total pollen sum in LPAZ 1 of the Lake Kinneret pollen record. The source area of *Quercus ithaburensis*-type pollen in the Lake Kinneret pollen record comprises the eastern slopes of the Lower Galilee, the Upper Jordan Valley, and the southern Golan Heights (Baruch, 1986). The *Pistacia* pollen of the Levantine records originate largely from *Pistacia palaestina*, which is the only species being reasonably represented in the pollen rain. *P. atlantica* and *P. lentiscus* are seriously underrepresented (Baruch, 1986). Regarding the ecology of the *Pistacia* species present, and their continuous occurrence in the whole record points to relatively mild winter temperatures (Rossignol-Strick, 1995).

Referring solely to the pollen record, it cannot be concluded whether the comparatively low ratios of Mediterranean trees and shrubs during the early Holocene in the Lake Kinneret region are caused by wood clearance of the Pottery Neolithic (PN) people, as assumed by Rollefson and Köhler-Rollefson (1992), or rather by an expansion of the Irano-Turanian steppe biom due to increasing aridity. An equivalent pattern can be observed in the revised pollen record from Lake Hula (PAZ 3) (van Zeist et al., 2009), and in the pollen record from the Dead Sea (PAZ 2) (Litt et al., 2012). Archaeological findings reveal no evidence for large-scale wood clearance activity during the PN, but rather conclude low settlement density (Ahlström, 1993). On the contrary, the reconstruction of the lake level of the Dead Sea shows low lake level stands between 9,000 and 7,000 cal BP (7,050 BCE and 5,505 BCE), indicating a period of increased aridity (Kushnir and Stein, 2010), which is consistent with the climatic deterioration, deduced by Rohling and Pälike (2005). Since the temporal correlation is in good agreement with the Lake Kinneret pollen record, and no

additional evidence for anthropogenic impacts is obvious, an increase of aridity can be assumed major reason for the observed change in vegetation, but which might not have affected the climate archive of Birkat Ram, located at a higher altitude and latitude (Fig. 3.2). A contradictory conclusion is drawn by Yasuda et al. (2000), who specify a sharp decrease of deciduous oaks around 9,000 yrs BP in a pollen record from Ghab Valley (Syria) as earliest evidence for large-scale anthropogenic deforestation. However, no correction for reservoir effects was applied to the measured radiocarbon ages of Yasuda et al. (2000), and the authors refer to the good correlation to the chronology of the Lake Hula profile (Baruch and Bottema, 1999), but which was rejected in the meantime (van Zeist et al., 2009). Adopting the suggested biostratighraphical correlation of an adjacent profile from Ghab Valley by Rossignol-Strick (1995), the age discrepancy might well add up to ~3,500 years, and hence the evidence for deforestation activities during the Pre-pottery Neolithic has to be questioned.

6.4.2 6,500-2,300 cal BP (Chalcolithic, Bronze, and Iron Age)

The Holocene in the Near East is characterised by increasing anthropogenic influence on the vegetation. The pronounced increase of *Olea europaea* pollen, which characterises the onset of the Chalcolithic period in the Levant (Litt et al., 2012; Neumann et al., 2007a) is obvious in the bottom part of LPAZ 3 in the Birkat Ram pollen record, and in the bottom part of LPAZ 2 in the Lake Kinneret record, respectively. The increase of olive pollen is the earliest observable evidence for olive cultivation, and therefore human impact on the vegetation. Regarding the Birkat Ram profile, the correlation of the lowermost rise of *Olea europaea* pollen is consistent with the results of Neumann et al. (2007a), and the magnetic susceptibility signal as independent proxy provides further support for the adoption of the age-to-depth model for the upper part of the profile (Fig. 5.2).

A similar pattern of the olive curve can be observed in the Dead Sea pollen record indicating an onset of the Chalcolithic period around 6,500 cal BP (4,550 BCE) based on reliable chronology (Litt et al., 2012). In the Lake Hula pollen record, olive curve pattern is correlatable, too, and the slight delay may be due to inaccuracy of the estimated chronology rather than actual offset (van Zeist et al., 2009). Archaeobotanical findings from several Chalcolithic sites also give evidence for olive cultivation (Lovell, 2002; Neef, 1990).

The consistency of this assumption perfectly matches with the proposed chronology of the Birkat Ram record (Fig. 4.7; onset of *Olea europaea* rise at ~530 cm, which is ~6,300 cal BP / 4,350 BCE). Concerning the Lake Kinneret chronology, the adoption of age-to-depth model II is further supported (Fig. 4.4) (onset of *Olea europaea* rise ~6,700 cal BP / 4,750 BCE) (see also chapter 5.1.2). Applying age-to-depth model I (Fig. 4.3), the increase of olive pollen would set in as early as ~7,100 cal BP (5,150 BCE), which is rather unlikely since neither any palynological nor any archaeobotanical record in the Levant verifies olive cultivation before ~6,500 cal BP (4,550 BCE). Therefore, the Lake Kinneret pollen record is discussed on the base of age-to-depth model II (Fig. 4.4) hereafter. Nevertheless, it has to be emphasised that the calibrated radiocarbon ages are to be considered tentative (see chapter 5.1.2).

Beneath the rise of *Olea europaea* pollen ratios, the remaining Mediterranean taxa reach high values during the Chalcolithic period. In the Birkat Ram record, *Quercus calliprinos*-type pollen ratios slightly increase, whereas *Quercus ithaburensis*-type pollen ratios decrease to some extent, which can be explained by woodland clearance and the subsequent replacement by olives. In addition, the fairly continuous occurrence of *Vitis vinifera* pollen from the Early Bronze Age (mid- LPAZ 3) might provide further evidence for human impact on the vegetation by grapevine cultivation, which is consistent with the findings from Neumann et al. (2007a). In the Lake Kinneret record, *Quercus ithaburensis*-type pollen reach higher values from the onset of the Chalcolithic period in comparison to the Neolithic period (Fig 5.1), regardless of the increase of *Olea europaea* percentages. *Quercus calliprinos*-type ratios remained stable.

Summarising, the Birkat Ram source area appears to have received a sufficient amount of precipitation for Mediterranean taxa to grow since the beginning of the Holocene. In contrast, the climatic conditions in the Lake Kinneret area seem to have ameliorated by around 6,500 cal BP (4,550 BCE), enabling an expansion of the Mediterranean vegetation. The fluctuations of the olive pollen during the Neolithic period (LPAZ 2) in the Lake Kinneret record (Fig. 5.1) clearly reflects changes of the magnitude of human activity rather than changes of the climatic conditions since the ratios of the remaining Mediterranean taxa hold steady. Analyses of the composition of diatoms in the Lake Kinneret sediment cores indicate increased anthropogenic impact during Chalcolithic period, and Early Bronze Age, too (Vossel, 2012).

The abandonment of olive groves around 4,600 cal BP (2,650 BCE; transition from LPAZ 3 to LPAZ 4, Birkat Ram) and around 4,900 cal BP (2,950 BCE; transition from LPAZ 2 to LPAZ 3, Lake Kinneret) occurred synchronously with an increase of oak pollen. In the Birkat Ram record, *Olea europaea* appears to have been replaced by deciduous oaks whereas in the Lake Kinneret record the *Quercus ithaburensis*-type, as well as *the Quercus calliprinos*-type values rise at the transition from LPAZ 2 to LPAZ 3. Apparently, the decline of olive cultivation did not occur due to the deterioration of the climatic conditions. This assumption is supported by the deduction of a highstand of the Lake Kinneret level around 5,000 cal BP (Hazan et al., 2005). The abandonment of the olive groves seems to have taken place as early as the Early Bronze age (5,500-4,150 cal BP / 3,550 BCE-2,200 BCE; after Levy, 1995) in northern Israel, which is consistent with the conclusions by van Zeist et al. (2009) regarding the Lake Hula record and the archaeological record (Baruch, 1986).

The chronologically well-constrained Dead Sea pollen record as well as archaeological and archaeobotanical findings (e.g., Berelov, 2006; Fall et al., 2004) indicate a decline of olive cultivation along with a decrease of settlement density and economic activities not before the Late Bronze Age (3,500-3,150 cal BP / 1,550 BCE-1,200 BCE; after Levy, 1995) in southern Israel. Regional differences in timing of the population development, as well as uncertainties in the chronologies might cause this offset. Nevertheless, the chronology is supported by the onset of regular occurrence of *Juglans regia*-type pollen since LPAZ 4 (Birkat Ram record) and LPAZ 3 (Lake Kinneret record), which is consistent with archaeobotanical evidence from the Middle Bronze Age from Megiddo (Liphschitz, 2000). During LPAZ 4, pollen ratios in the Birkat Ram record remain rather stable. The vegetation appears to have been predominated by Tabor oak woodland at low altitudes (<500m amsl) and evergreen oaks at higher altitudes. The availability of precipitation can be considered sufficient for the Mediterranean biom to grow in the Golan Heights. In contrast, pronounced changes of the AP/NAP-proportion in the Lake Kinneret record indicate fluctuations of the amount of precipitation in the more southern and more climate sensitive region (Zohary, 1982). A more exact chronology would be required to reliably correlate the changes in the composition of the vegetation with detected rapid climate changes (Mayewski et al., 2004; Rohling et al., 2009).

6.4.3 2,300 – 1,300 cal BP (Hellenistic, Roman / Byzantine period)

The sharp decrease of the ratio of *Quercus ithaburensis*-type pollen that distinguishes the transition from LPAZ 4 to LPAZ 5 in the Birkat Ram record (Fig. 5.3) can clearly be assigned to deforestation activities during the Hellenistic period (2,282-2013 cal BP / 332 BCE-63 BCE) (see also Neumann et al., 2007a). *Quercus calliprinos*-type pollen ratios slightly decrease, too, whereas olive pollen ratios increase steadily throughout LPAZ 5, indicating the re-establishment of olive cultivation during Hellenistic, Roman, and Byzantine times (2,282-1,312 cal BP / 332 BCE-638 CE).

Since the magnitude of the decline of oak pollen values by far exceeds the magnitude of the rise of olive pollen ratios, additional explanations have to be considered. Firstly, parts of the deforested areas could have been exploited for the cultivation of crops, which cannot be distinguished in the pollen record. Peas and lentils, for example, might have been cultivated, but which, being insect-pollinated, are characterised by poor pollen productivity. Moreover, they cannot be identified to the genus-level, and are hence included in the Fabaceae family (Behre, 1990). Secondly, areas could have been deforested to be used for grazing. This assumption is supported by the synchronous increase of *Sarcopoterium spinosum*, which is a spiny shrub, classified as secondary anthropogenic indicator by Behre (1990). *S. spinosum* is considered to reflect overgrazing, and to invade abandoned, formerly cultivated areas (Baruch, 1986).

Similar patterns are known from the Dead Sea record (Litt et al., 2012), as well as the Lake Hula record (van Zeist et al., 2009). Thirdly, timber industry can be assumed to have contributed to the forest clearance (Dar, 1993). The steep decrease of the *Quercus ithaburensis*-type signal is immediately compensated by a conspicuous rise of Poaceae pollen ratios, whereas *Olea europaea* values increase rather slightly. This pattern indicates that needs for arable farm land, and building land as well as the exploitation of timber predominated, while olive cultivation was developed gradually on the Golan Heights. Nevertheless, the maximum value of *Olea europaea* pollen during the second wave of olive cultivation in the Roman / Byzantine period is ~36% (132 cm composite core depth), which is more than three times the maximum value of the first olive peak during Chalcolithic times (~11% at 485 cm composite core depth). Therefore, the expansion of olive groves during the Hellenistic to Roman / Byzantine period appears to exceed by far the dimension of the Chalcolithic and Bronze Age areas.

In the Lake Kinneret record, the replacement of oaks by olives is also obvious, but the changes differ to some extent (Fig 5.1). The oak values as well as the Poaceae ratios decrease slightly, whereas the rise of *Olea europaea* values is fairly steep. This pattern is in good agreement with the pollen ratios recorded by Baruch (1986), who analysed sediment core KIN4D, cored in 1979 at a more southern part of the Lake Kinneret (Fig. 6.3). Assumingly, the trade with olive oil was established in the Lake Kinneret region earlier than on the Golan Heights (Zohary and Hopf, 1988). It can be suggested that people in the Birkat Ram region initially cultivated olives for their own requirements, and trading structures developed only subsequently (Kaniewski et al., 2009; Kaniewski et al., 2012).

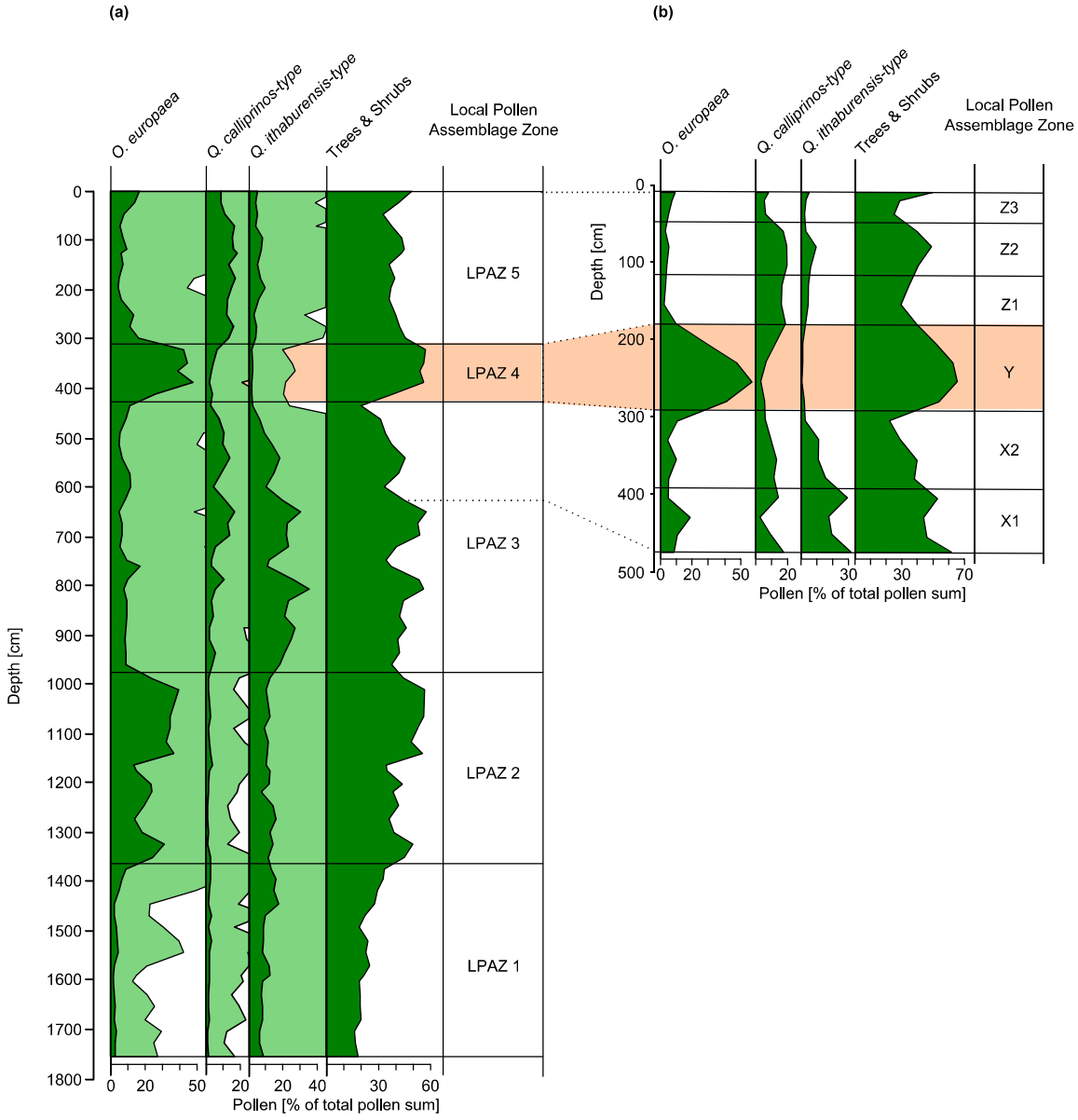

Fig. 6.3: Lake Kinneret; palynostratigraphical correlation of (a) the presented pollen record with (b) the pollen record after Baruch (1986), analysed samples originate from core KIN4D, cored 1979 at southern part of Lake Kinneret; colored horizon indicates olive cultivation during Hellenistic and Roman / Byzantine periods

6.4.4 1,300 cal BP – present (Early Islamic period to present)

After the abandonment of olive groves and the decline of economic structures during the Early Islamic period (Safrai, 1994), vacant areas were re-occupied by evergreen oaks and pistachios whereas *Quercus ithaburensis* did not recover since (LPAZ 6 and 7 in the Birkat Ram record, LPAZ 5 in the Lake Kinneret record). Compared to the high-stemmed Tabor oaks, the multi-stemmed shrubby *Quercus calliprinos* and *Pistacia palaestina* are less vulnerable for anthropogenic impact (e.g., grazing, cutting) (Baruch, 1990; Danin, 1988). High ratios of *Sarcopoterium spinosum* prevail throughout this period of woodland regeneration.

A similar succession is obvious from the Lake Hula record (van Zeist et al., 2009), as well as from the Dead Sea record (Litt et al., 2012). The former natural Mediterranean vegetation predominated of deciduous oaks, appears to have been replaced around 1,000 cal BP by macchia vegetation characterised by *Quercus calliprinos* and *Pistacia palaestina*, and batha vegetation characterised by *Sarcopoterium spinosum*. Pine pollen are a further important taxon in the uppermost part of the pollen record of Birkat Ram and Lake Kinneret. Remarkably high ratios occur since the Early Islamic period (LPAZ 6 and LPAZ 7 in the Birkat Ram profile; LPAZ 5 in the Lake Kinneret record). Possessing a good pollen productivity and dispersal, pines tend to be overrepresented in pollen assemblages (van Zeist et al., 2009).

Nevertheless, *Pinus halepensis* appears as an element of the recovering arboreal vegetation after the abandonment of olive groves. Pine trees are counted among the pioneer elements of the succession of vegetation during regeneration periods (Liphschitz and Biger, 2001). The distinct *Pinus* peak, which is more pronounced in the Lake Kinneret record (~10% of the total pollen sum) than in the Birkat Ram record (~5%), reflects human impact on the vegetation. The modern dispersion of Aleppo pines is a result of afforestation activities in the beginning of the 20th century, and does not represent the natural vegetation cover (Liphschitz and Biger, 2001). Alternation of plant assemblages in the Levant reflects largely anthropogenic interference with the natural vegetation rather than climate changes during the last 6,500 years (Litt et al., 2012; van Zeist et al., 2009).

7 Summary

Paleo-vegetation of northern Israel is reconstructed from palynological data over the Late Pleistocene and Holocene, and related to climate variation in the Levant, as well as anthropogenic impact on vegetation.

Being located in the arid-to-semi-arid climatic transitional zone, the modern and past vegetation in northern Israel comprises both, Mediterranean macchia, and Irano-Turanian steppe assemblages, and thus is highly sensitive to climate change. Palynological analyses were carried out on two lacustrine sediment profiles obtained during drilling campaigns, at Lake Kinneret in northern Israel (17.8 m composite core length), and at Birkat Ram in the Golan Heights (10.96 m composite core length). A chronological model was developed for both profiles based on radiocarbon dates. Variations in the composition of pollen assemblages were recorded.

Spanning ~30,000 years, and thus reaching further back than any other record in the southern Levant, the new Birkat Ram pollen record reflects predominating steppe vegetation indicating dry and cold climatic conditions during the Pleniglacial and the Last Glacial Maximum (23,000-19,000 cal BP). Deposition of sediments was very low and even discontinuous during the Late Glacial from around 17,000 cal BP to ~10,000 cal BP suggesting low lake levels to the point of desiccation of Birkat Ram by increased evaporation. Distinct peaks of *Artemisia* and Chenopodiaceae pollen yet reflect a characteristic eastern Mediterranean Younger Dryas-pattern (12,900-11,700 cal BP) in the Birkat Ram pollen record. A conspicuous increase of Mediterranean taxa is slightly delayed, and occurs after the onset of the Holocene (~11,700 cal BP) reflecting increased precipitation. There is strong evidence that the '8.2 ka Climate Event' can be verified in the Birkat Ram pollen record. A sharp decrease of Mediterranean taxa indicates distinct deterioration of climatic conditions.

The Lake Kinneret pollen record encompasses the past ~8,000 years. Moderately low ratios of Mediterranean taxa indicate relatively dry conditions from the bottom of the profile, and which slightly change to mesoclimatically more favoured condition until 6,500 cal BP. The Birkat Ram record, on the contrary, is characterised by high values of Mediterranean vegetation assemblages reflecting higher availability of precipitation in the Golan Heights over the entire early Holocene.

Increased ratios of olive pollen both from Birkat Ram and Lake Kinneret point to periods of enhanced human interference with vegetation between ~6,500 and ~4,700 cal BP (Chalcolithic period - Early Bronze Age), and between ~2,200 and ~1,500 cal BP (Hellenistic - Roman / Byzantine period). Regeneration of the vegetation after the first wave of olive cultivation was predominated by high-stemmed deciduous oaks whereas abandoned areas after the second wave of olive cultivation were re-occupied by multi-stemmed evergreen oaks which are less vulnerable for anthropogenic impact (e.g., grazing, logging) than deciduous oaks. From 19th to 20th century, pollen assemblages at Birkat Ram and Lake Kinneret pollen record indicate Pine afforestation, and the introduction of *Eucalyptus* and *Casuarina* being Neophytes from Australia.

The results of this study contribute to the discussion on temporal and geographical occurance of vegetation changes, as well as settlement periods in the Levant, and improve the data base for a better understanding of the development of vegetation changes over the climatically variable transition from Late Pleistocene to the Holocene. In addition, understanding interdependencies of past societies and their environments is indispensable to better asses and develop strategies for agriculture and food production during times of environmental and climate change, in particular in highly climate-sensitive areas such as the Levant.

8 Zusammenfassung

Basierend auf palynologischen Daten wurde die spätpleistozäne und holozäne Paläovegetation Nordisraels rekonstruiert und bezüglich ihrer Abhängigkeit von Klimavariationen in der Levante sowie von anthropogenem Einfluss diskutiert. Da das Untersuchungsgebiet im Übergangsbereich von aridem zu semi-aridem Klima liegt, wirken sich schon kleine Veränderungen der klimatischen Bedingungen auf die geographische Ausbreitung der vorkommenden Mediterranen Macchia und der Irano-Turanischen Steppenvegetation aus.

Die analysierten Sedimentkerne wurden im Rahmen einer Bohrkampagne im Norden Israels abgeteuft. Im See Genezareth konnte ein Kompositprofil von 17,8 m Länge gewonnen werden, das Kompositprofil aus dem Kratersee Birkat Ram umfasst 10,96 m. Für beide Profile wurde ein Altersmodell entwickelt, das sich auf Radiokarbondatierungen stützt. Die Veränderung der Pollenzusammensetzung entlang der Profile wurde erfasst.

Der Pollenrekord des Birkat Ram umfasst die letzten ~30.000 Jahre und reicht somit weiter zurück als die bisher in der südlichen Levante untersuchten Profile. Die Pollenzusammensetzung während des Hochglazials und des letzten glazialen Maximums (23.000-19.000 cal BP) deutet auf das Vorherrschen von Steppenvegetation und damit auf kalte, trockene Bedingungen hin. Da die Sedimentation während des Spätglazials zwischen ~17.000 und ~10.000 cal BP schwach bis diskontinuierlich war, kann auf sehr niedrige Seespiegel bis hin zur Austrocknung des Birkat Ram durch erhöhte Evaporation geschlossen werden. Ein für die Jüngere Dryas (12.900 - 11.700 cal BP) im ostmediterranen Raum charakteristisches Muster, bestehend aus deutlichen Maxima von *Artemisia* und Chenopodiaceae Pollen, kann dennoch im Birkat Ram Pollenrekord eindeutig nachgewiesen werden. Ein drastischer Anstieg der Pollen Mediterraner Taxa, der leicht verzögert nach dem Einsetzen des Holozän (11.700 cal BP) auftritt, spricht für eine erhöhte Verfügbarkeit von Niederschlag. Ein rapider Rückgang der Mediterranen Taxa in Pollenrekord des Birkat Ram, der eine deutliche Verschlechterung der Klimabedingungen anzeigt, resultiert vermutlich aus dem „8,2 ka-Klima-Event“.

Der Pollenrekord des See Genezareth umfasst die letzten ~8.000 Jahre. Im unteren Abschnitt des Profils deuten moderate Anteile Mediterraner Taxa an der Pollenzusammensetzung auf relativ trockene Bedingungen hin, die sich bis ~6.500 cal BP

geringfügig hin zu mesoklimatisch günstigeren Bedingungen verändern. Der Birkat Ram Pollenrekord dagegen weist hohe Werte Mediterraner Taxa auf, die für eine erhöhte Verfügbarkeit von Niederschlag während des gesamten Frühholozän in den Golan Höhen sprechen.

Sowohl im Profil des See Genezareth als auch in dem des Birkat Ram zeigen erhöhte Anteile von Olivenbaum-Pollen Perioden von intensivierten Wechselwirkungen zwischen Menschen und Vegetation von ~6.500 bis 4.700 cal BP (Chalkolitikum bis Frühbronzezeit) sowie zwischen ~2.200 und ~1.500 cal BP (Hellenistische bis Römisch / Byzantinische Periode) an. Die Regeneration der Vegetation nach der ersten Welle des Olivenanbaus war von hochstämmigen sommergünen Eichen geprägt, während aufgegebene Flächen nach der zweiten Phase des Olivenanbaus durch mehrstämmige immergrüne Eichen, die weniger anfällig für anthropogenenen Einfluss (z.B. Beweidung, Rodung) sind, wiederbesiedelt wurden. Seit dem 19. bis 20. Jahrhundert können in den Pollenzusammensetzungen des See Genezareth und des Birkat Ram Hinweise auf Aufforstung von Kiefern sowie für die Einführung von *Eucalyptus* und *Casuarina*, beides Neophyten aus Australien, gefunden werden.

Die Ergebnisse dieser Untersuchung tragen zur Diskussion möglicher zeitlicher und geographischer Vorkommen von Vegetations- und Siedlungsphasen in der Levante bei und erweitern die Datenbasis für ein besseres Verständnis der Entwicklung von Vegetationsveränderungen während des klimatisch variablen Überganges vom Spätpleistozän zum Holozän. Darüber hinaus sind Kenntnisse über Wechselwirkungen zwischen Bevölkerung und ihrer Umwelt insbesondere in klimatisch sensitiven Gebieten wie der Levante unerlässlich, um Strategien für Landwirtschaft und Nahrungsmittelproduktion in Zeiten von Umwelt- und Klimaänderungen zu entwickeln und einzuschätzen.

9 Résumé

La reconstitution de la paléo-végétation durant le Pléistocène Supérieur et l'Holocène au nord de l'Israël a fait l'object d'une étude palynologique qui a permis de mettre en évidence les interdépendances entre les paléo-environnements, le paléoclimat et l'impact anthropique sur la couverture végétale. Situé dans la zone climatique de transition entre domaines aride et semi-aride, la végétation fossile et moderne du nord de l'Israël comprend aussi bien des assemblages de maquis méditerranéen que des assemblages de steppe irano-turaniienne. Cette composition végétale est donc très sensible aux changements climatiques.

Des analyses palynologiques ont été effectuées sur deux carottes des sédiments lacustres qui ont été obtenues, l'une dans le lac de Tibériade (longueur du forage: 17,8 m), l'autre dans le lac de cratère Birkat Ram sur le plateau du Golan (longueur de forage: 10,96 m). Un modèle chronologique, développé sur la base de datations au radiocarbone, permet d'analyser les variations temporelles des assemblages de pollen qui ont été enregistrées dans ces lacs du nord de l'Israël.

Le profil palynologique de Birkat Ram couvre une période de ~30.000 ans et est ainsi le plus long profil jamais obtenue dans la région du Levant Sud. La composition pollinique reflète la prédominance d'une végétation steppique pendant la période pléniglaciaire et le dernier maximum glaciaire (23.000-19.000 cal BP) indiquant un climat froid et sec. Pendant la période tardiglaciaire entre ~17.000 cal BP et ~10.000 cal BP, le dépôt de sédiments a été faible, ou même discontinu suggérant une période de bas niveau de l'eau jusqu'à l'assèchement complet du lac de Birkat Ram, dû à une augmentation de l'évaporation. La présence des pics distincts de pollen d'*Artemisia* et de Chenopodiaceae reflète néanmoins le modèle caractéristique du Dryas récent (12.900-11.700 cal BP) dans la région de la Méditerranée orientale. Les abondances relatives des taxons méditerranéens augmentent considérablement après le début d'Holocène (11.700 cal BP) indiquant l'augmentation des précipitations. L'événement climatique de 8.200 ans est probablement marqué, dans le profil palynologique de Birkat Ram, par la forte diminution de l'abondance rélative des taxons méditerranéens, indiquant une détérioration des conditions climatiques.

Le profil pollinique du Lac de Tibériade couvre une période de ~8.000 ans. Dans la partie inférieure de l'enregistrement, les valeurs modérées d'abondance des taxons méditerranéens démontrent l'existence de conditions climatiques, devenant progressivement plus favorables jusqu'à 6.500 cal BP. Au contraire, le profil palynologique de Birkat Ram se caractérise, pendant tout le début de l'Holocène, par une prédominance des assemblages de végétation méditerranéenne indiquant de meilleures conditions de précipitations sur le plateau du Golan.

Deux phases d'augmentation du pollen d'olivier révèlent des périodes d'interference des activités humaines avec la végétation entre ~6.500 et ~4.700 cal BP (Chalcolithique - Bronze Ancien) et entre ~2.200 et ~1.500 cal BP (Période Hellénistique - Période Romano-Byzantine). La régénération de la végétation après la première vague de l'oléiculture a été prédominée par les chênes à feuilles caduques à haute tige tandis que des oliveraies abandonnées après la seconde vague ont été récolonisées par des chênes à feuilles persistantes à tiges multiples qui sont moins vulnérable à l'impact anthropique (le pâturage, l'abattage du bois) que les chênes à feuilles caduques. Depuis le 19^{ième} siècle les assemblages polliniques des profils de Birkat Ram et du Lac de Tibériade indiquent des boisements de pins et l'introduction d'*Eucalyptus* et *Casuarina*, deux neophytes provenant d'Australie.

Les résultats de cette étude contribuent à la discussion sur l'apparition temporelle et géographique des changements de la vegetation et des phases d'occupation humaine dans le Levant. De plus, l'élargissement de la base de données polliniques de la région du Levant permet une meilleure compréhension de l'évolution de la végétation en réponse à la transition climatique ayant eu lieu du Pléistocène supériuer à l'Holocène. Par ailleurs, la meilleure connaissance des interdépendances des sociétés du passé avec leur environnement est indispensable pour mieux évaluer et élaborer des stratégies pour l'agriculture et pour la production alimentaire pendant des périodes des changements environnementaux et climatiques, en particulier dans des régions sensibles, telles que le Levant.

10 Appendix

A.1

Israeli climate data; source: http://www.ims.gov.il; information relates to average time periods: 1981-2000 for temperature, and 1970/1971 - 1999/2000 for rainfall

	Har Kenaan (Zefat)			Jerusalem			Elat		
Elevation [m amsl]	934			815			12		
Month	Mean Maximum Air Temperature [°C]	Mean Minimum Air Temperature [°C]	Mean Rainfall [mm]	Mean Maximum Air Temperature [°C]	Mean Minimum Air Temperature [°C]	Mean Rainfall [mm]	Mean Maximum Air Temperature [°C]	Mean Minimum Air Temperature [°C]	Mean Rainfall [mm]
January	9.4	4.5	158.8	11.8	6.4	133.2	20.8	9.6	3.5
February	10.1	4.3	129.7	12.6	6.4	118.3	22.1	10.6	5.8
March	13.3	6.3	94.9	15.4	8.4	92.7	25.5	13.6	3.7
April	19.5	10.6	43.1	21.5	12.6	24.5	31.1	17.8	1.7
May	25.0	14.3	5.7	25.3	15.7	3.2	35.4	21.5	1.0
June	28.3	17.0	0.0	27.6	17.8	0.0	38.7	24.2	0.0
July	29.8	18.8	0.0	29.0	19.4	0.0	39.9	25.9	0.0
August	29.8	18.8	0.0	29.4	19.5	0.0	39.8	26.2	0.0
September	28.1	17.7	1.5	28.2	18.6	0.3	37.3	24.5	0.0
October	23.7	15.1	24.5	24.7	16.6	15.4	33.0	21.0	3.5
November	16.7	10.3	85.5	18.8	12.3	60.8	27.2	15.5	3.5
December	11.5	6.4	138.4	14.0	8.4	105.7	22.3	11.2	6.0

A.2

Lake Kinneret; structure of composite profile

Core Segment	Segment Depth [cm]	Composite Core Depth [cm]	Section Length [cm]
Ki10_I_V_1.3 top	6.5 - 98.0	0.0 - 91.5	91.5
Ki10_I_V_1.3 bottom	1.4 - 35.2	91.6 - 125.3	33.8
Ki10_I_1.3-2.3	5.1 - 74.7	125.4 - 194.9	69.6
Ki10_II_1.8-2.8	29.5 - 70.0	195.0 - 235.4	40.5
Ki10_I_2.3-3.3	15.0 - 86.1	235.5 - 306.5	71.1
Ki10_II_2.8-3.8	38.3 - 89.7	306.6 - 357.9	51.4
Ki10_I_3.3-4.3	47.4 - 92.3	558.0 - 402.8	44.9
Ki10_II_3.8-4.8	45.6 - 98.3	402.9 - 455.5	52.7
Ki10_I_4.3-5.3	46.7 - 84.8	455.6 - 493.6	38.1
Ki10_II_4.8-5.8	33.7 - 98.0	493.7 - 557.9	64.3
Ki10_I_5.3-6.3	38.7 - 91.6	558.0 - 610.8	52.9
Ki10_II_5.8-6.8	43.2 - 69.6	610.9 - 637.2	26.4
Ki10_I_6.3-7.3	18.4 - 95.6	637.3 - 714.4	77.2
Ki10_II_6.8-7.8	47.0 - 80.8	714.5 - 748.2	33.8
Ki10_I_7.3-8.3	17.1 - 62.1	748.3 - 793.2	45.0
Ki10_II_7.8-8.8	17.1 - 75.9	793.3 - 852.0	58.8
Ki10_I_8.3-9.3	20.0 - 75.1	852.1 - 907.1	55.1
Ki10_II_8.8-9.8	26.5 - 91.2	907.2 - 971.8	64.7
Ki10_I_9.3-10.3	40.2 - 99.4	971.8 - 1031.0	59.2
Ki10_II_9.8-10.8	49.6 - 54.5	1031.1 - 1035.9	4.9
Ki10_I_10.3-11.3	2.3 - 75.5	1036.0 - 1109.1	73.2
Ki10_II_10.8-11.8	23.8 - 88.9	1109.2 - 1174.2	65.1
Ki10_I_11.3-12.3	27.4 - 62.8	1174.3 - 1209.6	35.4
Ki10_II_11.8-12.8	20.4 - 58.1	1209.7 - 1247.3	37.7
Ki10_I_12.3-13.3	3.2 - 68.5	1247.4 - 1312.6	65.3
Ki10_II_12.8-13.8	17.7 - 99.1	1312.7 - 1394.0	81.4
Ki10_II_13.8-14.8	5.0 - 101.2	1394.1 - 1490.2	96.2
Ki10_II_14.8-15.8	0.9 - 98.6	1490.3 - 1587.9	97.7
Ki10_II_15.8-16.8	13.7 - 101.1	1588.0 - 1675.3	87.4
Ki10_II_16.8-17.8	1.4 - 99.3	1675.4 - 1773.2	97.9

A.3

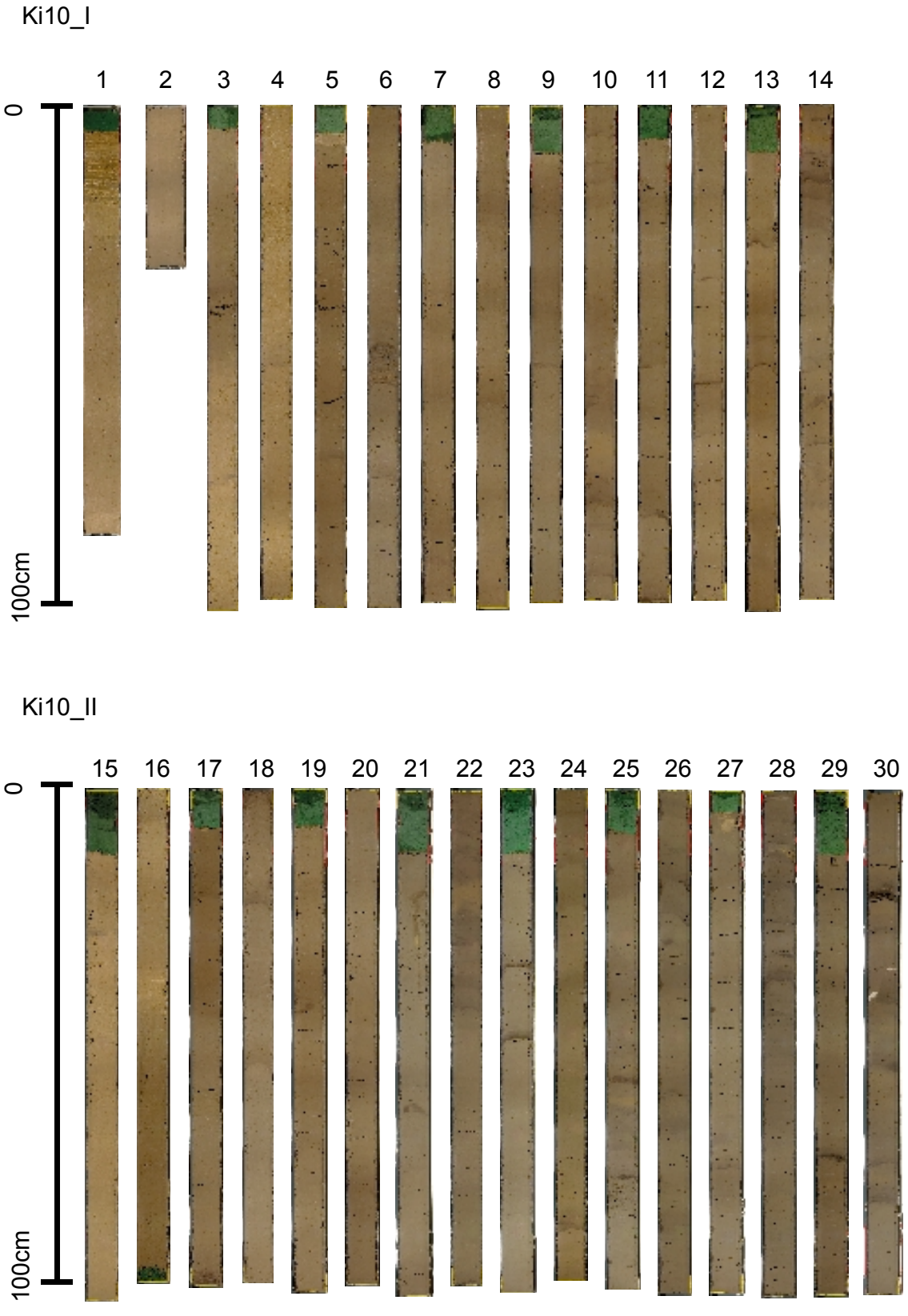

Lake Kinneret, segments of parallel cores, pictures by G. Oleschinski

Lake Kinneret; listing of pictured core segments

	Core Segment	Segment Length [cm]
1	Ki10_I_V1_1.3top	99.1
2	Ki10_I_V1_1.3bottom	37.4
3	Ki10_I_1.3-2.3	100.9
4	Ki10_I_2.3-3.3	99.0
5	Ki10_I_3.3-4.3	101.2
6	Ki10_I_4.3-5.3	98.9
7	Ki10_I_5.3-6.3	100.2
8	Ki10_I_6.3-7.3	100.0
9	Ki10_I_7.3-8.3	100.8
10	Ki10_I_8.3-9.3	99.5
11	Ki10_I_9.3-10.3	100.7
12	Ki10_I_10.3-11.3	99.7
13	Ki10_I_11.3-12.3	101.4
14	Ki10_I_12.3-13.3	99.4
15	Ki10_II_1.8-2.8	101.1
16	Ki10_II_2.8-3.8	99.0
17	Ki10_II_3.8-4.8	100.4
18	Ki10_II_4.8-5.8	100.4
19	Ki10_II_5.8-6.8	101.0
20	Ki10_II_6.8-7.8	99.5
21	Ki10_II_7.8-8.8	100.8
22	Ki10_II_8.8-9.8	99.6
23	Ki10_II_9.8-10.8	101.1
24	Ki10_II_10.8-11.8	100.0
25	Ki10_II_11.8-12.8	100.1
26	Ki10_II_12.8-13.8	100.6
27	Ki10_II_13.8-14.8	101.8
28	Ki10_II_14.8-15.8	99.4
29	Ki10_II_15.8-16.8	102.7
30	Ki10_II_16.8-17.8	99.7

Birkat Ram; listing of pictured core segments

	Core Segment	Segment Length [cm]
1	BR10_I_V1	96.8
2	BR10_I_V2top	74.3
3	BR10_I_V2bottom	54.5
4	BR10_I_0-1	91.9
5	BR10_I_1-2	98.2
6	BR10_I_2-3	88.5
7	BR10_I_3-4	97.6
8	BR10_I_4-5	90.1
9	BR10_I_5-6	73.7
10	BR10_I_6-7	119.2
11	BR10_I_7-8	104.5
12	BR10_I_8-9	99.0
13	BR10_I_9-10	76.0
14	BR 10_II_V1top	60.5
15	BR10_II_V1bottom	96.2
16	BR10_II_1.5-2.5	92
17	BR10_II_2.5-3.5	98
18	BR10_II_3.5-4.5	95
19	BR10_II_4.5-5.5	88.5
20	BR10_II_5.5-6.5	99.8
21	BR10_II_6.5-6.9	39.5
22	BR10_II_7.5-8.5	99
23	BR10_II_8.5-9.5	71.4
24	BR10_II_9.5-10.5	99.4
25	BR10_II_10.5-11.5	100.8

A.4

BR10_I

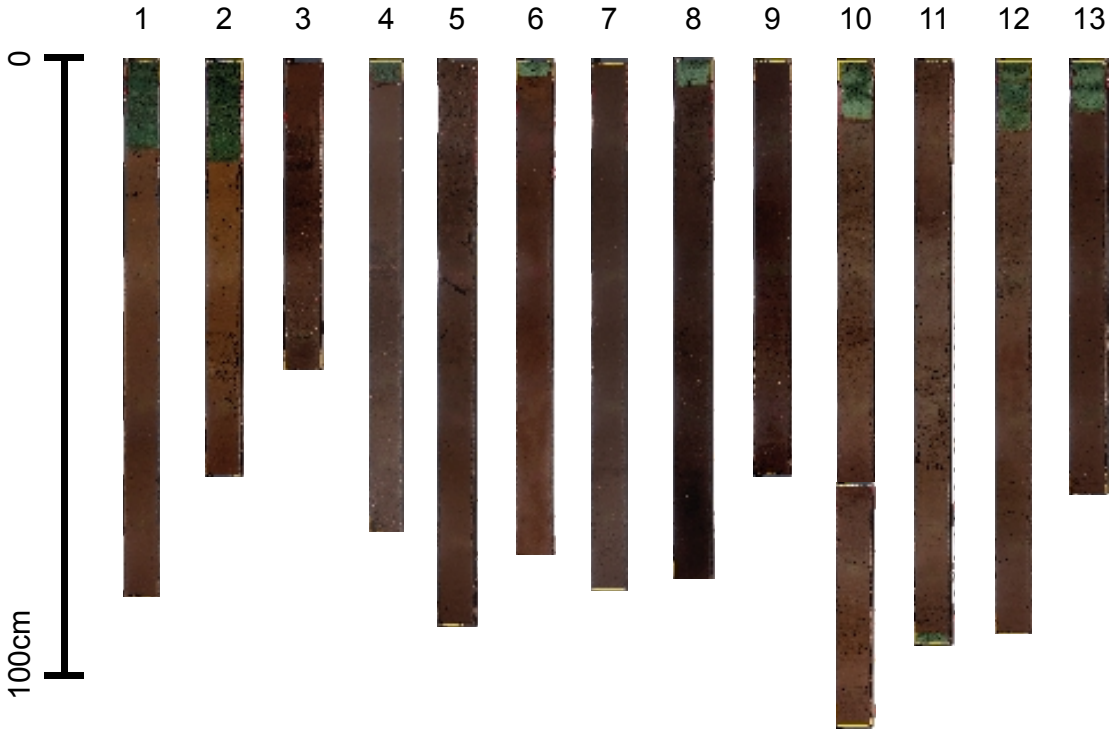

BR10_II

Birkat Ram; segments of parallel cores, pictures by G. Oleschinski

A.5

Lake Kinneret; detailed description of core segments after Rüßmann (2010)

Core Segment	Segment Lenght [cm]	Grain Size	Colour	Floral Foam; Segment Depth [cm]	Distinctly Colored Layers; Segment Depth [cm]
Ki10_I_V1top	99.1	U,t	light brown / grey	0.0 - 5.5	5.5 - 25.5 laminated deposition,
Ki10_I_V1bottom	37.4	U,t	light brown / grey	-	
Ki10_I_1.3-2.3	100.9	U,t	light brown / grey	0.0 - 4.0	
Ki10_I_2.3-3.3	99.0	U,t	light brown / grey	-	
Ki10_I_3.3-4.3	101.2	U,t	brown	0.0 - 6.0	
Ki10_I_4.3-5.3	98.9	U,t	brown	-	
Ki10_I_5.3-6.3	100.2	U,t	brown	0.0 - 7.5	
Ki10_I_6.3-7.3	100.0	U,t	brown	-	
Ki10_I_7.3-8.3	100.8	U,t	brown	0.0 - 9.0	
Ki10_I_8.3-9.3	99.5	U,t	brown	-	
Ki10_I_9.3-10.3	100.7	U,t	brown	0.0 - 7.0	
Ki10_I_10.3-11.3	99.7	U,t	brown	-	
Ki10_I_11.3-12.3	101.4	U,t	brown	0.0 - 9.0	81 -101-4 dark brown
Ki10_I_12.3-13.3	99.4	U,t	brown	-	0 - 28 dark brown
Ki10_II_1.8-2.8	101.1	U,t	light brown / grey	0.0 - 12.0	27.5 - 28.5 dark brown
Ki10_II_2.8-3.8	99.0	U,t	light brown / grey	96.0 - 99.0	
Ki10_II_3.8-4.8	100.4	U,t	brown / grey	0.0 - 7.5	
Ki10_II_4.8-5.8	100.4	U,t	brown / grey	-	21 - 23 dark grey
Ki10_II_5.8-6.8	101.0	U,t	brown / grey	0.0 - 7.5	
Ki10_II_6.8-7.8	99.5	U,t	brown / grey	-	
Ki10_II_7.8-8.8	100.8	U,t	brown / grey	0.0 - 12.5	62 - 64 dark brown
Ki10_II_8.8-9.8	99.6	U,t	brown / grey	-	19 - 23 light grey
Ki10_II_9.8-10.8	101.1	U,t	brown / grey	0.0 - 13.0	15 - 16 light grey, 35.5, 49.5 dark brown
Ki10_II_10.8-11.8	100.0	U,t	brown	-	
Ki10_II_11.8-12.8	100.1	U,t	brown / grey	0.0 - 9.0	
Ki10_II_12.8-13.8	100.6	U,t	brown / grey	-	
Ki10_II_13.8-14.8	101.8	U,t	brown / grey	0.0 - 4.0	
Ki10_II_14.8-15.8	99.4	U,t	brown / grey	-	32 - 33 dark grey
Ki10_II_15.8-16.8	102.7	U,t	brown / grey	0.0 - 13.0	75 - 76 dark grey
Ki10_II_16.8-17.8	99.7	U,t	brown / grey	-	20 - 22 dark grey, 81 - 82 dark brown

A.6

Lake Kinneret; samples analysed for pollen composition

Core Segment	Sample ID	Composite Depth [cm]
Ki10_I_V_1.3top	64	1
Ki10_I_V_1.3top	1	23
Ki10_I_V_1.3top	65	49
Ki10_I_V_1.3top	2	73
Ki10_I_V_1.3bottom	66	95
Ki10_I_V_1.3bottom	3	120
Ki10_I_1.3-2.3	67	125
Ki10_I_1.3-2.3	40	150
Ki10_I_1.3-2.3	68	175
Ki10_II_1.8-2.8	8	195
Ki10_II_1.8-2.8	69	220
Ki10_I_2.3-3.3	42	250
Ki10_I_2.3-3.3	70	275
Ki10_I_2.3-3.3	43	300
Ki10_II_2.8-3.8	71	323
Ki10_II_2.8-3.8	11	348
Ki10_I_3.3-4.3	72	366
Ki10_I_3.3-4.3	45	390
KI10_II_3.8-4.8	73	412
KI10_II_3.8-4.8	13	437
Ki10_I_4.3-5.3	74	464
Ki10_I_4.3-5.3	47	489
Ki10_II_4.8-5.8	75	515
Ki10_II_4.8-5.8	15	540
Ki10_I_5.3-6.3	76	574
Ki10_I_5.3-6.3	49	599
Ki10_II_5.8-6.8	77	626
Ki10_I_6.3-7.3	50	649
Ki10_I_6.3-7.3	78	674
Ki10_I_6.3-7.3	51	699
Ki10_II_6.8-7.8	79	722
Ki10_II_6.8-7.8	19	747
Ki10_I_7.3-8.3	52	761
Ki10_I_7.3-8.3	80	786
Ki10_II_7.8-8.8	20	806
Ki10_II_7.8-8.8	81	831
Ki10_I_8.3-9.3	54	862
Ki10_I_8.3-9.3	82	887
Ki10_II_8.8-9.8	22	911
Ki10_II_8.8-9.8	83	936
Ki10_II_8.8-9.8	23	961
Ki10_I_9.3-10.3	84	987
Ki10_I_9.3-10.3	57	1012
Ki10_I_10.3-11.3	58	1064
Ki10_I_10.3-11.3	85	1089
Ki10_I_10.8-11.8	26	1115
Ki10_I_10.8-11.8	86	1140
Ki10_I_10.8-11.8	27	1165
Ki10_I_11.3-12.3	60	1177
Ki10_I_11.3-12.3	87	1202
Ki10_II_11.8-12.8	28	1219
Ki10_II_11.8-12.8	88	1244
Ki10_I_12.3-13.3	62	1274
Ki10_I_12.3-13.3	89	1299
Ki10_II_12.8-13.8	30	1325
Ki10_II_12.8-13.8	90	1350
Ki10_II_12.8-13.8	31	1375
Ki10_II_13.8-14.8	91	1394
Ki10_II_13.8-14.8	32	1419
Ki10_II_13.8-14.8	92	1444
Ki10_II_13.8-14.8	33	1469
Ki10_II_14.8-15.8	93	1494
Ki10_II_14.8-15.8	34	1519
Ki10_II_14.8-15.8	94	1544
Ki10_II_14.8-15.8	35	1569
Ki10_II_15.8-16.8	95	1589
Ki10_II_15.8-16.8	36	1604
Ki10_II_15.8-16.8	96	1629
Ki10_II_15.8-16.8	37	1654
Ki10_II_16.8-17.8	97	1679
Ki10_II_16.8-17.8	38	1704
Ki10_II_16.8-17.8	98	1729
Ki10_II_16.8-17.8	39	1754

A.7

Birkat Ram; structure of composite profile

Core Segment	Segment Depth [cm]	Composite Core Depth [cm]	Section Length [cm]
BR10_I_0-1	5 - 99	0 - 94	94
BR10_I_1-2	0 - 60	95 - 155	60
BR10_II_1.5-2.5	15 - 82	156 - 223	67
BR10_I_2-3	24 - 72	224 - 272	48
BR10_II_2.5-3.5	30 - 48	273 - 291	18
BR10_I_3-4	9 - 86	292 - 369	77
BR10_II_3.5-4.5	27 - 72	370 - 415	45
BR10_I_4-5	36 - 74	416 - 454	38
BR10_II_4.5-5.5	20 - 75	455 - 510	55
BR10_I_5-6	37 - 68	511 - 542	31
BR10_II_5.5-6.9	19 - 79	543 - 603	60
BR10_I_6-7	22 - 98	604 - 681	76
BR10_I_7-8	0 - 21	682 - 776	21
BR10_II_7.5-8.5	25 - 79	777 - 831	54
BR10_I_8-9	48 - 88	832 - 872	40
BR10_II_8.5-9.5	23 - 54	873 - 904	31
BR10_I_9-10	33 - 47	905 - 919	14
BR10_II_9.5-10.5	20 - 95	920 - 995	75
BR10_II_10.5-11.5	0 - 100	996 - 1096	100

A.8

Birkat Ram; detailed description of core segments after Rüßmann (2012) and Geiger (2011)

Core Segment	Segment Lenght [cm]	Grain Size	Colour	Floral Foam; Segment Depth [cm]			Characteristics; Segment Depth [cm]
BR10_I_V1	96.8	U, t	brown / grey	0.0	-	16.5	
BR10_I_V2top	74.3	U, t	brown / grey	0.0	-	18.0	
BR10_I_V2bottom	54.5	U, t	dark brown / grey		-		
BR10_I_0-1	91.9	U, t	brown / grey	0.0	-	4.0	12 - 19 drk grey, 47 - 49 molluscs
BR10_I_1-2	98.2	U, t	brown / grey		-		0 - 4 molluscs
BR10_I_2-3	88.5	U, t	brown / grey	0.0	-	2.5	
BR10_I_3-4	97.6	U, t	brown / grey		-		
BR10_I_4-5	90.1	U, t	dark brown / grey	0.0	-	4.5	
BR10_I_5-6	73.7	U, t	dark brown / grey		-		
BR10_I_6-7	119.2	U, t	brown / grey	0.0	-	10.5	10.5 - 14.5 dark brown patches
BR10_I_7-8	104.5	U, t	brown / grey	103.0	-	104.5	55 - 74 porous
BR10_I_8-9	99.0	U, t	brown / grey	0.0	-	12.0	
BR10_I_9-10	76.0	U, t	dark brown / grey	0.0	-	9.0	
BR 10_II_V1top	60.5	U, t, fs	brown / grey	0.0	-	5.5	
BR10_II_V1bottom	96.2	U, t, fs	brown / grey		-		49 - 56 dark brown, 82 - 96 molluscs
BR10_II_1.5-2.5	92.0	U, t, fs	brown / grey	0.0	-	13.0	
BR10_II_2.5-3.5	98.0	U, t, fs	dark brown / grey		-		
BR10_II_3.5-4.5	95.0	U, t, fs	dark brown / grey	0.0	-	17.0	
BR10_II_4.5-5.5	88.5	U, t, fs	dark brown / grey		-		
BR10_II_5.5-6.5	99.8	U, t, fs	light brown / grey	0.0	-	8.5	
BR10_II_6.5-6.9	39.5	U, t	light brown / grey		-		23 - 33 porous
BR10_II_7.5-8.5	99.0	U, t	brown / grey	0.0	-	17.0	
BR10_II_8.5-9.5	71.4	U, t	brown / grey		-		
BR10_II_9.5-10.5	99.4	U, t	brown / grey	0.0	-	17.0	
BR10_II_10.5-11.5	100.8	U, t	dark brown / grey		-		

A.9

Birkat Ram; samples analysed for pollen composition

Core Segment	Sample ID	Composite Depth [cm]	Core Segment	Sample ID	Composite Depth [cm]
BR10_I_0-2	BR10-53	0	BR10_I_6-7_bottom	BR10-79	673
BR10_I_0-2	BR10-54	25	BR10_I_6-7_bottom	BR10-100	678
BR10_I_0-2	BR10-55	50	BR10_I_7-8	BR10-101	683
BR10_I_0-2	BR10-56	75	BR10_I_7-8	BR10-102	688
BR10_I_0-2	BR10-57	108	BR10_I_7-8	BR10-103	693
BR10_I_0-2	BR10-58	132	BR10_I_7-8	BR10-104	698
BR10_II_1.5-2.5	BR10-1	161	BR10_I_7-8	BR10-81	703
BR10_II_1.5-2.5	BR10-2	186	BR10_I_7-8	BR10-105	708
BR10_II_1.5-2.5	BR10-3	211	BR10_I_7-8	BR10-106	713
BR10_I_2-3	BR10-62	230	BR10_I_7-8	BR10-107	718
BR10_I_2-3	BR10-63	255	BR10_I_7-8	BR10-108	723
BR10_I_3-4	BR10-65	299	BR10_I_7-8	BR10-82	728
BR10_I_3-4	BR10-66	324	BR10_I_7-8	BR10-109	733
BR10_I_3-4	BR10-67	349	BR10_I_7-8	BR10-110	737
BR10_II_3.5-4.5	BR10-10	388	BR10_I_7-8	BR10-111	744
BR10_II_3.5-4.5	BR10-11	413	BR10_I_7-8	BR10-112	748
BR10_I_4-5	BR10-71	435	BR10_I_7-8	BR10-83	753
BR10_II-4.5-5.5	BR10-13	460	BR10_I_7-8	BR10-113	758
BR10_II-4.5-5.5	BR10-14	485	BR10_I_7-8	BR10-114	763
BR10_II-4.5-5.5	BR10-15	510	BR10_I_7-8	BR10-115	768
BR10_I_5-6	BR10-74	514	BR10_II_7.5-8.5	BR10-23	797
BR10_I_5-6	BR10-75	539	BR10_II_7.5-8.5	BR10-24	822
BR10_II_5.5-6.9	BR10-17	559	BR10_I_8-9	BR10-87	847
BR10_II_5.5-6.9	BR10-18	584	BR10_I_8-9	BR10-88	872
BR10_I_6-7_top	BR10-77	622	BR10_II_8.5-9.5	BR10-27	896
BR10_I_6-7_top	BR10-92	627	BR10_I_9-10	BR10-90	907
BR10_I_6-7_top	BR10-93	631	BR10_II_9.5-10.5	BR10-29	920
BR10_I_6-7_top	BR10-94	637	BR10_II_9.5-10.5	BR10-30	945
BR10_I_6-7_top	BR10-95	642	BR10_II_9.5-10.5	BR10-31	970
BR10_I_6-7_top	BR10-78	647	BR10_II_9.5-10.5	BR10-32	995
BR10_I_6-7_top	BR10-96	652	BR10_II_10.5-11.5	BR10-33	1015
BR10_I_6-7_bottom	BR10-97	657	BR10_II_10.5-11.5	BR10-34	1040
BR10_I_6-7_bottom	BR10-98	662	BR10_II_10.5-11.5	BR10-35	1065
BR10_I_6-7_bottom	BR10-99	667	BR10_II_10.5-11.5	BR10-36	1090

A 10 (Lake Kinneret pollen diagram)

and

A11 (Birkat Ram pollen diagram)

being folded pages inside back cover of the thesis

11 Table of figures and charts

Fig. 3.1:	Map of Israel and adjacent areas; Birkat Ram, and Lake Kinneret	11
Fig. 3.2:	Topographical map of Israel and adjacent areas	13
Fig. 3.3:	Geological map of the Lake Kinneret area, and Birkat Ram area	14
Fig. 3.4:	Israeli climate diagrams	16
Fig. 3.5:	Map of Israel and adjacent areas indicating mean annual precipitation	17
Fig. 3.6:	Distribution of vegetation zones in Israel and adjacent areas	20
Fig. 4.1:	Lake Kinneret, uppermost 25 cm laminated sediments	24
Fig. 4.1:	Lake Kinneret; composite profile of parallel cores	25
Fig. 4.2:	Lake Kinneret; age-to-depth model I	29
Fig. 4.3:	Lake Kinneret; age-to-depth model II	30
Fig. 4.4:	Birkat Ram; oxidised root cast fragments	31
Fig. 4.5:	Birkat Ram; composite profile of parallel cores	32
Fig. 4.6:	Birkat Ram; age-to-depth model	36
Fig. 5.1:	Lake Kinneret; pollen diagram	43
Fig. 5.2:	Birkat Ram; correlation with a profile from Birkat Ram in 1999	48
Fig. 5.3:	Birkat Ram; pollen diagram	52
Fig. 6.1:	Birkat Ram; fruit of *Polygonum sp*.,	59
Fig. 6.2:	Correlation of pollen records along a north-to-south-transect	64
Fig. 6.3:	Lake Kinneret; correlation with a profile from Lake Kinneret 1979	70

Table 2.1:	Chronology of archaeological and historical periods in the Near East	9
Table 4.1:	Lake Kinneret; AMS ^{14}C data	28
Table 4.2:	Birkat Ram; AMS ^{14}C data	34
Table 4.3:	Birkat Ram; AMS ^{14}C data from Birkat Ram profile, cored in 1999	35
Table 5.1:	Lake Kinneret, pollen zonation of composite profile	44
Table 5.2:	Lake Kinneret, pollen zonation of composite profile	53

12 References

AHLSTRÖM, G. W. (1993). The History of Ancient Palestine from the Palaeolithic Period to Alexander's Conquest. *Journal for the Study of the Old Testament*, Supplement Series 146.

ALLEY, R. B. & ÁGÚSTSDÓTTIR, A. M. (2005). The 8k event: cause and consequences of a major Holocene abrupt climate change. *Quaternary Science Reviews*, 24:1123-1149.

ALLEY, R. B., MAYEWSKI, P. A., SOWERS, T., STUIVER, M., TAYLOR, K. C. & CLARK, P. U. (1997). Holocene climatic instability: A prominent, widespread event 8200 yr ago. *Geology*, 25:483-486.

ALPERT, P., NEEMAN, B. U. & SHAY-EL, Y. (1990). Climatological analysis of Mediterranean cyclones using ECMWF data. *Tellus Series a-Dynamic Meteorology and Oceanography*, 42:65-77.

ANDERSON, J. (1995). The impact of Rome on the periphery: the case of Palestina-Roman Period (63 BCE-324 CE). In *The archaeology of society in the Holy Land*, ed. T. E. Levy. London: Leicester Univ. Press, 1995.

AVIAM, M. (2011). Socio-Economic Hierarchy and its Economic Foundations in First Century Galilee: The Evidence from Yodefat and Gamla. In *Flavius Josephus*, ed. J. Pastor, P. Stern & M. Mor. Leiden: Koninklijke Brill NV, 2011.

AYALON, A., BAR-MATTHEWS, M., FRUMKIN, A. & MATTHEWS, A. (2013). Last Glacial warm events on Mount Hermon: the southern extension of the Alpine karst range of the east Mediterranean. *Quaternary Science Reviews*, 59:43-56.

BAR-MATTHEWS, M. & AYALON, A. (2005). Speleothems as paleoclimate indicators, a case study from Soreq Cave located in the eastern Mediterranean Region, Israel. In *Past Climate through Europe and Africa: Developments in Paleoenvironmental Research*, ed. R. W. Battarbee, F. Gasse & C. E. Stickley. Dordrecht: Springer, 2005.

BAR-MATTHEWS, M., AYALON, A., KAUFMAN, A. & WASSERBURG, G. J. (1999). The Eastern Mediterranean paleoclimate as a reflection of regional events: Soreq cave, Israel. *Earth and Planetary Science Letters*, 166:85-95.

BAR-YOSEF, O. (1995). Earliest food producers - Pre-Pottery Neolithic (8,000-5,500). In *The archaeology of society in the Holy Land*, ed. T. E. Levy. London: Leicester Univ. Press, 1995.

BAR-YOSEF, O. (1998). The Natufian culture in the Levant, threshold to the origins of agriculture. *Evolutionary Anthropology: Issues, News, and Reviews*, 6:159-177.

BAR-YOSEF, O. (2000). The impact of radiocarbon dating on Old World archaeology: past achievements and future expectations. *Radiocarbon*, 42:23-40.

BAR-YOSEF, O. (2011). Climatic Fluctuations and Early Farming in West and East Asia. *Current Anthropology*, 52:S175-S193.

BARD, E., HAMELIN, B. & DELANGHE-SABATIER, D. (2010). Deglacial Meltwater Pulse 1B and Younger Dryas Sea Levels Revisited with Boreholes at Tahiti. *Science*, 327:1235-1237.

BARTINGTON-INSTRUMENTS-LIMITED. (1995). Preliminary Specification for the MS2E Sensor: Bartington Instruments Limited, Oxford, 1995.

BARUCH, U. (1986). The Late Holocene Vegetational History of Lake Kinneret (Sea of Galilee), Israel. *Paléorient*:37-48.

BARUCH, U. (1990). Palynological evidence of human impact on the vegetation as recorded in Late Holocene lake sediments in Israel. In *Man's Role in the Shaping of the Eastern Mediterranean Landscape*, ed. S. Bottema, Entjes-Nieborg, G. & vanZeist, W. Rotterdam: Balkema, 1990, pp. 283-293.

BARUCH, U. & BOTTEMA, S. (1991). Palynological evidence for climatic changes in the Levant ca. 17,000-9,000 BP. In *The Natufian culture in the Levant*, ed. O. Bar-Yosef & F. R. Valla, 1991.

BARUCH, U. & BOTTEMA, S. (1999). A new pollen diagram from Lake Hula: vegetational, climatic and anthropogenic implications. In *Ancient Lakes: Their Cultural and Biological Diversity, Kenobi Productions*, ed. H. Kawanabe, G. W. Coulter & A. C. Roosevelt. Ghent: Kenobi Productions, 1999, pp. 75–86.

BEHRE, K.-E. (1990). Some reflections on anthropogenic indicators and the record of prehistoric occupation phases in pollen diagrams from the Near East. *Man's role in the shaping of the eastern Mediterranean landscape. Balkema, Rotterdam*:219-231.

BELFER-COHEN, A. & BAR-YOSEF, O. (2002). Early Sedentism in the Near East. *Life in Neolithic Farming Communities*:19-38.

BELFER-COHEN, A. & GORING-MORRIS, A. N. (2011). Becoming Farmers: The Inside Story. *Current Anthropology*, 52:S209-S220.

BERELOV, I. (2006). Signs of sedentism and mobility in an agro-pastoral community during the Levantine Middle Bronze Age: Interpreting site function and occupation strategy at Zahrat adh-Dhra' 1 in Jordan. *Journal of Anthropological Archaeology*, 25:117-143.

BERGLUND, B. E., BIRKS, H. J. B., RALSKA-JASIEWICZOWA, M. & WRIGTH, H. E. (1996). *Palaeoecological Events During the Last 15 000 Years*. West Sussex: John Wiley & Sons.

BERGLUND, B. E. & RALSKA-JASIEWICZOWA, M. (1986). Pollen analysis and pollen diagrams. In *Handbook of Holocene palaeoecology and palaeohydrology*, ed. B. E. Berglund & M. Ralska-Jasiewiczowa. New York: Wiley, 1986, pp. 455-484.

BERLIN, A. M. (1997). Archaeological Sources for the History of Palestine: Between Large Forces: Palestine in the Hellenistic Period. *The Biblical Archaeologist*, 60:2-51.

BEUG, H.-J. (2004). *Leitfaden der Pollenbestimmung für Mitteleuropa und angrenzende Gebiete*. München: Verlag Dr. Friedrich Pfeil

BIRKS, H. J. B. & BIRKS, H. H. (1980). *Quaternary palaeoecology*. London: Arnold.

BITAN, A. (1974). The wind regime in the north-west section of the Dead-Sea. *Theoretical and Applied Climatology*, 22:313-335.

BITAN, A. (1981). Lake Kinneret (Sea of Galilee) and its exceptional wind system. *Boundary-Layer Meteorology*, 21:477-487.

BLAAUW, M. (2010). Methods and code for 'classical' age-modelling of radiocarbon sequences. *Quaternary Geochronology*, 5:512-518.

BOND, G., SHOWERS, W., CHESEBY, M., LOTTI, R., ALMASI, P., DEMENOCAL, P., PRIORE, P., CULLEN, H., HAJDAS, I. & BONANI, G. (1997). A Pervasive Millennial-Scale Cycle in North Atlantic Holocene and Glacial Climates. *Science*, 278:1257-1266.

BONHOMMET, N. & ZÄHRINGER, J. (1969). Paleomagnetism and potassium argon age determinations of the Laschamp geomagnetic polarity event. *Earth and Planetary Science Letters*, 6:43-46.

BOTTEMA, S. (1992). Prehistoric cereal gathering and farming in the Near East: the pollen evidence. *Review of Palaeobotany and Palynology*, 73:21-33.

BOTTEMA, S. (1995). The Younger Dryas in the Eastern Mediterranean. *Quaternary Science Reviews*, 14:883-891.

BOUCHER, K. (1975). *Global Climate*. London: English Universities Press.

BOYD, B. (2006). On 'Sedentism' in the Later Epipalaeolithic (Natufian) Levant. *World Archaeology*, 38:164-178.

BROECKER, W. S., DENTON, G. H., EDWARDS, R. L., CHENG, H., ALLEY, R. B. & PUTNAM, A. E. (2010). Putting the Younger Dryas cold event into context. *Quaternary Science Reviews*, 29:1078-1081.

BUNIMOWITZ, S. (1995). On the edge of empires - Late Bronze Age (1,500-1,200 BCE). In *The archaeology of society in the Holy Land*, ed. T. E. Levy. Londone: Leicester Univ. Press, 1995.

BURTON, M. & LEVY, T. E. (2001). The Chalcolithic Radiocarbon Record And Its Use In Southern Levantine Archaeology. *Radiocarbon*, 43.

CHANCEY, M. A. & PORTER, A. L. (2001). The Archaeology of Roman Palestine. *Near Eastern Archaeology*, 64:164-203.

CHILDE, G. (1936). *Man Makes Himself*: Oxford university press.

DANIN, A. (1988). *Flora and vegetation of Israel and adjacent areas*. Den Haag, PAYS-BAS: Junk.

DANIN, A. (1999). Desert rocks as plant refugia in the Near East. *The botanical review*:93.

DANIN, A. (2001). Near East ecosystems, plant diversity. In *Encyclopedia of Biodiversity*, ed. S. Levin: Academic Press, 2001.

DANIN, A. & PLITMANN, U. (1987). Revision of the plant geographical territories of Israel and Sinai. *Plant Systematics and Evolution*, 156:43-53.

DANSGAARD, W., JOHNSEN, S. J., CLAUSEN, H. B., DAHL-JENSEN, D., GUNDESTRUP, N. S., HAMMER, C. U., HVIDBERG, C. S., STEFFENSEN, J. P., SVEINBJORNSDOTTIR, A. E., JOUZEL, J. & BOND, G. (1993). Evidence for general instability of past climate from a 250-kyr ice-core record. *Nature*, 364:218-220.

DAR, S. (1993). Settlements and cult sites on Mount Hermon, Israel. Iturean Culture in the Hellenistic and Roman Periods. In *BAR International Series 589*, 1993, pp. 325.

DAVIES, C. P. & FALL, P. L. (2001). Modern pollen precipitation from an elevational transect in central Jordan and its relationship to vegetation. *Journal of Biogeography*, 28:1195-1210.

DAVIS, M. B. (2000). Palynology after Y2K – understanding the source area of pollen in sediments. *Annual Review of Earth and Planetary Sciences*, 28:1-18.

DAYAN, U., ZIV, B., SHOOB, T. & ENZEL, Y. (2008). Suspended dust over southeastern Mediterranean and its relation to atmospheric circulations. *International Journal of Climatology*, 28:915-924.

DEEVEY, E. S., GROSS, M. S., HUTCHINSON, G. E. & KRAYBILL, H. L. (1954). The Natural C14 Contents of Materials from Hard-Water Lakes. *Proceedings of the National Academy of Sciences*, 40:285-288.

DESCHAMPS, P., DURAND, N., BARD, E., HAMELIN, B., CAMOIN, G., THOMAS, A. L., HENDERSON, G. M., OKUNO, J. I. & YOKOYAMA, Y. (2012). Ice-sheet collapse and sea-level rise at the Bolling warming 14,600 years ago. *Nature*, 483:559-564.

DEVELLE, A. L., GASSE, F., VIDAL, L., WILLIAMSON, D., DEMORY, F., VAN CAMPO, E., GHALEB, B. & THOUVENY, N. (2011). A 250ka sedimentary record from a small karstic lake in the Northern Levant (Yammoûneh, Lebanon): Paleoclimatic implications. *Palaeogeography, Palaeoclimatology, Palaeoecology*, 305:10-27.

DEVELOPMENT-CORE-TEAM. (2011). R: A language and environment for statistical computing. R Foundation for Statistical Computing, Vienna, Austria. ISBN 3-900051-07-0, 2011.

DEVER, W. G. (1995). Social structure in the Early Bronze IV period in Palestine. In *The archaeology of society in the Holy Land*, ed. T. E. Levy. London: Leicester Univ. Press, 1995.

EHRLICH, A. & SINGER, A. (1976). Late Pleistocene Diatom Succession in a Sediment Core from B irket Ram, Golan Heights. *Israel Journal of Earth Science*, 25:138-151.

EIG, G., ZOHARY, M. & FEINBRUN, N. (1931). *The Plants of Palestine: an analytical key*. Jerusalem University Press.

EPSTEIN, C. (1977). The Chalcolithic Culture of the Golan. *The Biblical Archaeologist*, 40:57-62.

EPSTEIN, C. (1998). The Chalcolithic Culture of the Golan. In *Israel Antiquities Authority Report 4*, 1998, pp. 352.

FAEGRI, K. & IVERSEN, J. (1989). *Textbook of pollen analysis*. Chichester: Wiley.

FALL, P. L. (2012). Modern vegetation, pollen and climate relationships on the Mediterranean island of Cyprus. *Review of Palaeobotany and Palynology*, 185:79-92.

FALL, P. L., LINES, L. & FALCONER, S. E. (2004). Seeds of Civilization: Bronze Age Rural Economy and Ecology in the Southern Levant. *Annals of the Association of American Geographers*, 88:107-125.

FANTALKIN, A., FINKELSTEIN, I. & PIASETZKY, E. (2011). *Iron Age Mediterranean Chronology: A Rejoinder*.

FINKELSTEIN, I. & PIASETZKY, E. L. I. (2009). Radiocarbon-Dated Destruction Layers: a Skeleton for Iron Age Chronology in the Levant. *Oxford Journal of Archaeology*, 28:255-274.

FINKELSTEIN, I., SILBERMAN, N. A. & MAGALL, M. (2004). *Keine Posaunen vor Jericho*: Dtv.

FRUMKIN, A., FORD, D. C. & SCHWARCZ, H. P. (1999). Continental Oxygen Isotopic Record of the Last 170,000 Years in Jerusalem. *Quaternary Research*, 51:317-327.

GAT, J. R. & MAGARITZ, M. (1980). Climatic variations in the Eastern Mediterranean Sea area. *Naturwissenschaften*, 67:80-87.

GEIGER, K. (2011). *Sedimentologische Analyse von Bohrkernen des Birkat Ram-Sees, Golan Höhen, Israel*, Rheinischen Friedrich-Wilhelms-Universität Bonn. Unpublished.

GEOLOGICAL-SURVEY-OF-ISRAEL. (2012). www.gsi.gov.il, 2012.

GEYH, M. A., SCHOTTERER, U. & GROSJEAN, M. (1998). *Temporal changes of the (super 14) C reservoir effect in lakes*.

GIBSON, S. & ROWAN, Y. (2006). The Chalcolithic in the Central Highlands of Palestine: A Reassessment Based on a New Examination of Khirbet es-Sauma'a. *Levant*, 38:85-108.

GIESECKE, T., FONTANA, S., VAN DER KNAAP, W., PARDOE, H. & PIDEK, I. (2010). From early pollen trapping experiments to the Pollen Monitoring Programme. *Vegetation History and Archaeobotany*, 19:247-258.

GOPHER, A. (1995). Early pottery-bearin groups in Israel - the Pottery Neolithic period. In *The archaeology of society in the Holy Land*, ed. T. E. Levy. London: Leicester Univ. Press, 1995.

GOPHNA, R. (1995). Early Bronze Age Canaan: Some spatial and demographic observations. In *The archaeology of society in the Holy Land*, ed. T. E. Levy. London: Leicester Univ. Press, 1995.

GORING-MORRIS, A. N. & BELFER-COHEN, A. (2011). Neolithization Processes in the Levant: The Outer Envelope. *Current Anthropology*, 52:S195-S208.

GREENBERG, R. (2011). Life In the City: Tel Bet Yerah in the Early Bronze Age. In *Daily Life, Materiality, and Complexity in Early Urban Communities of the Southern Levant - Papers in Honour of Walter E. Rast and R. Thomas Schaub*, ed. M. S. Chesson. Winona Lake, Indiana: Eisenbrauns, 2011, pp. 41-54.

GREENBERG, R. & PAZ, Y. (2005). The Early Bronze Age Fortifications of Tel Bet Yerah. *Levant*, 37:81-103.

GRIMM, E. C. (1987). CONISS: a FORTRAN 77 program for stratigraphically constrained cluster analysis by the method of incremental sum of squares. *Computers & Geosciences*, 13:13-35.

GRIMM, E. C. (2011). TILIA: a Pollen Program for Analysis and Display. Illinois, 2011.

GRIMM, E. C., MAHER JR, L. J. & NELSON, D. M. (2009). The magnitude of error in conventional bulk-sediment radiocarbon dates from central North America. *Quaternary Research*, 72:301-308.

GROOTES, P. M., STUIVER, M., WHITE, J. W. C., JOHNSEN, S. & JOUZEL, J. (1993). Comparison of oxygen isotope records from the GISP2 and GRIP Greenland ice cores. *Nature*, 366:552-554.

GROSMAN, L. (2003). Preserving Cultural Traditions in a Period of Instability: The Late Natufian of the Hilly Mediterranean Zone. *Current Anthropology*, 44:571-580.

GVIRTZMAN, G. & WIEDER, M. (2001). Climate of the last 53,000 Years in the eastern Mediterranean, based on soil-sequence Stratigraphy in the coastal plain of Israel. *Quaternary Science Reviews*, 20:1827-1849.

HAJAR, L., HAÏDAR-BOUSTANI, M., KHATER, C. & CHEDDADI, R. (2010). Environmental changes in Lebanon during the Holocene: Man vs. climate impacts. *Journal of Arid Environments*, 74:746-755.

HAJAR, L., KHATER, C. & CHEDDADI, R. (2008). Vegetation changes during the late Pleistocene and Holocene in Lebanon: a pollen record from the Bekaa Valley. *The Holocene*, 18:1089-1099.

HAZAN, N. (2004). Lake Kinneret levels and active faulting in the Tiberias area. *Israel Journal of Earth-Sciences*, 53:199.

HAZAN, N., STEIN, M., AGNON, A., MARCO, S., NADEL, D., NEGENDANK, J. F. W., SCHWAB, M. J. & NEEV, D. (2005). The late Quaternary limnological history of Lake Kinneret (Sea of Galilee), Israel. *Quaternary Research*, 63:60-77.

HOLLADAY JR, J. S. (1995). The kingdoms of Israel and Judah: Political and economic centralization in the Iron IIA - B (ca. 1,000-750 BCE). In *The archaeology of society in the Holy Land*, ed. T. E. Levy. London: Leicester Univ. Press, 1995.

HOROWITZ, A. (1971). Climatic and vegetational developments in northeastern Israel during Upper Pleistocene-Holocene times. *Pollen et Spores*, 13:255-278.

HOROWITZ, A. (1979). *The Quaternary of Israel*. New York/London: Academic Press.

HOROWITZ, A. (1984). Continuous Late Cenozoic pollen diagrams from Israel: stratigraphy, paleoclimatology and global correlations. *Proc. Int. Palynol., Congr., 6th, Calgary*, 66.

ILAN, D. (1995). The dawn of internationalism - the Middle Bronze Age. In *The archaeology of society in the Holy Land*, ed. T. E. Levy. London: Leicester Univ. Press, 1995.

ISRAEL-OCEEANOGRAPHIC&LIMNOLOGICAL-RESEARCH. (2010). http://isramar.ocean.org.il, 2010.

ISSAR, A. & ZOHAR, M. (2004). *Climate change: environment and civilization in the Middle East*: Springer Verlag.

JAFFE, S. (1988). Climate of Israel. In *The Zoogeography of Israel*, ed. Y. Yom Tov & E. Tchernov, 1988, pp. 79-95.

JANSSEN, C. R. (1973). Local and regional pollen deposition. In *Quaternary plant ecology*, ed. H. J. B. Birks & R. G. West. Oxford: Blackwell, 1973, pp. 31-42.

KANIEWSKI, D., PAULISSEN, E., VAN CAMPO, E., BAKKER, J., VAN LERBERGHE, K. & WAELKENS, M. (2009). Wild or cultivated Olea europaea L. in the eastern Mediterranean during the middle—late Holocene? A pollen-numerical approach. *The Holocene*, 19:1039-1047.

KANIEWSKI, D., VAN CAMPO, E., BOIY, T., TERRAL, J.-F., KHADARI, B. & BESNARD, G. (2012). Primary domestication and early uses of the emblematic olive tree: palaeobotanical, historical and molecular evidence from the Middle East. *Biological Reviews*, 87:885-899.

KARMON, Y. (1994). *Israel. Eine geographische Landeskunde*. Darmstadt: Wissenschaftliche Buchgesellschaft.

KOLODNY, Y., STEIN, M. & MACHLUS, M. (2005). Sea-rain-lake relation in the Last Glacial East Mediterranean revealed by δ18O-δ13C in Lake Lisan aragonites. *Geochimica et Cosmochimica Acta*, 69:4045-4060.

KOTTHOFF, U., MÜLLER, U. C., PROSS, J., SCHMIEDL, G., LAWSON, I. T., VAN DE SCHOOTBRUGGE, B. & SCHULZ, H. (2008). Lateglacial and Holocene vegetation dynamics in the Aegean region: an integrated view based on pollen data from marine and terrestrial archives. *The Holocene*, 18:1019-1032.

KUIJT, I. & GORING-MORRIS, N. (2002). Foraging, Farming, and Social Complexity in the Pre-Pottery Neolithic of the Southern Levant: A Review and Synthesis. *Journal of World Prehistory*, 16:361-440.

KUSHNIR, Y. & STEIN, M. (2010). North Atlantic influence on 19th–20th century rainfall in the Dead Sea watershed, teleconnections with the Sahel, and implication for Holocene climate fluctuations. *Quaternary Science Reviews*, 29:3843-3860.

LANGGUT, D., ALMOGI-LABIN, A., BAR-MATTHEWS, M. & WEINSTEIN-EVRON, M. (2011). Vegetation and climate changes in the South Eastern Mediterranean during the Last Glacial-Interglacial cycle (86 ka): new marine pollen record. *Quaternary Science Reviews*, 30:3960-3972.

LEROY, S. A. G. (2010). Pollen analysis of core DS7-1SC (Dead Sea) showing intertwined effects of climatic change and human activities in the Late Holocene. *Journal of Archaeological Science*, 37:306-316.

LEV, L., BOARETTO, E., HELLER, J., MARCO, S. & STEIN, M. (2007). *The Feasibility of Using Melanopsis Shells as Radiocarbon Chronometers, Lake Kinneret, Israel*.

LEVY, T. E. (1995). *The archaeology of society in the Holy Land*. London: Leicester Univ. Press.

LIPHSCHITZ, N. (2000). Archaeobotanical Findings. In *Megiddo III - The 1992-1996 Seasons*, ed. I. Finkelstein, D. Ussishkin & B. Halpem. Tel Aviv: Tel Aviv University, 2000.

LIPHSCHITZ, N. & BIGER, G. (2001). Past distribution of Aleppo pine (Pinus halepensis) in the mountains of Israel (Palestine). *The Holocene*, 11:427-436.

LITT, T., BRAUER, A., GOSLAR, T., MERKT, J., BAŁAGA, K., MÜLLER, H., RALSKA-JASIEWICZOWA, M., STEBICH, M. & NEGENDANK, J. F. W. (2001). Correlation and synchronisation of Lateglacial continental sequences in northern central Europe based on annually laminated lacustrine sediments. *Quaternary Science Reviews*, 20:1233-1249.

LITT, T., KRASTEL, S., STURM, M., KIPFER, R., ÖRCEN, S., HEUMANN, G., FRANZ, S. O., ÜLGEN, U. B. & NIESSEN, F. (2009). 'PALEOVAN', International Continental Scientific Drilling Program (ICDP): site survey results and perspectives. *Quaternary Science Reviews*, 28:1555-1567.

LITT, T., OHLWEIN, C., NEUMANN, F. H., HENSE, A. & STEIN, M. (2012). Holocene climate variability in the Levant from the Dead Sea pollen record. *Quaternary Science Reviews*, 49:95-105.

LITT, T. & STEBICH, M. (1999). Bio- and chronostratigraphy of the lateglacial in the Eifel region, Germany. *Quaternary International*, 61:5-16.

LOVELL, J. (2002). Shifting Subsistence Patterns : some Ideas about the End of the Chalcolithic in the southern Levant. *Paléorient*:89-102.

LOWE, D. J. (2011). Tephrochronology and its application: A review. *Quaternary Geochronology*, 6:107-153.

MAYEWSKI, P. A., ROHLING, E. E., CURT STAGER, J., KARLÉN, W., MAASCH, K. A., DAVID MEEKER, L., MEYERSON, E. A., GASSE, F., VAN KREVELD, S., HOLMGREN, K., LEE-THORP, J., ROSQVIST, G., RACK, F., STAUBWASSER, M., SCHNEIDER, R. R. & STEIG, E. J. (2004). Holocene climate variability. *Quaternary Research*, 62:243-255.

MAZAR, A. (1992). *Archaeology of the land of the Bible: 10,000-586 B.C.E.* New York: Doubleday.

MEADOWS, J. (2005). The Younger Dryas episode and the radiocarbon chronologies of the Lake Huleh and Ghab Valley pollen diagrams, Israel and Syria. *The Holocene*, 15:631-636.

MIX, A. C., BARD, E. & SCHNEIDER, R. (2001). Environmental processes of the ice age: land, oceans, glaciers (EPILOG). *Quaternary Science Reviews*, 20:627-657.

MOORE, P. D., WEBB, J. A. & COLLINSON, M. E. (1991). *Pollen analysis*. Oxford: Blackwell.

MURPHY, M. A. (1999). Special-International Stratigraphic Guide--An abridged version. *Episodes*, 22:255.

NEEF, R. (1990). Introduction, development and environmental implications of olive culture: The evidence from Jordan. In *Man's Role in the Shaping of the Eastern Mediterranean Landscape*, ed. Bottema, Entjes-Nieborg & W. van Zeist. Rotterdam: Balkema, 1990, pp. 295-306.

NEUMANN, F., SCHÖLZEL, C., LITT, T., HENSE, A. & STEIN, M. (2007a). Holocene vegetation and climate history of the northern Golan heights (Near East). *Vegetation History and Archaeobotany*, 16:329-346.

NEUMANN, F. H., KAGAN, E. J., LEROY, S. A. G. & BARUCH, U. (2010). Vegetation history and climate fluctuations on a transect along the Dead Sea west shore and their impact on past societies over the last 3500 years. *Journal of Arid Environments*, 74:756-764.

NEUMANN, F. H., KAGAN, E. J., SCHWAB, M. J. & STEIN, M. (2007b). Palynology, sedimentology and palaeoecology of the late Holocene Dead Sea. *Quaternary Science Reviews*, 26:1476-1498.

NIKLEWSKI, J. & VAN ZEIST, W. (1970). A late Quaternary pollen diagram from northwestern Syria. *Acta Botanica Neerlandica*, 19:737-754.

NISHRI, A., STILLER, M., RIMMER, A., GEIFMAN, Y. & KROM, M. (1999). Lake Kinneret (The Sea of Galilee): the effects of diversion of external salinity sources and the probable chemical composition of the internal salinity sources. *Chemical Geology*, 158:37-52.

OLSSON, I. (1991). Accuracy and precision in sediment chronology. *Hydrobiologia*, 214:25-34.

PAIN, S. (2013). Coffee dregs: is this the end of coffee? *New Scientist*, 217:32-35.

PASTOR, J. (1997). *Land and Economy in Ancient Palestine*. London: Routledge.

PAZ, Y. (2011). 'Raiders on the Storm': The Violent Destruction of Leviah, an Early Bronze Age Urban Centre in the Southern Levant. *Journal of Conflict Archaeology*, 6:3-21.

PETIT, J. R., JOUZEL, J., RAYNAUD, D., BARKOV, N. I., BARNOLA, J. M., BASILE, I., BENDER, M., CHAPPELLAZ, J., DAVIS, M., DELAYGUE, G., DELMOTTE, M., KOTLYAKOV, V. M., LEGRAND, M., LIPENKOV, V. Y., LORIUS, C., PEPIN, L., RITZ, C., SALTZMAN, E. & STIEVENARD, M. (1999). Climate and atmospheric history of the past 420,000 years from the Vostok ice core, Antarctica. *Nature*, 399:429-436.

PICARD, L. (1952). The Pleistocene peat of lake Hula. *Bull. Res. Counc. Isr. G*, 2:147-156.

PLENIER, G., VALET, J.-P., GUÉRIN, G., LEFÈVRE, J.-C., LEGOFF, M. & CARTER-STIGLITZ, B. (2007). Origin and age of the directions recorded during the Laschamp event in the Chaîne des Puys (France). *Earth and Planetary Science Letters*, 259:414-431.

PLICHT, J. V. D., BRUINS, H. J. & NIJBOER, A. J. (2009). The Iron Age around the Mediterranean: A High Chronology Perspective from the Groningen Radiocarbon Database.

PRENTICE, I. C. & WEBB, T. (1986). Pollen percentages, tree abundances and the Fagerlind effect. *Journal of Quaternary Science*, 1:35-43.

PROSS, J., KOTTHOFF, U., MÜLLER, U. C., PEYRON, O., DORMOY, I., SCHMIEDL, G., KALAITZIDIS, S. & SMITH, A. M. (2009). Massive perturbation in terrestrial ecosystems of the Eastern Mediterranean region associated with the 8.2 kyr B.P. climatic event. *Geology*, 37:887-890.

REILLE, M. (1990-1999). *Pollen et spores d'Europe et d'Afrique du nord*. Marseille: Index.

REIMER, P. J. (2009). INTCAL 09 and MARINE09 radiocarbon age calibration curves, 0-50,000 years Cal BP. *Radiocarbon*, 51:1111.

ROBERTS, N., EASTWOOD, W. J., KUZUCUOĞLU, C., FIORENTINO, G. & CARACUTA, V. (2011). Climatic, vegetation and cultural change in the eastern Mediterranean during the mid-Holocene environmental transition. *The Holocene*, 21:147-162.

ROBINSON, S. A., BLACK, S., SELLWOOD, B. W. & VALDES, P. J. (2006). A review of palaeoclimates and palaeoenvironments in the Levant and Eastern Mediterranean from 25,000 to 5000 years BP: setting the environmental background for the evolution of human civilisation. *Quaternary Science Reviews*, 25:1517-1541.

ROHLING, E. J., HAYES, A., MAYEWSKI, P. A. & KUCERA, M. (2009). Holocene climate variability in the eastern Mediterranean, and the end of the Bronze Age. In *Forces of Transformation: The End of the Bronze Age in the Mediterranean.* , ed. C. Bachhuber & G. Roberts. Oxford: Oxbow Press, 2009.

ROHLING, E. J. & PÄLIKE, H. (2005). Centennial-scale climate cooling with a sudden cold event around 8,200 years ago. *Nature*, 434:975-979.

ROLLEFSON, G. O. & KÖHLER-ROLLEFSON, I. (1992). Early neolithic exploitation patterns in the Levant: Cultural impact on the environment. *Population & Environment*, 13:243-254.

ROSEN, A. M. & RIVERA-COLLAZO, I. (2012). Climate change, adaptive cycles, and the persistence of foraging economies during the late Pleistocene/Holocene transition in the Levant. *Proceedings of the National Academy of Sciences*, 109:3640-3645.

ROSSIGNOL-STRICK, M. (1993). Late Quaternary climate in the Eastern Mediterranean Region. *Paléorient*:135-152.

ROSSIGNOL-STRICK, M. (1995). Sea-land correlation of pollen records in the Eastern Mediterranean for the glacial-interglacial transition: Biostratigraphy versus radiometric time-scale. *Quaternary Science Reviews*, 14:893-915.

ROWAN, Y. & GOLDEN, J. (2009). The Chalcolithic Period of the Southern Levant: A Synthetic Review. *Journal of World Prehistory*, 22:1-92.

RUBIO DE CASAS, R. (2002). On the historical presence of the wild olive Olea europaea L. var. sylvestris (Miller) Lehr. in the Eurosiberian North of the Iberian Peninsula. *Anales del Jardín Botánico de Madrid*, 59:342.

RÜßMANN, M. (2010). *Sedimentologische Analyse der Bohrkerne des See Genezareths, Israel*, Rheinische Friedrich-Wilhelms-Universität Bonn. Unpublished.

RÜßMANN, M. (2012). *Geochemische Analyse an Sedimentbohrkernen des Birkat Ram Sees*, Steinmann-Institut für Geologie, Mineralogie, Paläontologie Bereich Paläobotanik. Unpublished.

SADE, A. R., TIBOR, G., HALL, J. K. & DIAMANT, M. (2008). Multibeam Bathymetry of the Sea of Galilee (Lake Kinneret), ed. Poster, 2008.

SAFRAI, Z. (1994). *The Economy of Roman Palestine*. London: Routledge.

SAYEJ, G. J. (2010). *Palestinian Archaeology: Knowledge, Awareness and Cultural Heritage*.

SCHWAB, M. J., NEUMANN, F., LITT, T., NEGENDANK, J. F. W. & STEIN, M. (2004). Holocene palaeoecology of the Golan Heights (Near East): investigation of lacustrine sediments from Birkat Ram crater lake. *Quaternary Science Reviews*, 23:1723-1731.

SEGEV, A. & RYBAKOV, M. (2011). History of faulting and magmatism in the Galilee (Israel) and across the Levant continental margin inferred from potential field data. *Journal of Geodynamics*, 51:264-284.

SHAANAN, U., PORAT, N., NAVON, O., WEINBERGER, R., CALVERT, A. & WEINSTEIN, Y. (2011). OSL dating of a Pleistocene maar: Birket Ram, the Golan heights. *Journal of Volcanology and Geothermal Research*, 201:397-403.

SHAKUN, J. D. & CARLSON, A. E. (2010). A global perspective on Last Glacial Maximum to Holocene climate change. *Quaternary Science Reviews*, 29:1801-1816.

SHARON, D. & KUTIEL, H. (1986). The distribution of rainfall intensity in Israel, its regional and seasonal variations and its climatological evaluation. *Journal of Climatology*, 6:277-291.

SHMIDA, A. (1980). Kermes oaks in the land of Israel. *Israel Land and Nature*, 6:9-16.

SINGER, A. & EHRLICH, A. (1978). Paleolimnology of a late Pleistocene-Holocene crater lake from the Golan Heights, eastern Mediterranean. *Journal of Sedimentary Research*, 48:1331-1340.

STEIN, M., MIGOWSKI, C., BOOKMAN, R. & LAZAR, B. (2004). *Temporal changes in radiocarbon reservoir age in the Dead Sea-Lake Lisan system*.

STEIN, M., TORFSTEIN, A., GAVRIELI, I. & YECHIELI, Y. (2010). Abrupt aridities and salt deposition in the post-glacial Dead Sea and their North Atlantic connection. *Quaternary Science Reviews*, 29:567-575.

STEININGER, F. F. (1999). *Empfehlungen (Richtlinien) zur Handhabung der stratigraphischen Nomenklatur*.

STILLER, M. (2001). Calibration of lacustrine sediment ages using the relationship between 14C levels in lake waters and in the atmosphere: the case of Lake Kinneret. *Radiocarbon*, 43:821.

STILLER, M., CARMI, I. & KAUFMAN, A. (1988). Organic and inorganic 14C concentrations in the sediments of lake kinneret and the dead sea (Israel) and the factors which control them. *Chemical Geology: Isotope Geoscience section*, 73:63-78.

STOCKMAR, J. (1971). Tablets with spores used in absolute pollen analysis. *Pollen et Spores*, 13 615-621.

STUIVER, M. & POLACH, H. A. (1977). *Discussion; reporting of C-14 data*.

SUGITA, M. (1997). Reconstruction of fire disturbances and forest succession from fossil pollen in lake sediments: Potential and limitations. In *Sediment records of biomass burning and global change. NATO ASI Series I: Global environmental change*, ed. J. S. Clark, H. Cahcier, J. G. Goldammer & B. Stocks, 1997, pp. 387-412.

SUGITA, S. (1994). Pollen Representation of Vegetation in Quaternary Sediments: Theory and Method in Patchy Vegetation. *Journal of Ecology*, 82:881-897.

THEUERKAUF, M., KUPARINEN, A. & JOOSTEN, H. (2012). Pollen productivity estimates strongly depend on assumed pollen dispersal. *The Holocene*.

THOMA, B. (PhD thesis; in prep.). *PhD thesis*, Rheinische Friedrich-Wilhelm Universität. Unpublished.

THOMPSON, T. L. (1979). *The settlement of Palestine in the Bronze Age*. Wiesabden: Reichert.

TZEDAKIS, P. C. (2007). Seven ambiguities in the Mediterranean palaeoenvironmental narrative. *Quaternary Science Reviews*, 26:2042-2066.

TZEDAKIS, P. C., HOOGHIEMSTRA, H. & PÄLIKE, H. (2006). The last 1.35 million years at Tenaghi Philippon: revised chronostratigraphy and long-term vegetation trends. *Quaternary Science Reviews*, 25:3416-3430.

URMAN, D. (1985). The Golan. A profile of a region during the Roman and Byzantine periods. In *BAR International Series 269*, 1985, pp. 251.

VAKS, A., BAR-MATTHEWS, M., AYALON, A., SCHILMAN, B., GILMOUR, M., HAWKESWORTH, C. J., FRUMKIN, A., KAUFMAN, A. & MATTHEWS, A. (2003). Paleoclimate reconstruction based on the timing of speleothem growth and oxygen and carbon isotope composition in a cave located in the rain shadow in Israel. *Quaternary Research*, 59:182-193.

VALLA, F. R. (1995). The first settled societies - Natufian (12,500-10,200 BP). In *The archaeology of society in the Holy Land*, ed. T. E. Levy. London: Leicester Univ. Press, 1995.

VAN ZEIST, W., BARUCH, U. & BOTTEMA, S. (2009). Holocene Palaeoecology of the Hula Area, Northeastern Israel. In *A Timeless Vale. Archaeological and related essays on the Jordan Valley in honour of Gerrit van der Kooij on the occasion of his sixty-fifth birthday. Archaeological Studies Leiden University*, ed. E. Kaptijn & L. P. Petit: Leiden University Press, 2009, pp. 29-64.

VAN ZEIST, W. & BOTTEMA, S. (1982). Vegetational history of the Eastern Mediterranean and the Near East during the last 20,000 years. In *BAR International Series 133*, ed. J. L. Bintliff & W. Van Zeist, 1982, pp. 277-323.

VAN ZEIST, W. & BOTTEMA, S. (1991). *Late Quaternary vegetation of the Near East*. Wiesbaden: Dr. Ludwig Reichert Verlag.

VAN ZEIST, W. & WOLDERING, H. (1980). Holocene vegetation and climate of northwestern Syria. *Palaeohistoria*.

VOSSEL, H. (2012). *Diatomeen-Analyse an Sedimentbohrkernen aus dem See Genezareth (Israel)*, Rheinische Friedrich-Wilhelms-Universität Bonn. Unpublished.

WALTER, H. & STRAKA, H. (1970). *Arealkunde - floristisch-historische Geobotanik. Einführung in die Phytologie*.

WEINSTEIN, A. (1989). Geographic variation and phenology of Pinus halepensis, P. brutia and P. eldarica in Israel. *Forest Ecology and Management*, 27:99-108.

WEINSTEIN, M. (1976a). The Late Quaternary Vegetation of the Northern Golan. *Pollen et Spores*, 18.

WEINSTEIN, M. (1976b). The Late Quaternay Vegetation of the Northern Golan. *Pollen et Spores*, 18:553-562.

WICK, L., LEMCKE, G. & STURM, M. (2003). Evidence of Lateglacial and Holocene climatic change and human impact in eastern Anatolia: high-resolution pollen, charcoal, isotopic and geochemical records from the laminated sediments of Lake Van, Turkey. *The Holocene*, 13:665-675.

YASUDA, Y., KITAGAWA, H. & NAKAGAWA, T. (2000). The earliest record of major anthropogenic deforestation in the Ghab Valley, northwest Syria: a palynological study. *Quaternary International*, 73–74:127-136.

YECHIELI, Y., MAGARITZ, M., LEVY, Y., WEBER, U., KAFRI, U., WOELFLI, W. & BONANI, G. (1993). Late Quaternary Geological History of the Dead Sea Area, Israel. *Quaternary Research*, 39:59-67.

ZANCHETTA, G., SULPIZIO, R., ROBERTS, N., CIONI, R., EASTWOOD, W. J., SIANI, G., CARON, B., PATERNE, M. & SANTACROCE, R. (2011). Tephrostratigraphy, chronology and climatic events of the Mediterranean basin during the Holocene: An overview. *The Holocene*, 21:33-52.

ZEDER, M. A. (2011). The origins of agriculture in the Near East. *Current Anthropology*, 52:221-235.

ZHOU, A.-F., CHEN, F.-H., WANG, Z.-L., YANG, M.-L., QIANG, M.-R. & ZHANG, J.-W. (2011). *Temporal Change of Radiocarbon Reservoir Effect in Sugan Lake, Northwest China during the Late Holocene*.

ZIV, B., DAYAN, U., KUSHNIR, Y., ROTH, C. & ENZEL, Y. (2006). Regional and global atmospheric patterns governing rainfall in the southern Levant. *International Journal of Climatology*, 26:55-73.

ZOHARY, D. & HOPF, M. (1988). *Domestication of plants in the Old World. The origin and spread of cultivated plants in West Asia, Europe and the Nile Valley*: Clarendon Press.

ZOHARY, M. (1962). Plant Life of Palestine: Israel and Jordan. *Chronica Botanica*, 33.

ZOHARY, M. (1966). *Flora palaestina*. Jerusalem.

ZOHARY, M. (1972). *Flora Palaestina*.

ZOHARY, M. (1973). *Geobotanical Foundations of the Middle East*. Stuttgart: Gustav Fischer Verlag.

ZOHARY, M. (1982). *Vegetation of Israel and adjacent areas*. Wiesbaden: Dr. Ludwig Reichert Verlag.

A 10 Lake Kinneret, Complete Pollen Diagram

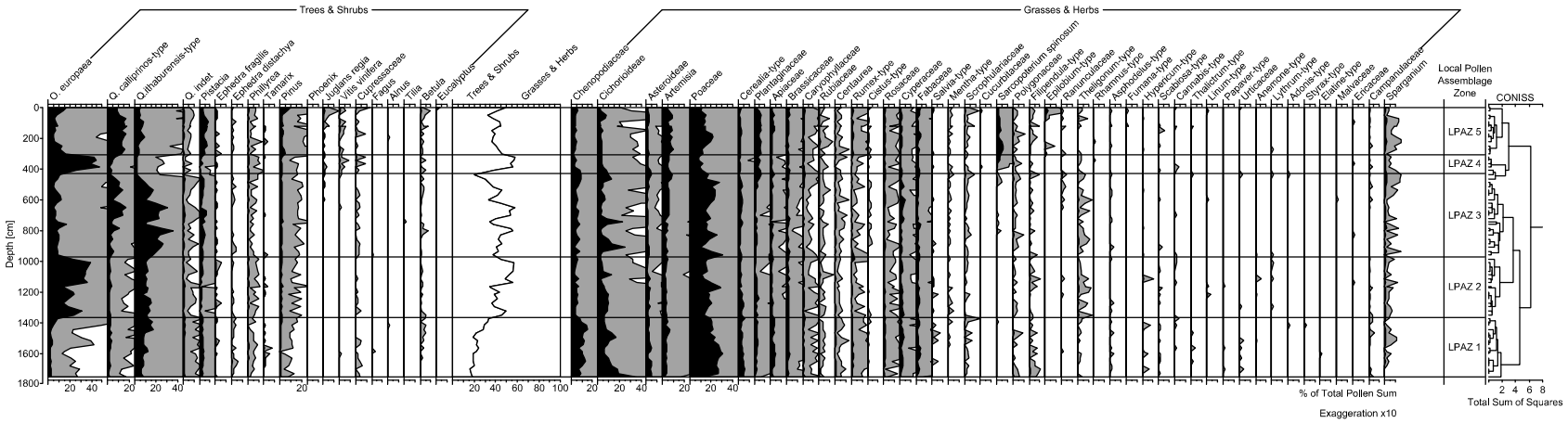

A 11 Birkat Ram, Complete Pollen Diagram